ACOUSTICAL OCEANOGRAPHY OF THE LEVANTINE SEA

Nazim Cubukcu

NAVAL POSTGRADUATE SCHOOL
Monterey, California

THESIS

ACOUSTICAL OCEANOGRAPHY OF THE

LEVANTINE SEA

by

Nazım Çubukçu

September 1978

Thesis Advisor: A. B. Chace

Approved for public release; distribution unlimited.

SECURITY CLASSIFICATION OF THIS PAGE (When Data Entered)

REPORT DOCUMENTATION PAGE

READ INSTRUCTIONS BEFORE COMPLETING FORM

1. REPORT NUMBER	2. GOVT ACCESSION NO.
3. RECIPIENT'S CATALOG NUMBER	
4. TITLE (and Subtitle) Acoustical Oceanography of the Levantine Sea	5. TYPE OF REPORT & PERIOD COVERED Master's Thesis; September 1978
	6. PERFORMING ORG. REPORT NUMBER
7. AUTHOR(s) Nazım Çubukçu	8. CONTRACT OR GRANT NUMBER(s)
9. PERFORMING ORGANIZATION NAME AND ADDRESS Naval Postgraduate School Monterey, CA 93940	10. PROGRAM ELEMENT, PROJECT, TASK AREA & WORK UNIT NUMBERS
11. CONTROLLING OFFICE NAME AND ADDRESS Naval Postgraduate School Monterey, CA 93940	12. REPORT DATE September 1978
	13. NUMBER OF PAGES 147
14. MONITORING AGENCY NAME & ADDRESS (if different from Controlling Office) Naval Postgraduate School Monterey, CA 93940	15. SECURITY CLASS. (of this report) Unclassified
	15a. DECLASSIFICATION/DOWNGRADING SCHEDULE

16. DISTRIBUTION STATEMENT (of this Report)

Approved for public release; distribution unlimited.

17. DISTRIBUTION STATEMENT (of the abstract entered in Block 20, if different from Report)

18. SUPPLEMENTARY NOTES

19. KEY WORDS (Continue on reverse side if necessary and identify by block number)

20. ABSTRACT (Continue on reverse side if necessary and identify by block number)

Data on oceanographic conditions in the Levantine Sea in the eastern end of the Mediterranean Sea were compiled. Water masses, bottom sediments, and bottom topography are described. Four locations were chosen as representative of the Levantine Sea. Acoustic propagation was modelled

DD FORM 1 JAN 73 1473 EDITION OF 1 NOV 65 IS OBSOLETE
S/N 0102-014-6601 |

SECURITY CLASSIFICATION OF THIS PAGE (When Data Entered)

for four different months in the 50 to 5000 Hz frequency range for source and receiver depths of 21 to 300 ft at each location. Optimum passive detection of submarine targets was found to occur when source and receiver were at the same depth. This could be achieved with the sonar either on a submarine or lowered below a surface ship.

Approved for public release; distribution unlimited.

Acoustical Oceanography of the Levantine Sea

by

Nazim Cubukcu
Lieutenant, Turkish Navy
Turkish Navy Academy, 1971

Submitted in partial fulfillment of the
requirements for the degree of

MASTER OF SCIENCE IN OCEANOGRAPHY

from the

NAVAL POSTGRADUATE SCHOOL
September 1978

ABSTRACT

Data on oceanographic conditions in the Levantine Sea in the eastern end of the Mediterranean Sea were compiled. Water masses, bottom sediments, and bottom topography are described. Four locations were chosen as representative of the Levantine Sea. Acoustic propagation was modelled for four different months in the 50 to 5000 Hz frequency range for source and receiver depths of 21 to 300 ft at each location. Optimum passive detection of submarine targets was found to occur when source and receiver were at the same depth. This could be achieved with the sonar either on a submarine or lowered below a surface ship.

TABLE OF CONTENTS

LIST OF TABLES

LIST OF FIGURES

ACKNOWLEDGEMENTS

I would like to express my appreciation for the guidance and assistance given by LCDR A. B. Chace who generously shared his experience in the field of acoustical oceanography in numerous invaluable discussions and timely encouragement throughout the entire study.

I also wish to recognize the efforts of my wife, Mehtap, during the last two years. Her patience and understanding helped to make the entire learning experience at the Naval Postgraduate School an enjoyable one.

I. INTRODUCTION

The most important naval application of oceanography is sound propagation through the sea. There have been many attempts to establish relationships between oceanic properties and sound propagation. Effective naval use of the seas requires detailed description and understanding of the important environmental factors. The Eastern Mediterranean has received little attention yet relative to antisubmarine warfare (ASW); it is a critical area.

The purpose of this thesis is to examine environmental properties of the Levantine Sea such as water mass, bottom topography, sediments and their compositions, and to relate them to sound propagation. The vertical sound velocity profile and acoustical transmission loss are examined at four specific sites using a range of frequencies (from 50 to 5000 Hz), target depths, and sonar depths. Four selected months were used to obtain the seasonal picture.

II. GEOGRAPHY OF THE LEVANTINE SEA

The Mediterranean Sea is divided into two major sections, Western and Eastern, by the ridge which includes Italy, Sicily, and the submerged parts of the sill between Europe and Africa.

The Eastern Mediterranean exclusive of the Aegean Sea generally has been divided into two parts, the Ionian and Levantine basins (Sverdrup, Johnson, and Fleming, 1942). The boundary between these basins formerly was placed at the ridge extending from Greece to Africa. Recent bathymetric data, however, show that the two continents are not connected by a ridge. A better western boundary is a line from Ras-al Hilal on the Libyan coast to the island of Crete by way of Gavdhos Island (Figure 1).

The area covered by the Levantine Sea is approximately 320,000 square kilometers with a maximum depth of 4384 m (Carter, Flanagan, Jones, Marchant, Murchison, Rebman, Sylvester, and Whitney, 1972).

The Levantine Sea is bordered on the north by Crete, the Dodecanese Islands, and Turkey. On the east it is bordered by Syria, Lebanon, and Israel and to the south by Egypt and Libya. The Island of Cyprus is located in the northeast quadrant of the basin. The northwest margin of the basin includes an island arc extending from Crete through the Dodecanese Islands to Rhodes.

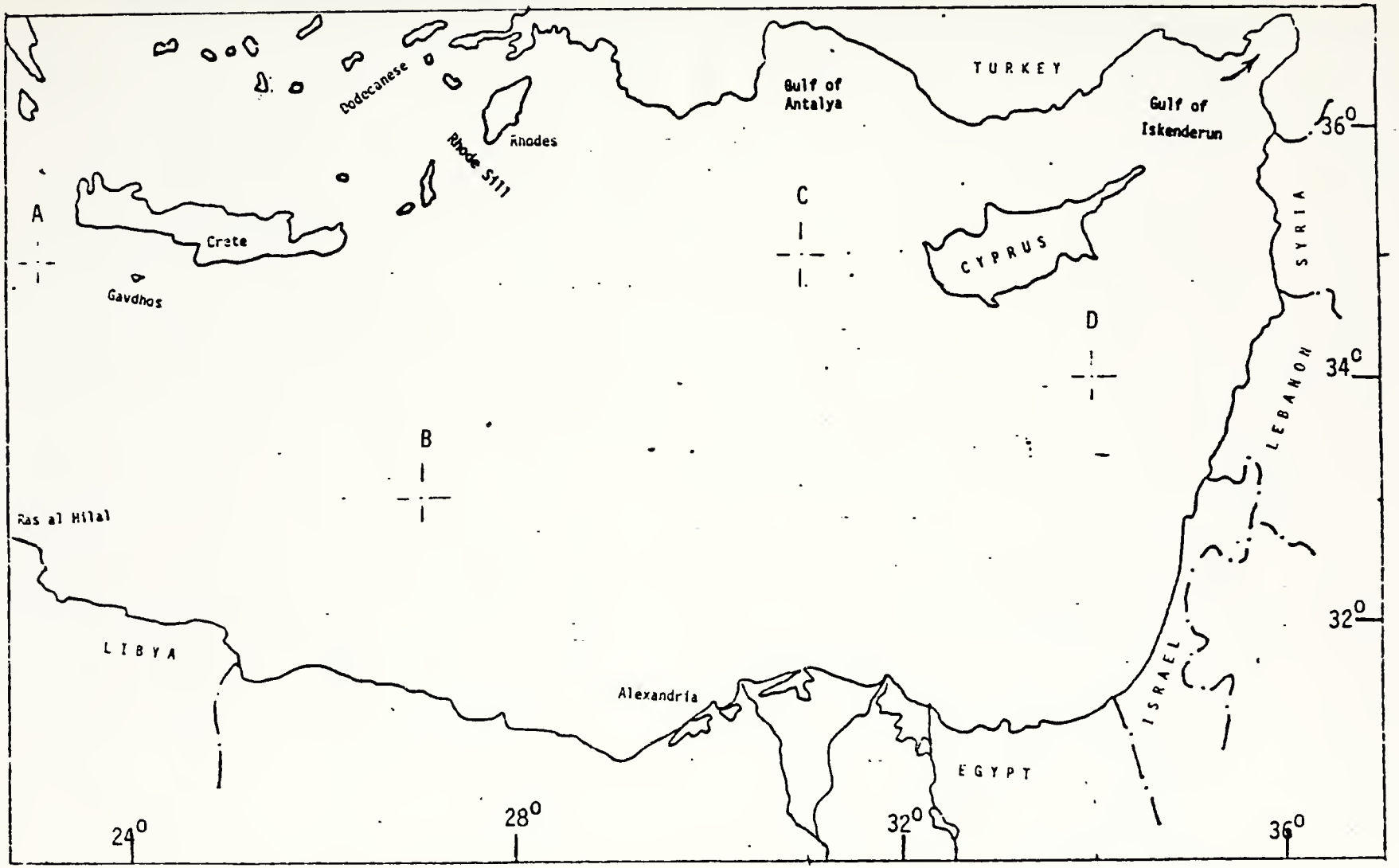

Figure 1. Location map of the Levantine Sea.

III. HYDROLOGY

The physical oceanography of the Mediterranean Sea is primarily controlled by the climatology of the region. Water loss by evaporation is greater than the gain resulting from precipitation and river discharge. Lacombe and Tchernia (1972) describe the Mediterranean as a machine which balances both its water and salt contents. Incoming water from the Atlantic is evaporated and in the winter season cooled at the surface, and to a lesser extent diluted by rain and river outflow, resulting in the typical dense and salty Mediterranean water mass which ultimately flows back into the Atlantic at subsurface depths through the Strait of Gibraltar. The mechanism of this machine determines not only the physical properties of the Mediterranean water masses, but their main flow patterns as well.

A. VERTICAL STRUCTURE OF WATER MASSES

There are four distinct water masses in the Mediterranean Sea (Wüst, 1961). The Levantine Sea has all of these masses; in fact, this area is very important because it is the source of intermediate Levantine water.

Vertical convection currents which can cause a complete overturning of the entire water column are an important factor in the formation of subsurface water and are most likely to occur during periods of minimum surface temperature (Pollak, 1951).

By means of the vertical distribution of salinity, oxygen, and temperature, the Levantine Sea water is separated into four different water masses:

1. Near Surface Water of Atlantic origin between the surface and 75 m depth,

2. The Intermediate Water between 200 m and 600 m depth,

3. The Deep Water between 1500 m and 3000 m depth,

4. The Bottom Water at depths to 4200 m.

Each of these water masses is now treated in more detail.

1. Near Surface Water

Summer prevailing winds strengthen the eastward flowing surface currents. These waters of Atlantic origin are recognizable by their relatively low salinity and are found everywhere in the Levantine Sea. North to northwest winds (Etesian winds) prevail over this area in summer. These winds are both strong and consistent in direction which results in effective mixing of the near surface waters. Zonal transport of Central Mediterranean surface waters adds to the Levantine surface water with the winds mixing them to a depth of 20 to 75 m.

In winter the influence of the Atlantic surface water in the Levantine Sea is decreased because in the Central Mediterranean much of it is deflected north toward the Adriatic.

During the summer and winter seasons the circulation of the surface waters of the Levantine Sea is very complex. Figure 2 shows the general circulation January through December. The most intensive and stable feature is the cyclonic gyre north of Crete. Between Crete and Africa there is a flow from the central basin into the Levantine Sea in the surface layer. This easterly surface current in the Levantine Sea weakens in summer (Ovchinnikov and Fedoseyev, 1968).

Nielsen (1912) showed the most commonly presented picture of the currents in the Eastern Mediterranean. His description should be modified on the basis of later studies; for example, studying the influence of the Nile flood waters along the Israeli coast two varieties of water

Figure 2. General surface circulation, January through December (Swanson, 1966).

developing side by side have been discovered (Engel, 1967). On the other hand, hydrological conditions in the Gulf of Iskenderun (northeastern corner of Levantine Sea) show that the surface circulation there forms two eddies.

The velocity of the currents seldom exceeds 6-12 nautical miles per day. The general pattern of the geostrophic circulation at the surface and at a depth of 20 m, indicating general counterclockwise flow in the eastern part of the Levantine Sea, are shown in Figures 3 and 4, respectively.

The seasonal variation of the surface salinity in the Levantine Sea is affected primarily by evaporation and to a lesser extent by the annual cycle of rainfall. In fall and winter the surface water temperature is higher than the air temperature. The surface waters of the northern Levantine Sea are slightly cooler than those to the south. The average values of air and surface temperatures calculated for a strip of five degree squares along the Turkish and Egyptian coasts are shown in Table I. The seasonal air-sea temperature differences are such that evaporation and cooling are a minimum in summer (May-July) and a maximum in fall and winter. The annual cycle of rainfall in this region, shown in Table II, tends to reduce the salinity in the winter season. The minimum salinity occurs earlier in the southern Levantine Sea, presumably under the influence of the Atlantic Ocean surface water entering from the west (Morcos, 1972). More salinity and temperature information for the Levantine Sea are shown in Appendix B and Figures 11 through 19.

2. Intermediate Water

The formation of Intermediate Water depends mainly on climatological conditions resulting in vertical mixing and sinking of relatively

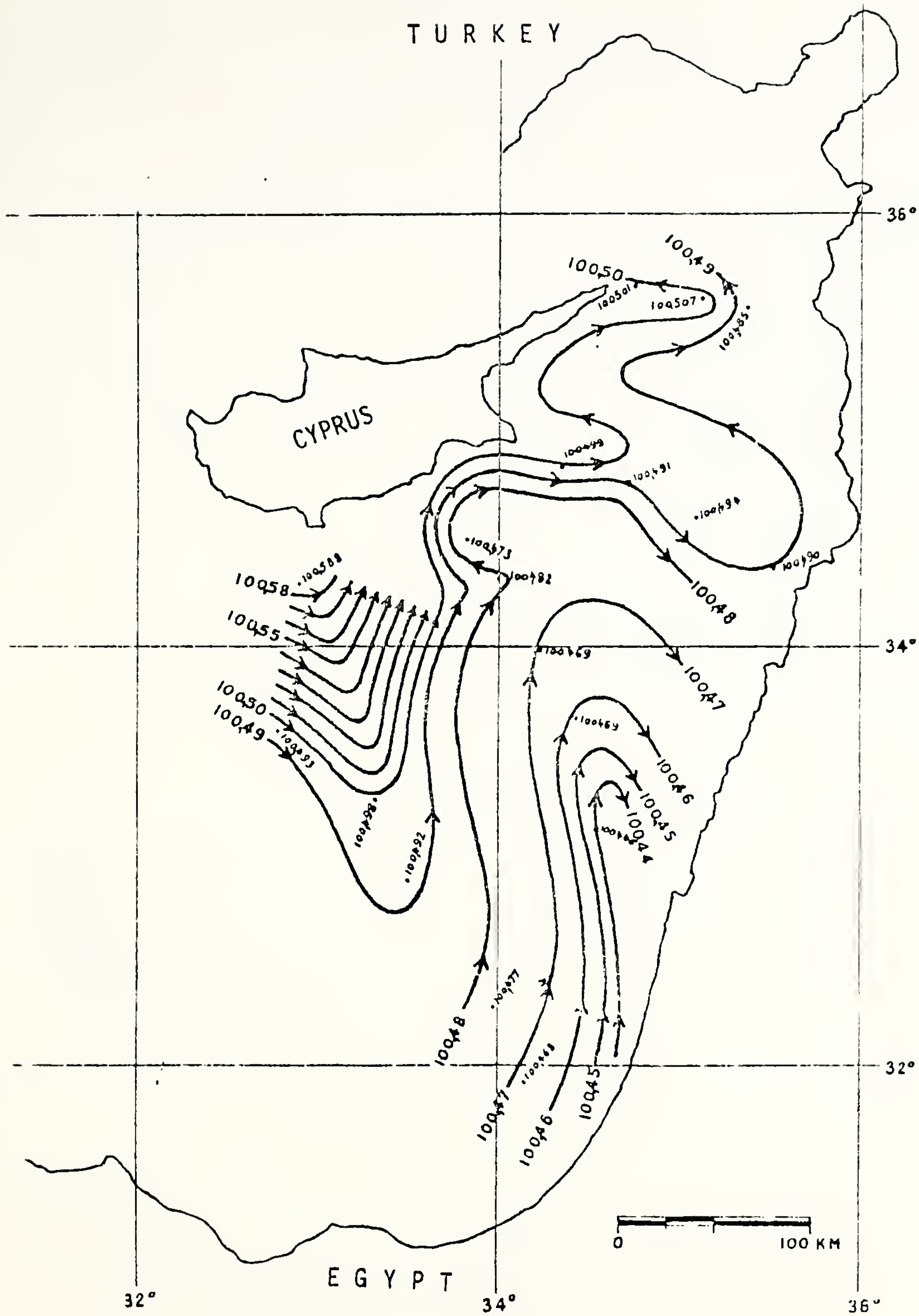

Figure 3. Contours of pressure of a water column at the sea surface to a depth of 20 m (Engel, 1967).

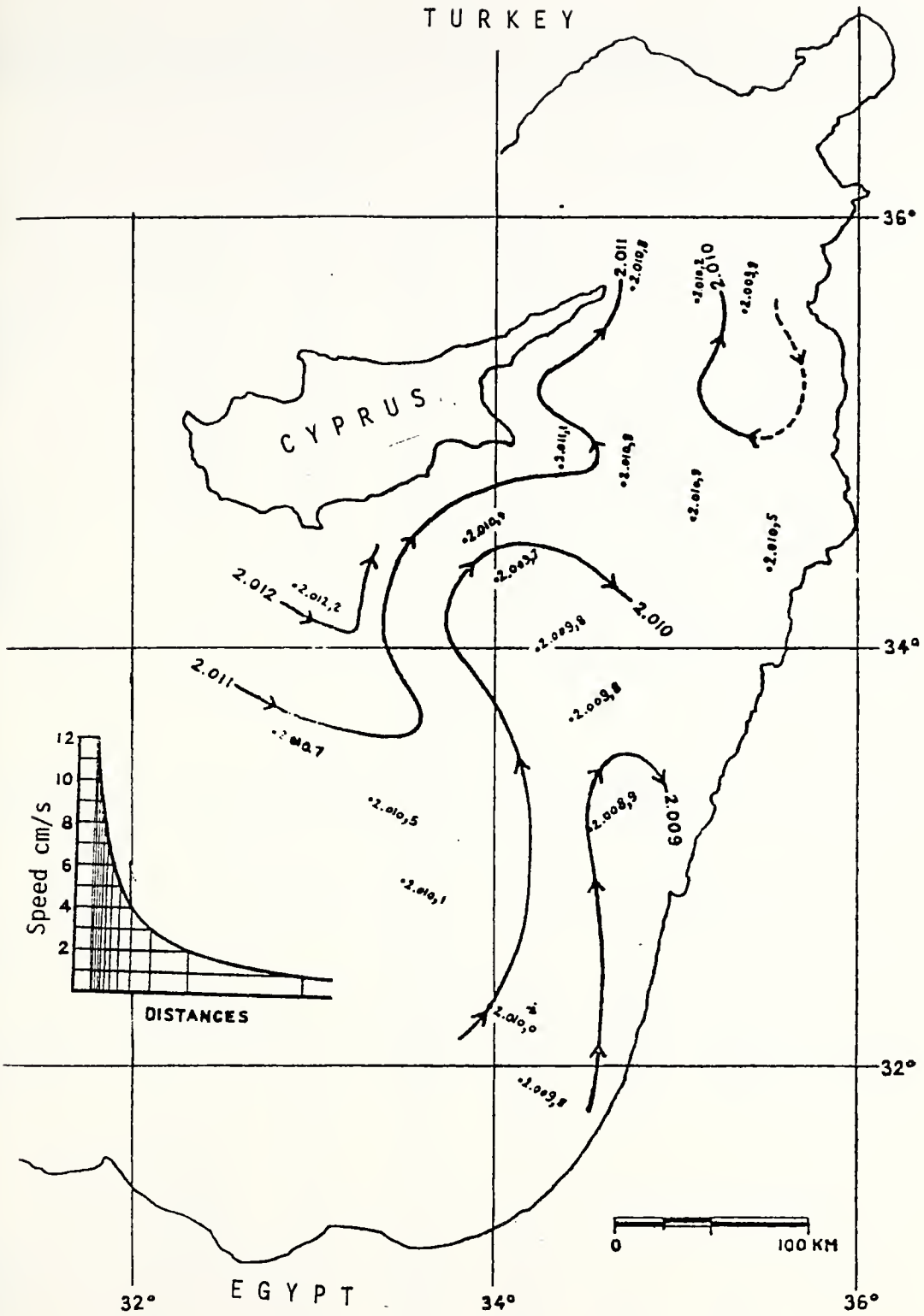

Figure 4. Contours of pressure of a water column at the sea surface to a depth of 20 m (Engel, 1967).

TABLE I

AVERAGE MONTHLY TEMPERATURE OF SEA SURFACE AND OVERLYING AIR IN A STRIP OF 5^{o} SQUARES ALONG THE TURKISH AND EGYPTIAN COASTS (^{o}C) (Morcos, 1972)

Months	Turkish Coast (^{o}C)			Egyptian Coast (^{o}C)		
	Sea Water	Air	$t_w - t_u$	Sea Water	Air	$t_w - t_u$
January	17.0	15.2	1.8	17.2	15.9	1.3
February	15.5	14.4	1.1	16.3	15.4	0.9
March	16.2	15.6	0.6	16.0	16.3	-0.3
April	16.9	17.3	-0.4	17.4	17.9	-0.5
May	19.5	20.2	-0.7	20.0	20.6	-0.6
June	22.0	23.5	-1.5	22.9	23.5	-0.6
July	24.8	25.8	-1.0	24.9	25.5	-0.6
August	26.5	27.1	-0.6	25.8	26.2	-0.4
September	25.2	25.4	-0.2	25.4	25.2	0.2
October	23.3	23.1	0.2	24.0	23.5	0.5
November	20.6	19.6	1.0	21.9	20.8	1.1
December	18.2	16.6	1.6	19.2	17.8	1.4
Annual range	11.0	12.7		9.8	10.8	

TABLE II

AVERAGE MONTHLY PRECIPITATION AT COASTAL METEOROLOGICAL STATIONS IN THE NORTHERN AND SOUTHERN LEVANTINE SEA (mm)(Morcos, 1972)

Months	Northern Levant Sea (mm)			Southern Levant Sea (mm)		
	Rhodes	Antalya	Cyprus Cape Andreas	Port Said	Alex-andria	Saloum
January	237	247	96	18	48	21
February	123	151	74	13	24	15
March	110	75	47	10	11	8
April	25	39	36	5	3	<1
May	30	27	22	3	2	5
June	0.5	13	2	0.0	0.0	<1
July	0.0	2	0.0	0.0	0.0	<1
August	0.0	1	<0.1	0.0	<0.1	0.0
September	4	11	16	0.0	1	<1
October	96	49	26	3	6	2
November	152	129	61	10	33	26
December	199	267	138	15	56	18
Total	973	1011	518	77	184	95

cold saline waters to intermediate depths. Along the coast of Asia Minor, the temperature drops in February to values of about 15.5°-16.0°C. At the same time the surface salinity is high (39.0‰). The combination of low temperature and high salinity forms relatively dense surface water on both sides of Rhodes. This large homogenous water mass is formed in the upper 250 m, then spreads at subsurface depths as a core layer that is called Levantine Intermediate Water (Morcos, 1972). While spreading westward, it mixes with lower salinity water from above and below resulting in a decrease in salinity and temperature, with an associated increase in depth from 50-100 m to 100-250 m and finally to 300-400 m. T-S diagrams of the core layer of the Intermediate Water in the northern and southern Levantine Sea are shown in Figure 5.

After having passed the central Ionian Basin the main flow goes over the Sicilian ridge through the Strait of Sardinia. Distributions of salinity within the core of the Levantine Intermediate Water in winter and summer are shown in Figures 6 and 7, respectively.

In the summer, the Levantine Intermediate current is perceptibly weaker than in winter. Apart from this fact the main trends of the distribution of the salinity within the core layer remain the same in summer as in winter (Wüst, 1961). During the summer the circulation of the intermediate waters in the Levantine Sea shows a degree of complexity similar to that of the surface layer.

3. Deep Water

According to Nielsen (1912) the source of the deep water is the southern Aegean Sea, but Pollak (1951) showed that this is not true. Only one of the three passages from the southern Aegean into the Mediterranean has an appreciable sill depth. This is the Andikithara Channel, north of Crete, with a maximum depth of 805 m. The other two channels have

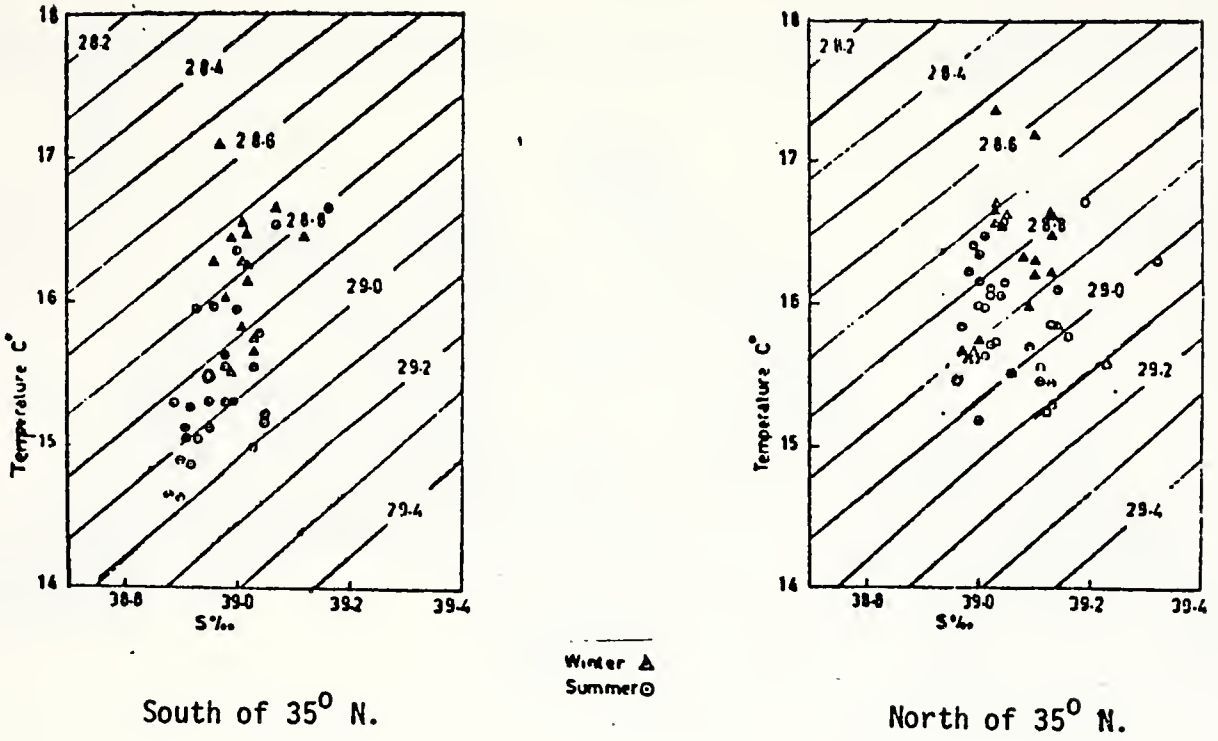

Figure 5. T-S diagrams of the core layer of the Levantine intermediate water (Morcos, 1972).

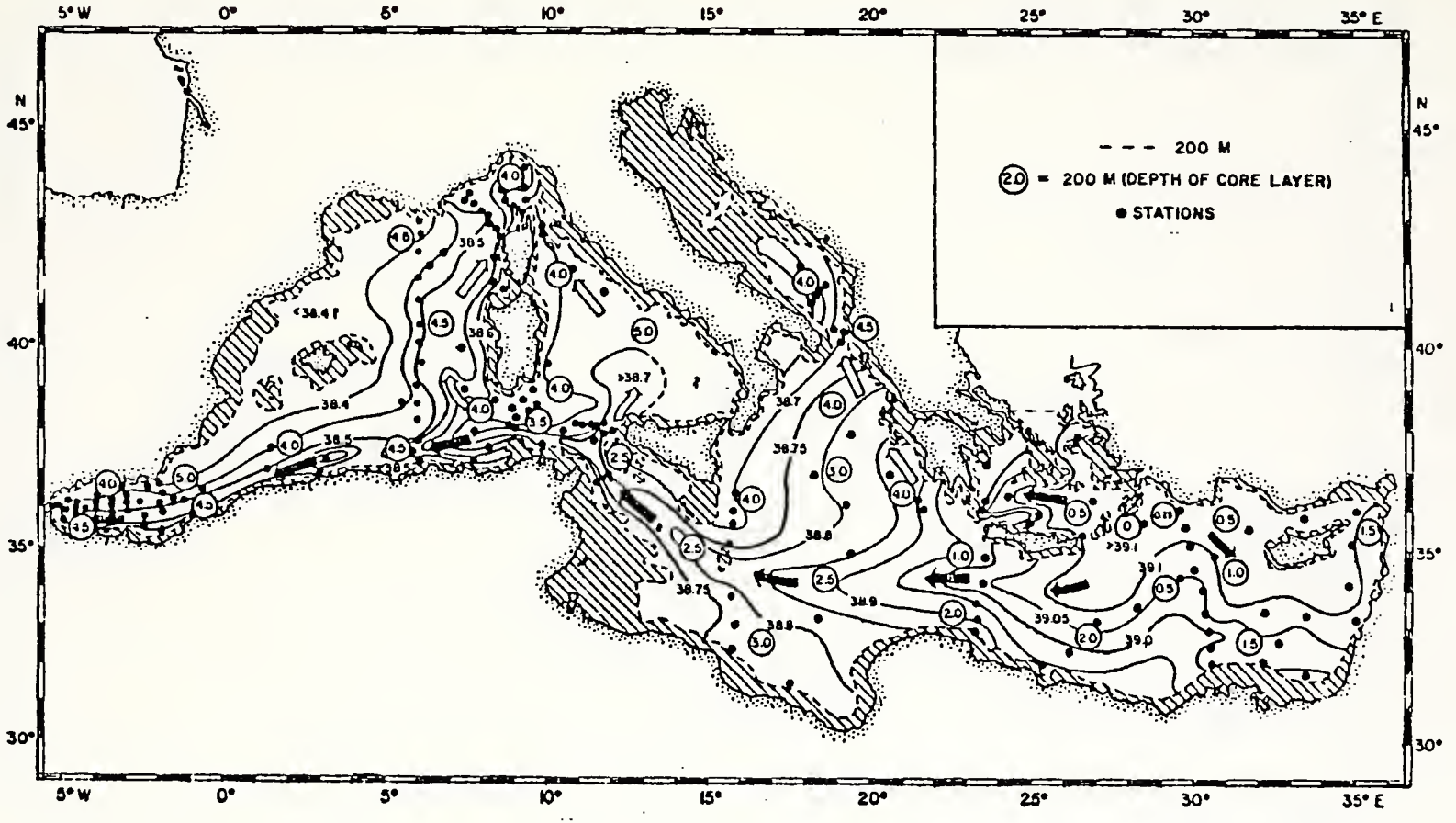

Figure 6. Distribution of salinity within the core layer of intermediate water in winter (Wüst, 1961).

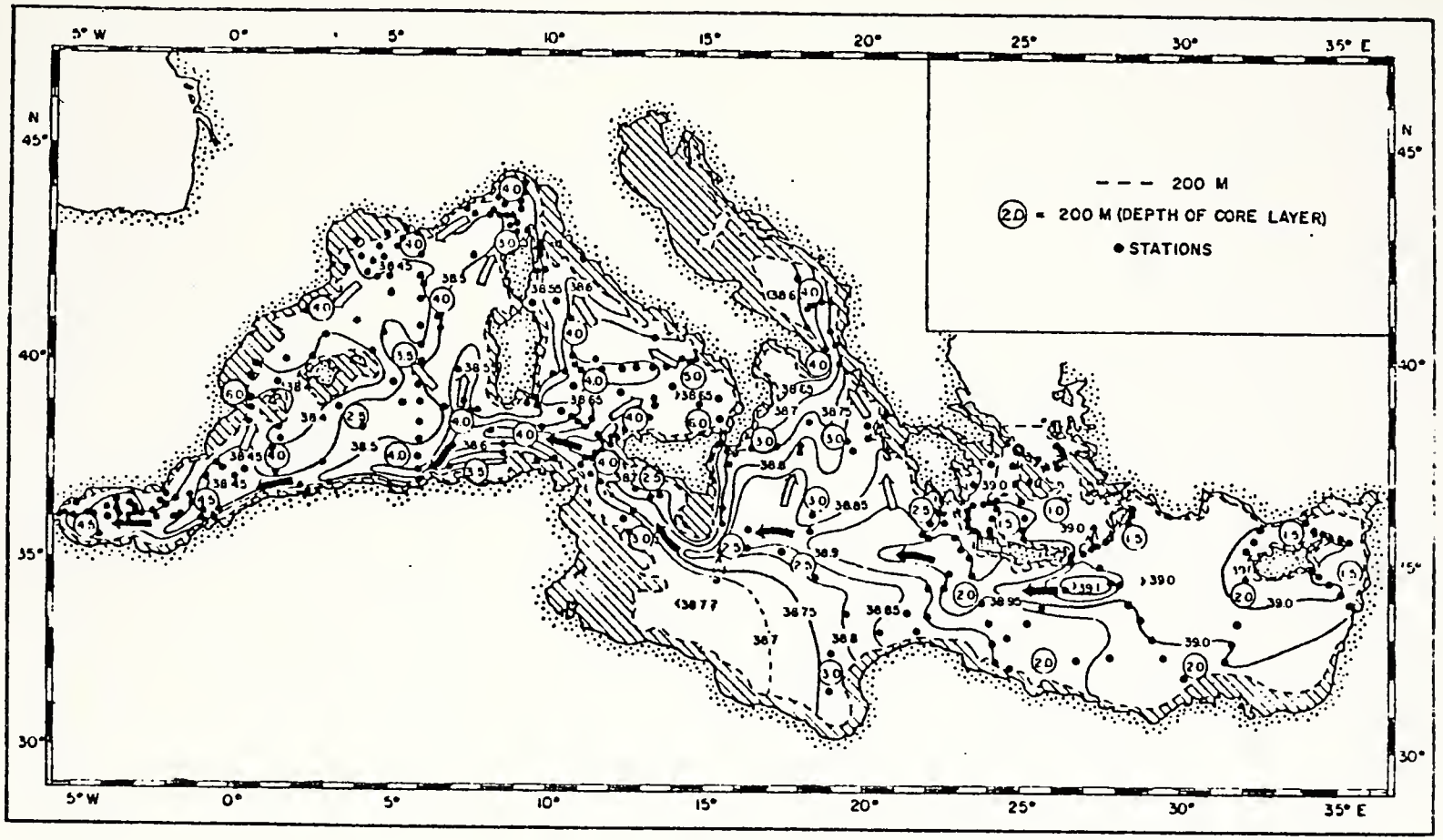

Figure 7. Distribution of salinity within the core layer of intermediate water in summer (Wüst, 1961).

depths of 137 m and 290 m. Moskalenko and Ovchinnikov (1968) state that formation of deep water depends to some extent on the warmer and saltier waters which penetrate the Levantine Sea from the Crete Basin of the Aegean Sea. This idea is consistent with Nielsen (1912) but is contrary to Pollak (1951). Wüst (1961) showed, on the basis of the oxygen distribution in the deep water (Figure 8), that the main source region for the high oxygen content Levantine Sea Deep Water is the Adriatic Sea. On the basis of these investigations it appears that the Adriatic Sea is the principal source of the Levantine Deep Water and that a significant Aegean source would be unlikely due to the shallow sill depths. Future research may provide confirmation.

If the upper limit of the deep water in the Levantine Basin were defined by marked changes in the gradient of water properties, a depth of about 700 m would be selected; on the other hand Pollak (1951) using absolute values as criterion, specified 1600 m as the upper limit for deep water. The deep water mass has nearly uniform temperature and salinity values ($13.5\ ^{o}C < T < 13.7\ ^{o}C$ -- $36.6‰ < S < 36.8‰$).

4. Bottom Water

Bottom waters in the western and eastern Mediterranean are separate and distinct due to the shallow 330 m depth of the Sicilian sill.

Bottom waters are best characterized by potential temperature, salinity, and potential density (Wüst, 1961). The map of potential temperature, which is the temperature that a water sample would attain if raised adiabatically to the sea surface (Sverdrup et al., 1942), is shown in Figure 9 for the bottom waters. At the borders there is a weak temperature gradient, which means that the isotherms are here nearly parallel to the contour lines of depth.

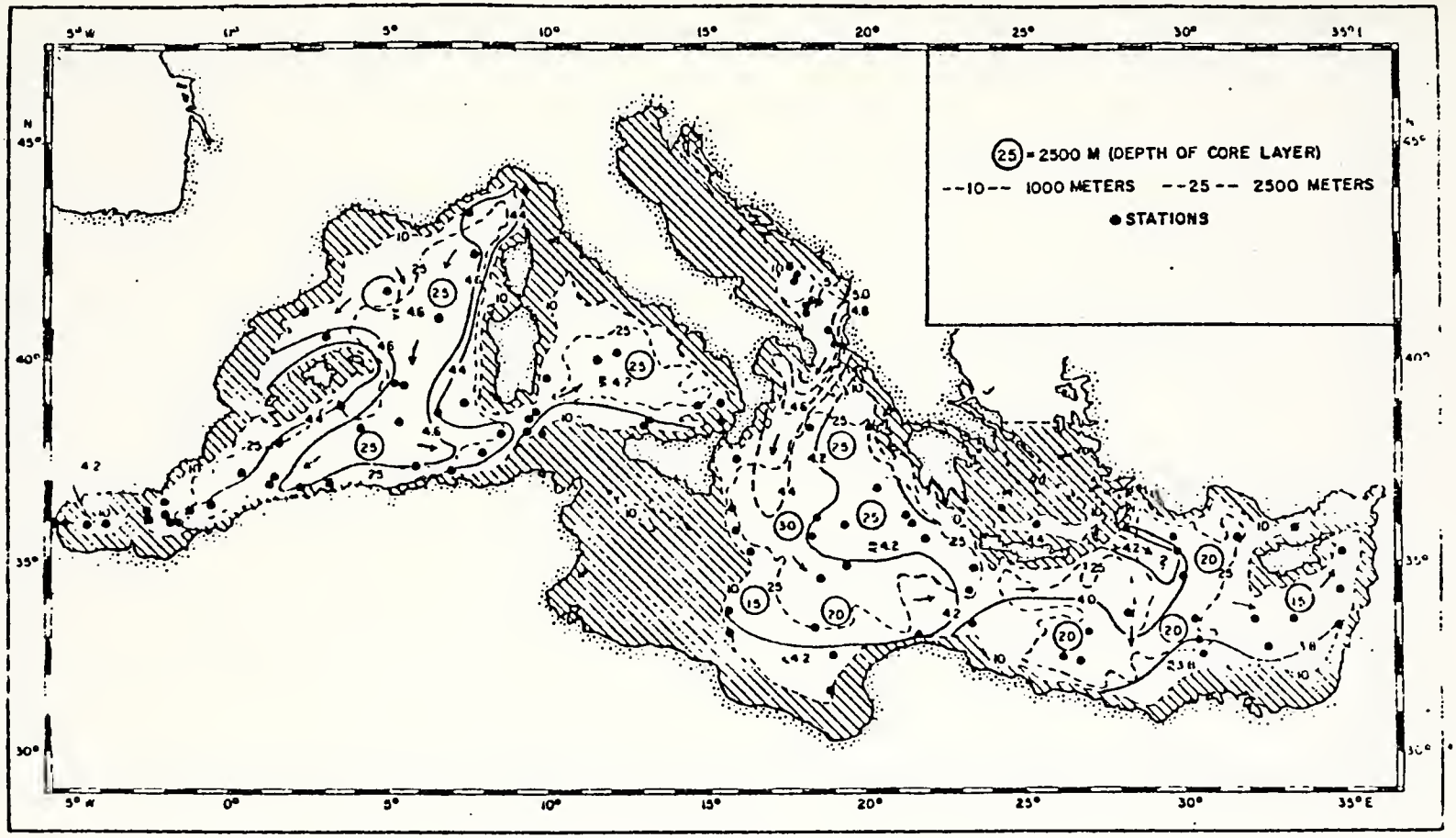

Figure 8. Distribution of oxygen within the core layer of the deep water (Wüst, 1961).

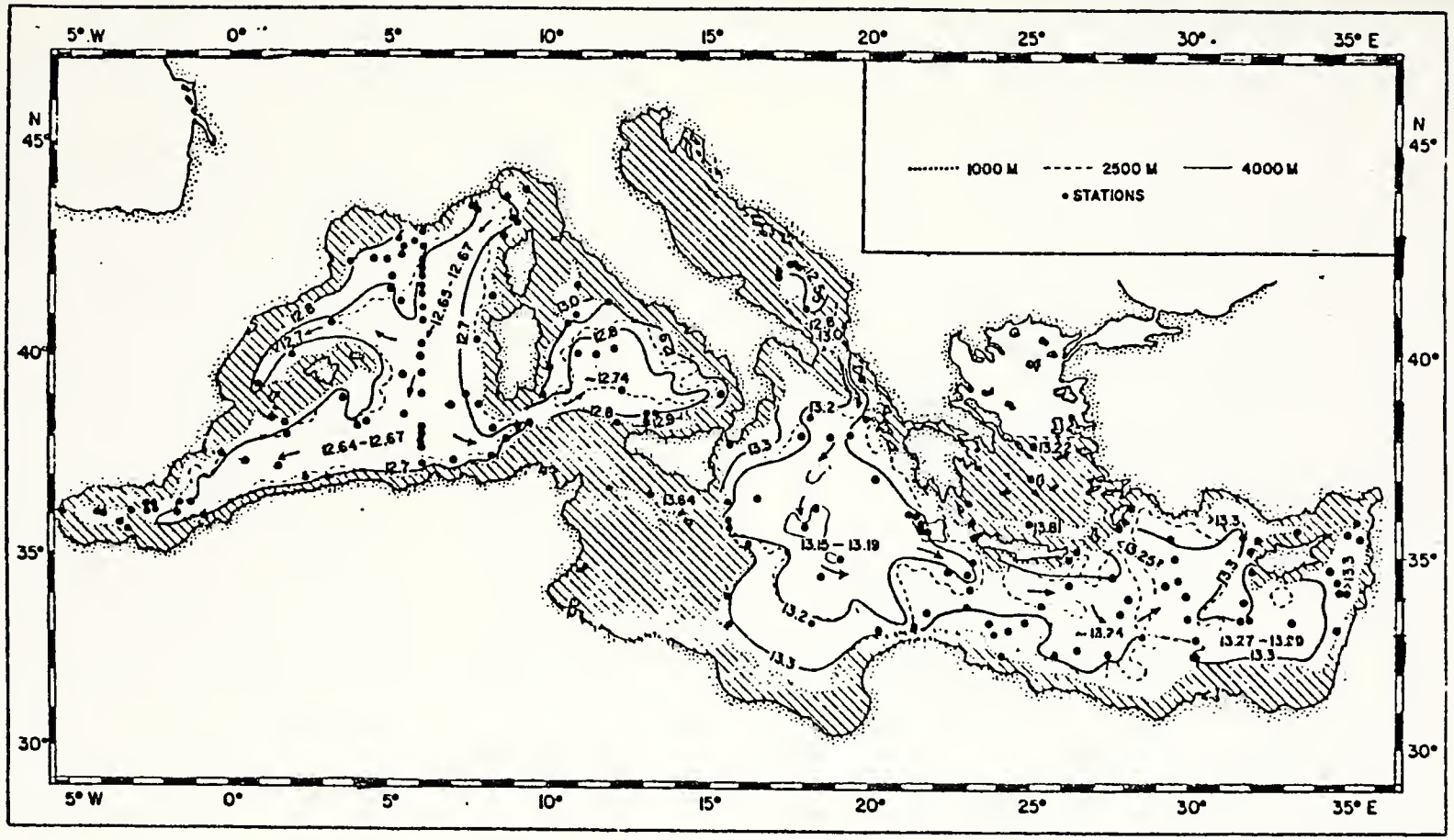

Figure 9. Map of the potential bottom temperatures (at depths of more than 1500 m) (Wüst, 1961).

The bottom water in the Levantine Basin originates at the surface in the Adriatic Sea in winter. The main flow of Adriatic bottom water is at first directed to the south and accompanied by marked vertical mixing on the Otranto Sill (between Italy and Albania). From here, similar to the deep water, it turns to the east and enters the Levantine Basin where it flows with a nearly constant temperature of 13.27 ^{o}C into the great depths south of the Rhode Sill and Cyprus (Wüst, 1961).

There is a thick transition layer between intermediate and deep waters, but between deep and bottom waters no significant transition layer exists. Wüst (1961) described the properties of deep and bottom waters using temperature, salinity, and oxygen. The differences between these water masses are slight so that it is difficult to determine a boundary between them. Lack of detailed observations from the eastern Mediterranean compounds the problem.

B. SALINITY AND TEMPERATURE DISTRIBUTION

In the Levantine Sea vertical salinity gradients are small. Isohaline conditions are approached from near the surface to the bottom. Figure 10 shows locations of the salinity profile sections during summer which are shown in Figures 11 and 12, respectively.

In the horizontal salinity distribution the maximum surface salinity occurs in both seasons in the Gulf of Iskenderun. Figures 13 and 14 show the horizontal surface salinity distribution in summer and in winter, respectively. In the intermediate water, the gradient of the horizontal salinity distribution becomes smaller than at the surface. Figures 15 and 16 show this distribution for the depth of 300 m in summer and in winter. Figure 17 shows both the surface and the east-west vertical salinity distribution in the Levantine Sea.

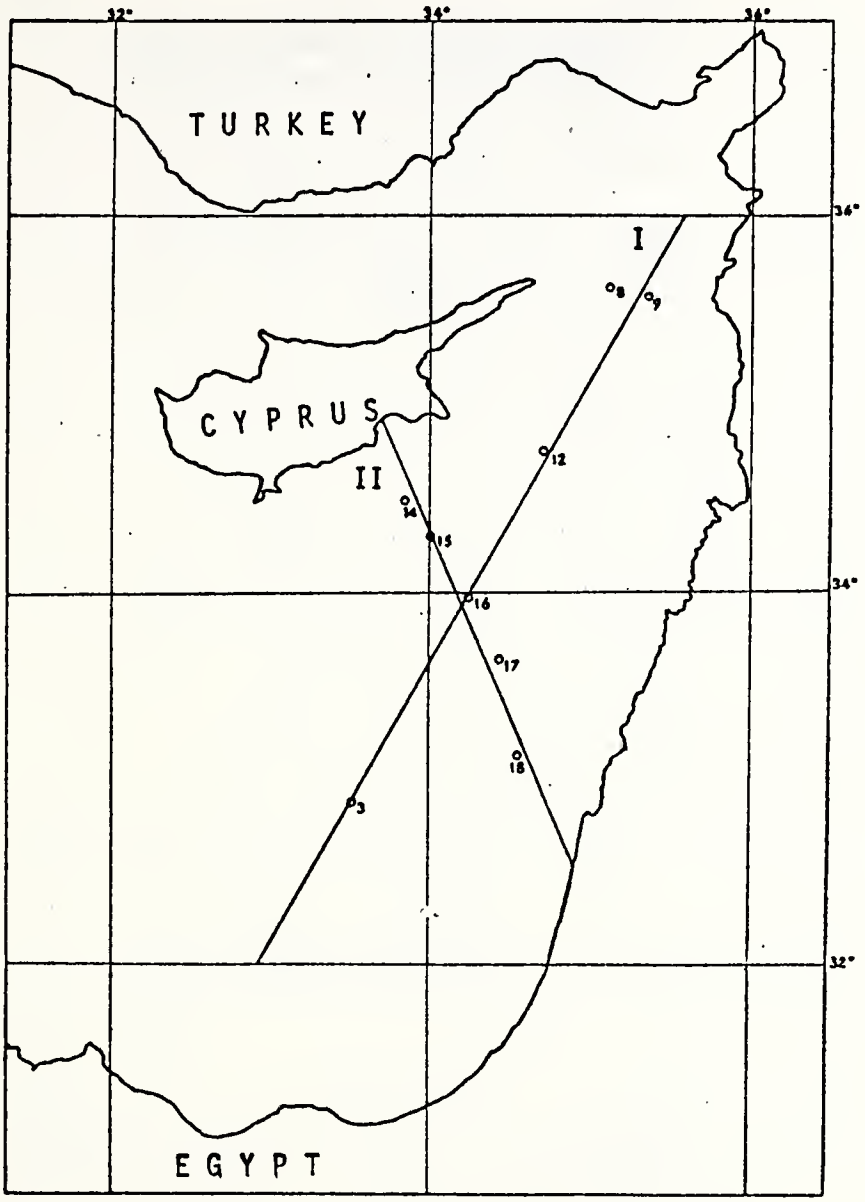

Figure 10. Locations of the salinity and temperature profile sections (Engel, 1968).

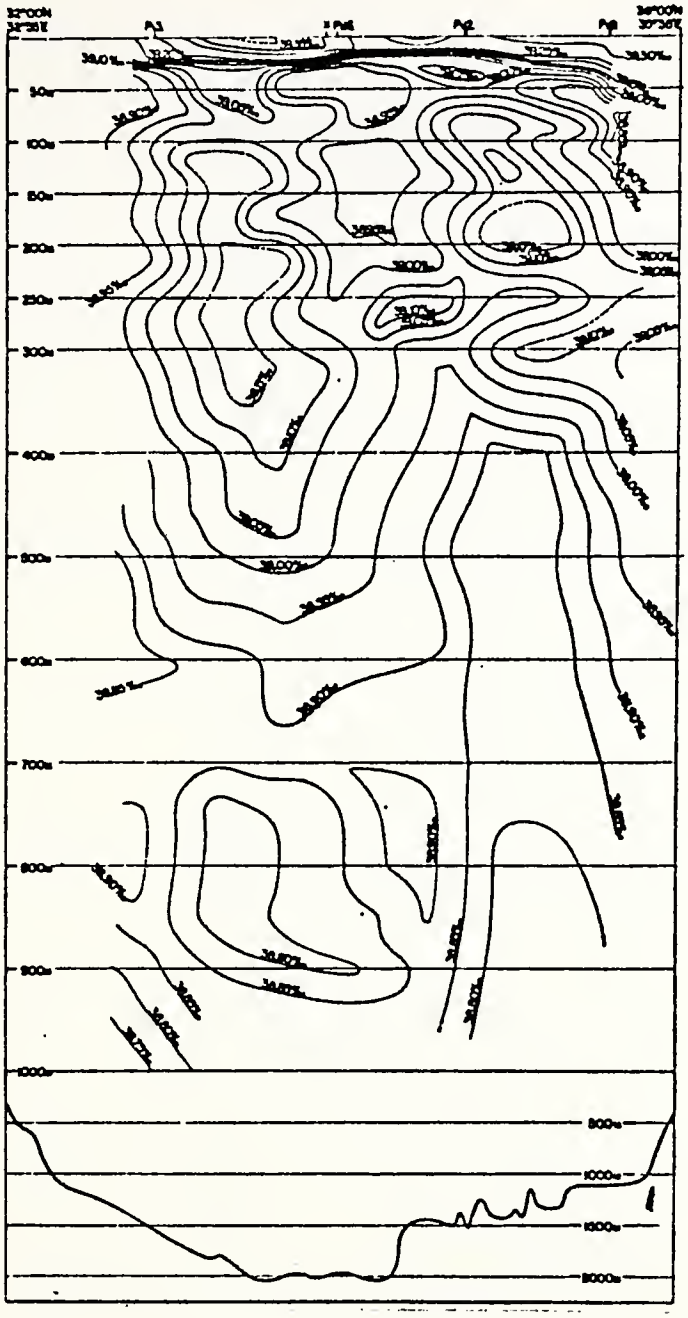

Figure 11. Vertical salinity distribution in Section I during summer (Engel, 1968).

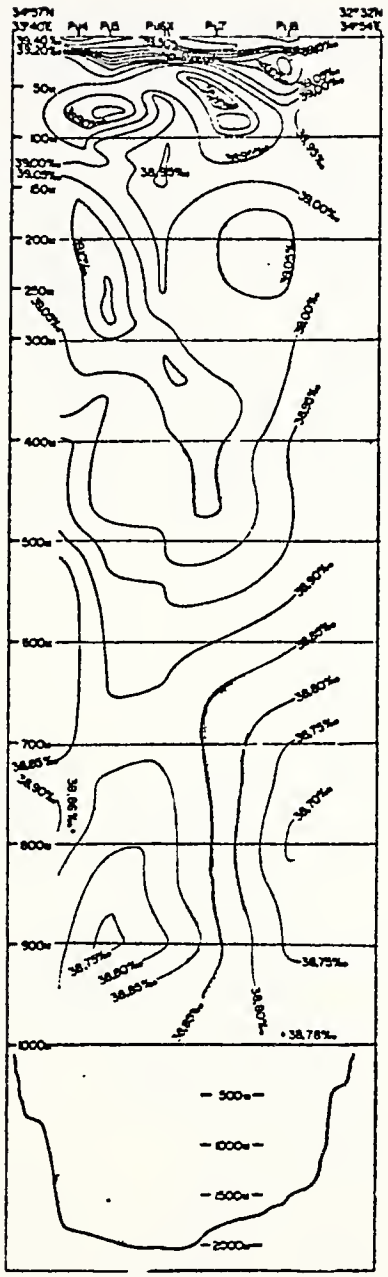

Figure 12. Vertical salinity distribution in Section II during summer (Engel, 1968).

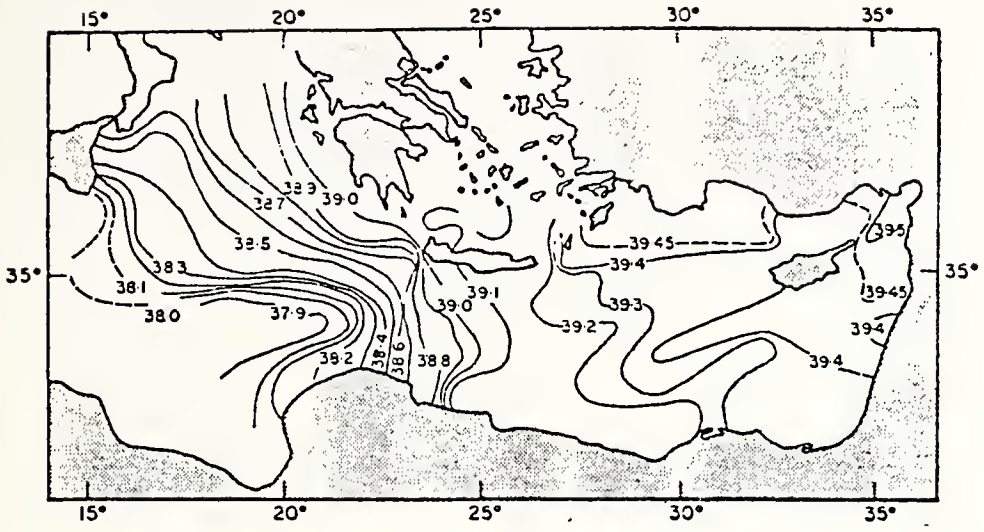

Figure 13. Surface isohalines in summer (Armanda, 1969).

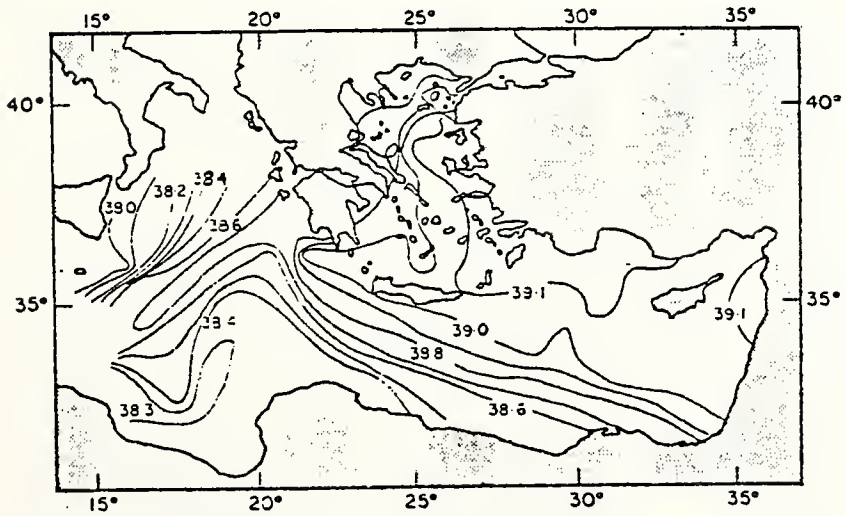

Figure 14. Surface isohalines in winter (Armanda, 1969).

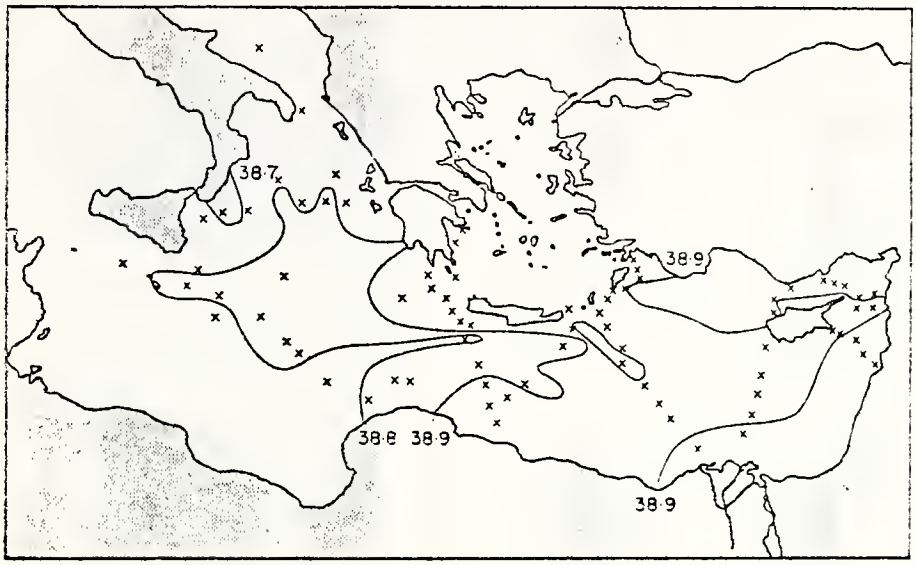

Figure 15. Isohalines for the depth of 300 m in summer (Armanda, 1969).

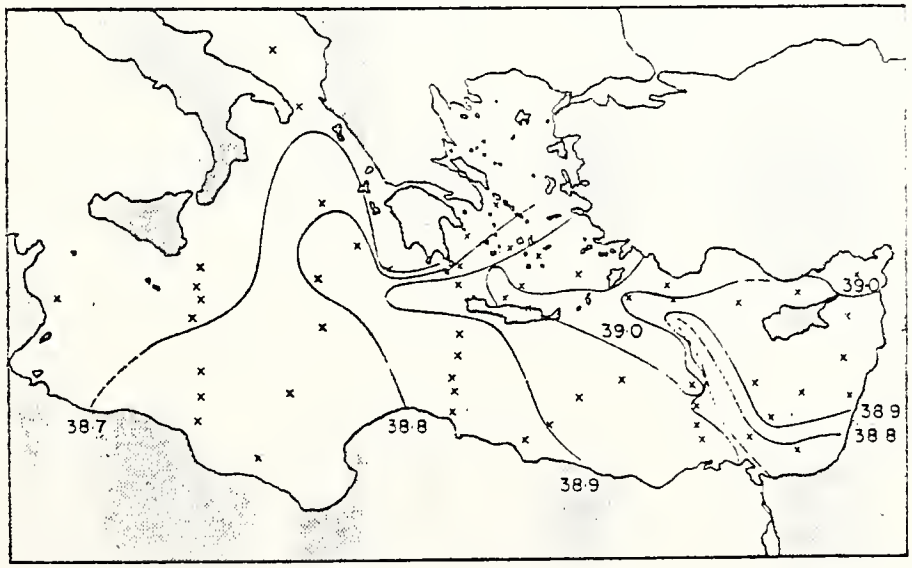

Figure 16. Isohalines for the depth of 300 m in winter (Armanda, 1969).

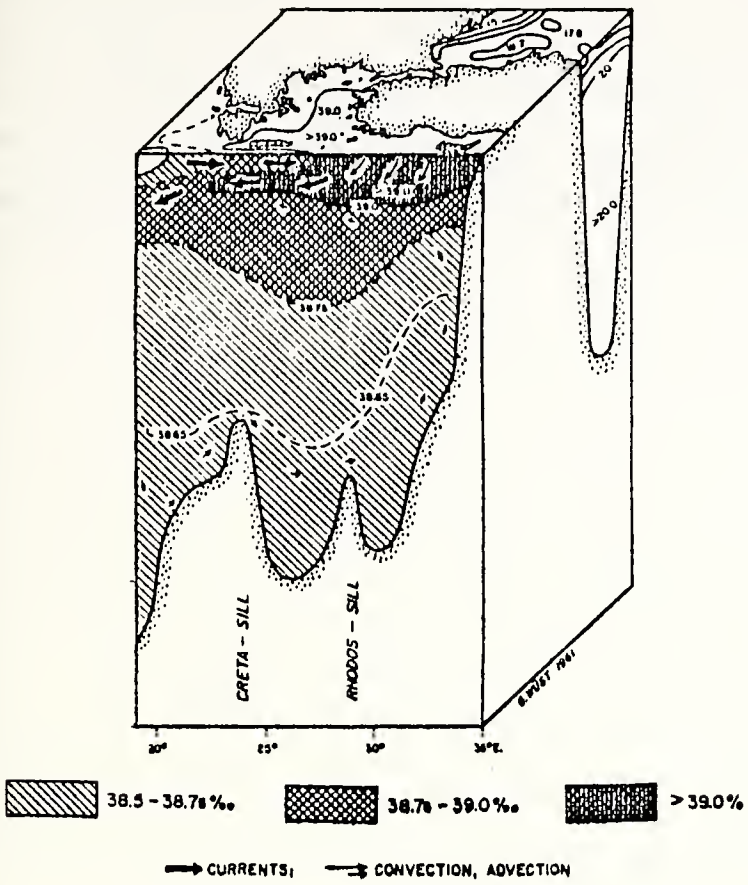

Figure 17. Schematic block diagram of salinity distribution and circulation in the Levantine Sea (Wüst, 1961).

Vertical temperature distribution for the sections of Figure 10 are shown in Figures 18 and 19. Surface and intermediate water masses show seasonal temperature variation. A surface maximum occurs in summer. Winter has both the coldest and deepest surface water masses.

Appendix B shows the monthly BT data at four different points.

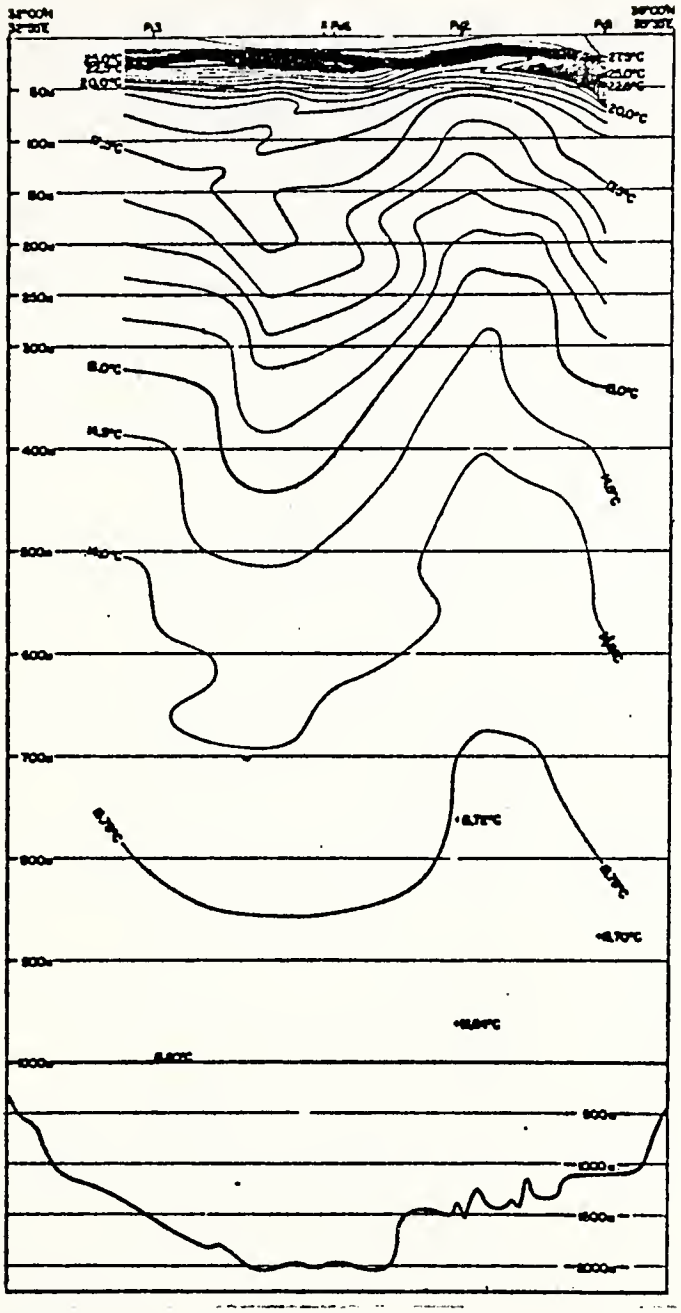

Figure 18. Vertical temperature distribution in Section I during summer (Engel, 1968).

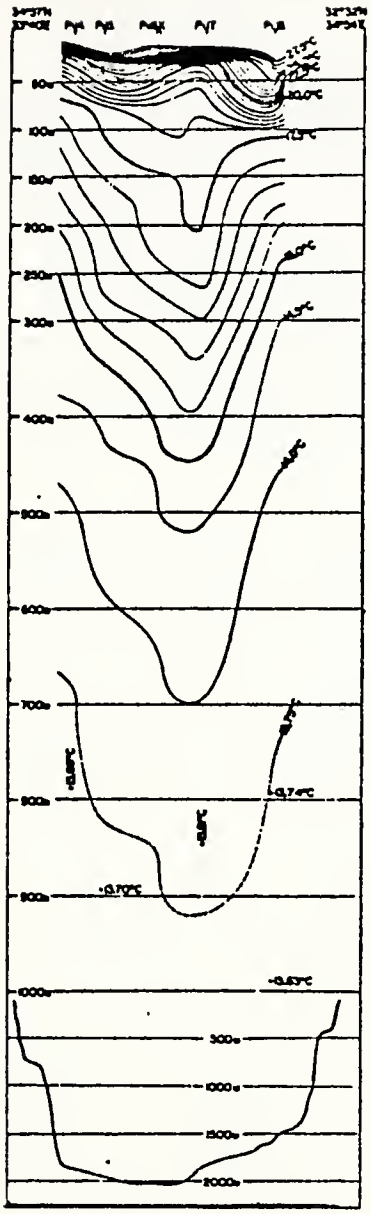

Figure 19. Vertical temperature distribution in Section II during summer (Engel, 1968).

IV. BATHYMETRY

Information about the depth of the Mediterranean Sea is reported in early literature beginning with Herodotus in 450 B.C. (Emery, Heezen, and Allan, 1966). Since then there have been many additional attempts to determine the bathymetry. The bathymetry and physiographic provinces of the Levantine Sea are shown in Figure 20. Recent studies show that the deepest part of the sea is the Rhodes Abyssal Plain with a depth of 4700 m (Emery et al., 1966).

The Mediterranean Sea is almost entirely located within the Alpine Geosynclinal Belt (Goncharov and Mikhailov, 1963). The largest forms of bottom relief in the eastern part are determined by the complex inter-relation between the structural elements of the north, in the zone of young folding (the Aegean and the Sea of Marmara), and of the southern regions adjacent to the ancient Africa-Arabian shelf. The largest bottom relief in the eastern Mediterranean is the complex formed by the island arc of Crete and Rhodes. The crest of this arc extends northwest into Greece and east into Turkey. Deep troughs stretch along this arc from the Ionian Islands to the Gulf of Antalya. The troughs, located on the convex side of the arc, are separated by anticlines but they are a single system and are connected with a deep 1500 km long regional rift.

The troughs generally have a V-shaped profile with a maximum depth of 4000 to 5000 m (Goncharov and Mikhailov, 1964). Between Cyprus and the continental slope of Egypt there is a plateau bordered on the north and south by two troughs.

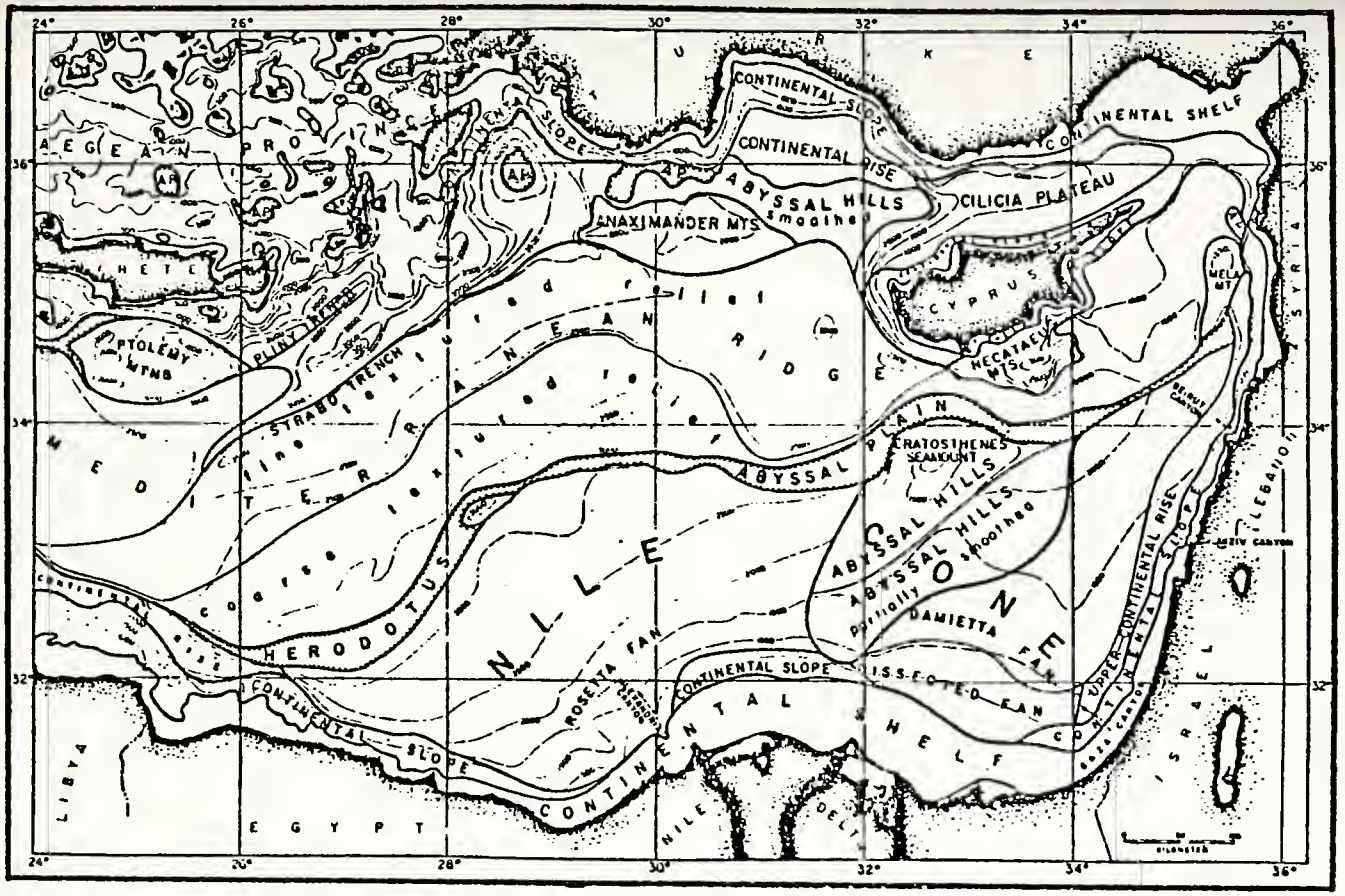

Figure 20. Chart of Levantine Sea showing bottom contours at 500 m intervals and boundaries of physiographic provinces based upon precision sounding profiles (Emery et al., 1966).

A. CONTINENTAL SHELF, SLOPE, AND RISE

If the Nile Cone and Gulf of Iskenderun are omitted the width of the continental shelf of the Eastern Mediterranean Sea is less than 15 kilometers. In these two regions the continental shelf may exceed 70 km and both areas are of depositional origin.

The shelf break off the Nile Delta usually occurs at a depth of about 95 m, somewhat shallower than the average of 110 m off the south coast of Israel. Continental shelves elsewhere in the region (see Figure 20) are too poorly sounded to depict details of the topography, terraces, or even a reliable depth of the shelf break. Due to sediment deposition near the eastern and western edges of the Nile Cone there is no significant shelf break. Profiles of the Nile Cone also indicate several terrace levels. Figures 22, 23, and 24 show characteristics of sounding profiles of various physiographic features taken from the area shown in Figure 21.

The continental slope is the region between shelf break and continental rise. It has a variable depth range between 800 and 2200 m. On the continental slope of the Afro-Arabian platform two types of relief can be distinguished. A steep slope, which stretches along the coast of Syria and the Lebanon and also occurs west of the Nile Cone, and a gentle slope, which is located off the coast of Egypt where it is covered by alluvium from the Nile and also in the Gulf of Sidra along the coast of Libya just off Figure 21 (Goncharov and Mikhailov, 1964).

Profiles 1 and 13 of Figure 23 and Profile 2 of Figure 24 show that the topography of the upper continental rise is irregular (Emery et al., 1966). The continental rise consists of sediments contributed to the sea by the Nile River and carried northeastward by the regional current.

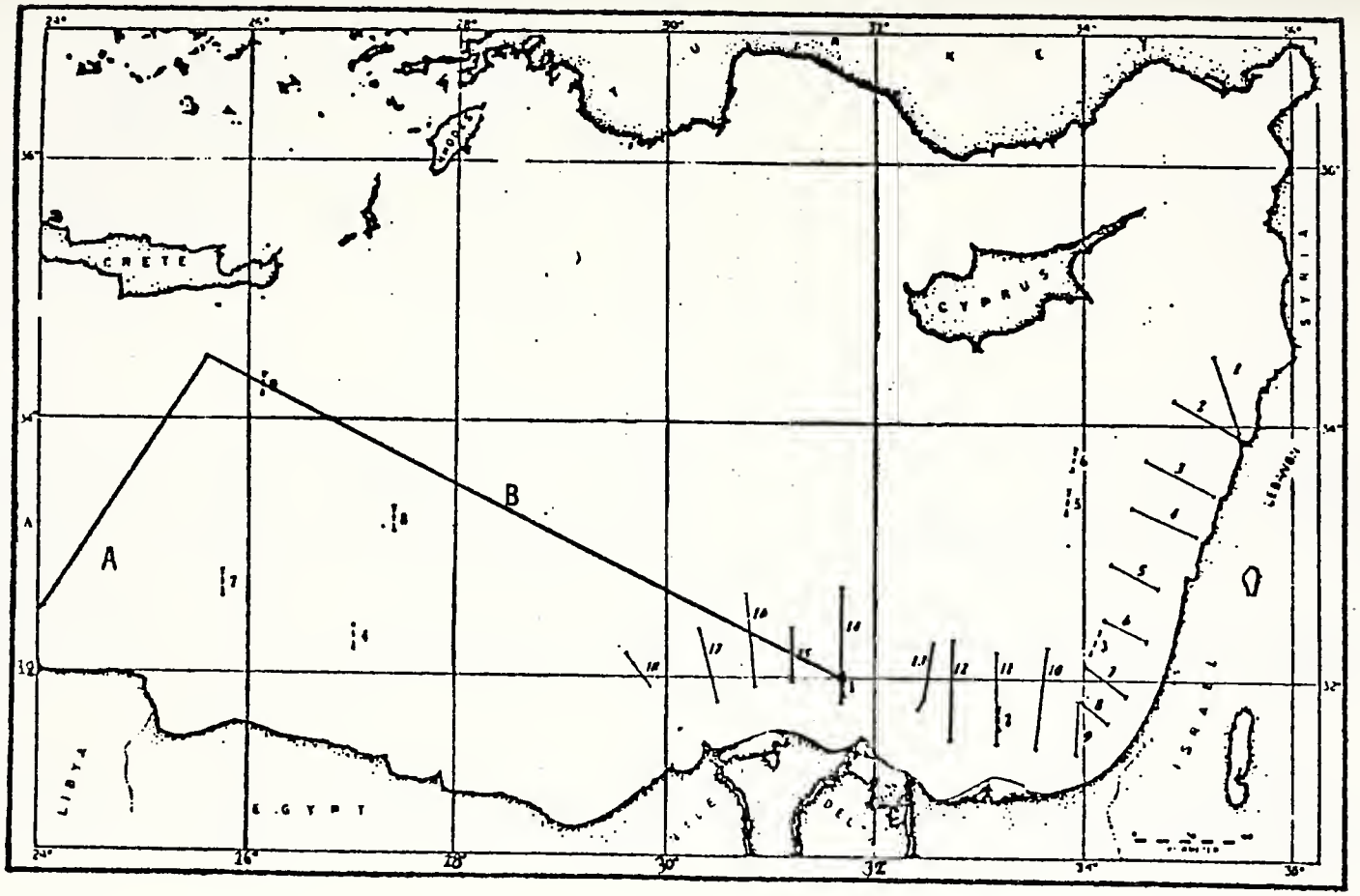

Figure 21. Locations of selected sounding profiles (Emery et al., 1966).

Leg A

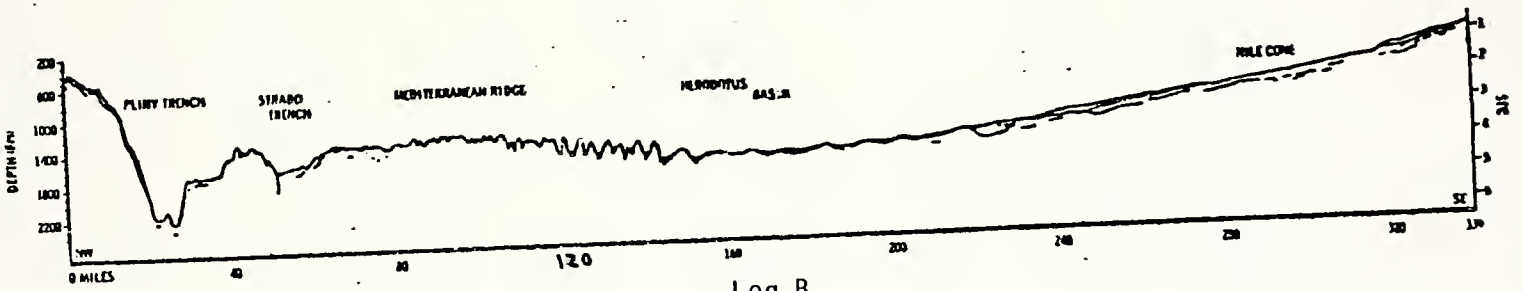

Leg B

Figure 22. Bottom topography of the two sections that are shown in Figure 21 (Engel, 1968).

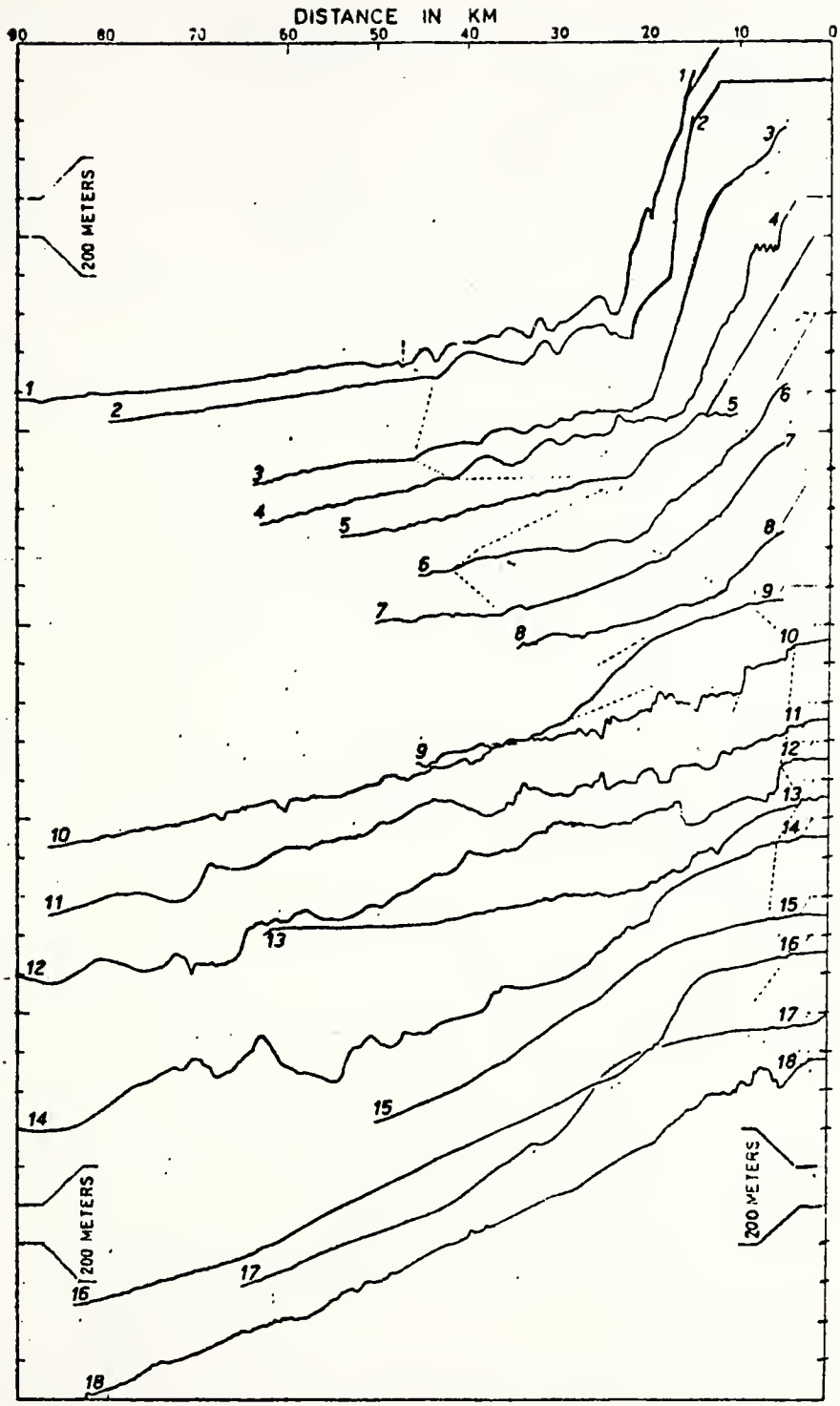

Figure 23. Profiles of the continental slope, rise, and Nile Cone. Location of each numbered profile is shown in Figure 21 (Emery et al., 1966).

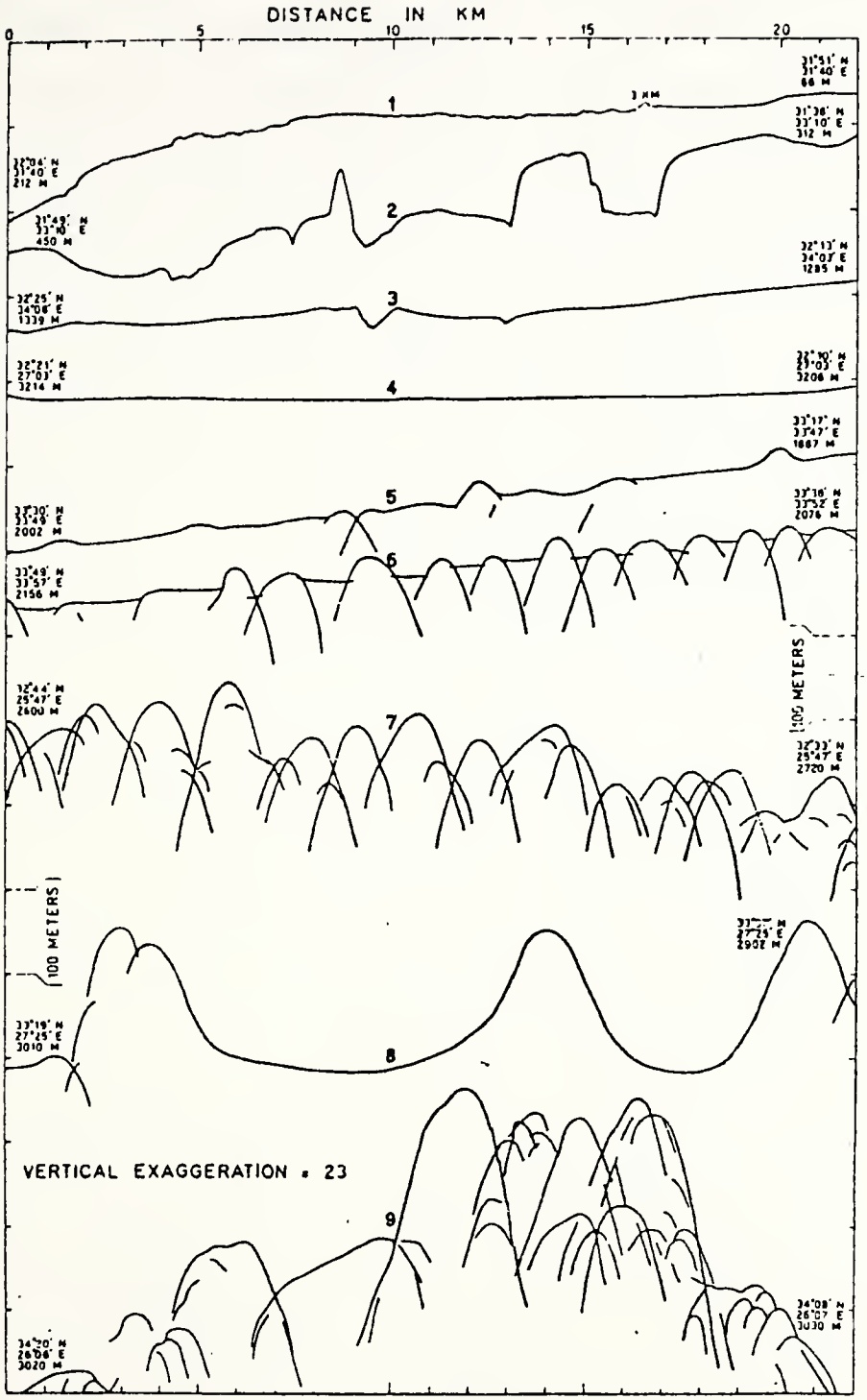

Figure 24. Characteristics of sounding profiles over various physiographic features (Emery et al., 1966).

B. AEGEAN PROVINCE, MOUNTAINS, AND ABYSSAL HILLS

The Aegean Province extends south from Greece and western Turkey past Crete to a southeastern boundary at the Pliny and Strabo trenches. The most characteristic feature is the presence of numerous small islands bounded at the south by Crete and Rhodes. Topography of the Aegean Province is determined by its tectonic and volcanic origin only slightly smoothed by subsequently deposited sediments (Emery, et al., 1966).

The Levantine Basin contains several mountainous areas. South of Crete there are the Ptolemy Mountains, the shallowest of which has a depth of 1000 m. Others include the Aleximander Mountains, Hecataeus Mountains, Eratosthenes Seamount, and Mela Mountain, all shown in Figure 20. The two most extensive mountain provinces are completely separated from each other by trenches. For example, Pliny Trench reaches depths of 3200 m.

C. MEDITERRANEAN RIDGE

A deep sea ridge termed the Mediterranean Ridge extends from southern Italy passing between Crete and Libya and curving sinuously northeastward to Cyprus. Cyprus and the shallow area northeast of the island may be considered as a shallow continuation of the ridge. The ridge is about 1600 km long and averages about 150 km wide. Both sides of the ridge are marked by slopes which have an average gradient of about 1:10 and a relief of 200-600 m. They descend onto an abyssal plain along the south side and into trenches along most of the north side. Crest depths from Crete to Cyprus vary from 2200 m to 2500 m. The greatest relief on the ridge occurs between Crete and Libya where it is flanked by Pliny and Strabo Trenches to the north and by the Herodotus Basin to the south.

The ridge resembles other mid-ocean ridges. Its sinuous course through the Eastern Mediterranean Sea places it almost equidistant between the

African and European shores (Emery et al., 1966). Most earthquake foci in the Levantine Sea lie on a belt along the axis of the ridge. Earthquakes are less frequent than in the Aegean Arc (Comninakis and Papazachos, 1972).

D. TRENCHES, ABYSSAL PLAINS, AND SUBMARINE CANYONS

The northwestern flank of the Mediterranean Ridge is bounded by two subparallel, northeast and southwest trending trenches within the area. The Pliny Trench, which divides and rejoins, surrounds the Ptolemy Mountains. Farther east the Mediterranean Ridge is bounded by Strabo Trench, the southern end of which cuts into the ridge. The northeastern end diverges from the ridge toward a small circular abyssal plain east of Rhodes.

The Rhodes Abyssal Plain contains the greatest depths in the Levantine Basin, about 4700 m. Figure 20 shows long and narrow Herodotus Abyssal Plain which separates the irregular topography of the Mediterranean Ridge from the smoother surface of the Nile Cone. It represents ponding of sediments from the Nile River against the medial ridge.

There are four submarine canyons in the Levantine Basin. They indent the shelf-break and extend down to at least 1000 m depth. The largest is Alexandria Canyon off the Egyptian coast. Gaza Canyon is named for the ancient still existing city near its head. A sounding line crosses its extension on the Domietta Fan as a leveed channel (see Figure 23, Profile 9). A third canyon lies just off the Israel-Lebanon boundary near the former Arab town of Akziv, for which it was named. Beirut Canyon, the fourth one, lies off the north coast of Syria.

V. SEDIMENTS

The Levantine Sea floor topography has been modified by deposition of sediments. The chief area of deposition is the Nile Cone. Sediments elsewhere beyond the continental slopes of the region are too thin to have greatly modified the topography, but they are nearly ten meters thick in most cores (Emery et al., 1966). Figure 26 shows the general stratigraphy of 32 sediment cores located as shown in Figure 25.

The distribution of sediment types is dependent upon the water depth and bottom morphology. In those areas with a broad shelf, coarse-grained sediments (sand) cover broad zones and are conspicuous on bottom sediment charts. These sediments are seldom found deeper than 50 to 100 m. Muds cover most of the continental slope and abyssal sea floor.

There are three general types of sediment in the Levantine Basin (Emelyanov, 1972):

1. Terrigenous sediments occur in the geosynclinal areas of the basin. Usually they are gray in color with a moisture content ranging from 24 to 81 percent. The Nile terrigenous sediments are generally quartz sands and pelitic muds. Muds occur in limited regions on the shelf and extend continuously over the continental slope and basin between the Nile Cone, Cyprus, and Syria. They are characterized by high water content, from 55 to 68 percent, and gray color (Emelyanov, 1972).

2. Biogenic sediments are widely distributed between Cyrenaica, Crete, and Alexandria. They are highly calcareous (50 to 69 percent $CaCO_3$), tough, viscous, and light brown in color.

3. Chemogenic sediments of calcareous composition (oolites) probably cover the south edge of the Levantine Sea (Emelyanov, 1972).

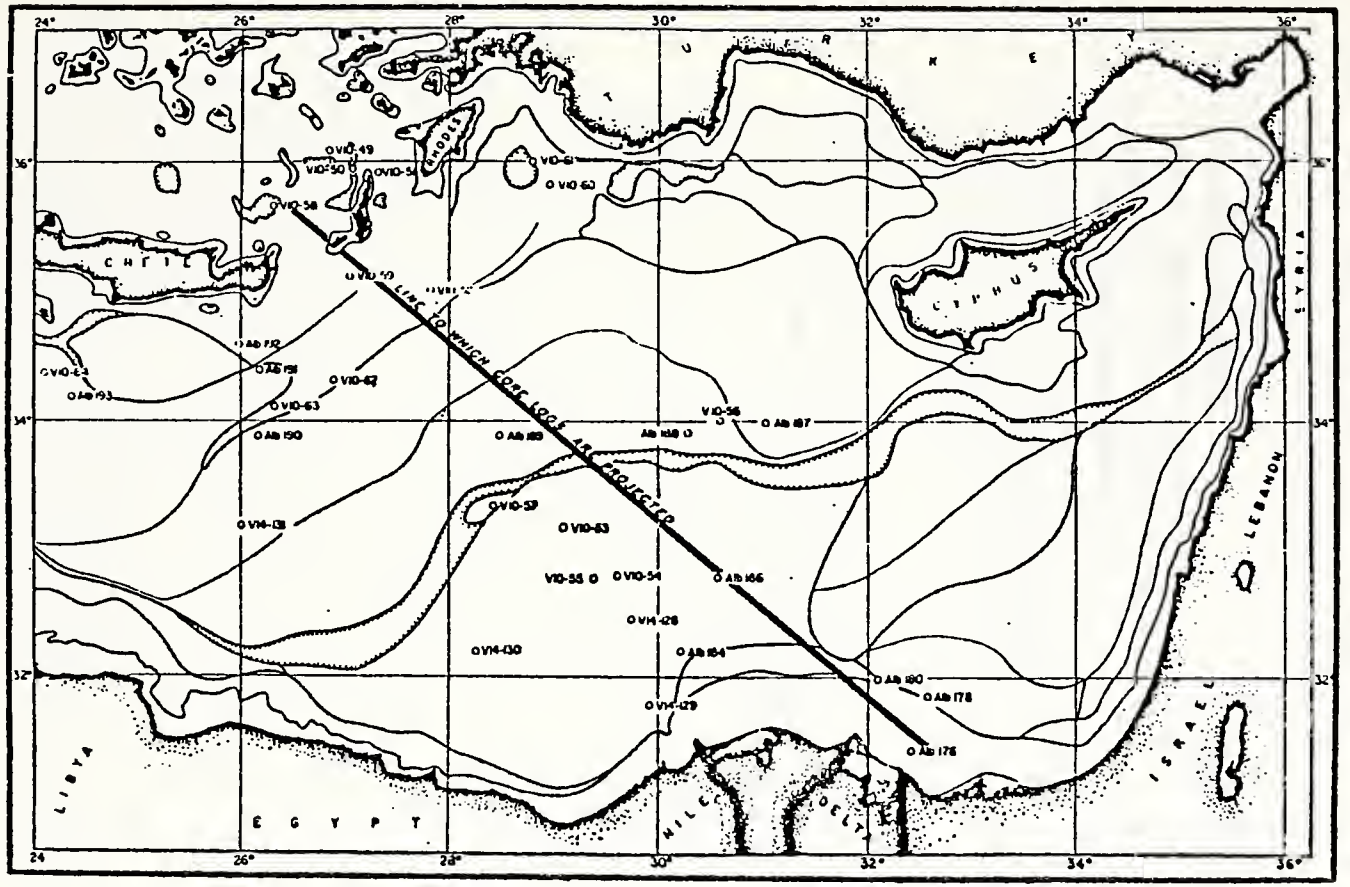

Figure 25. Locations of piston cores obtained in the eastern Mediterranean Sea (Emery et al., 1966).

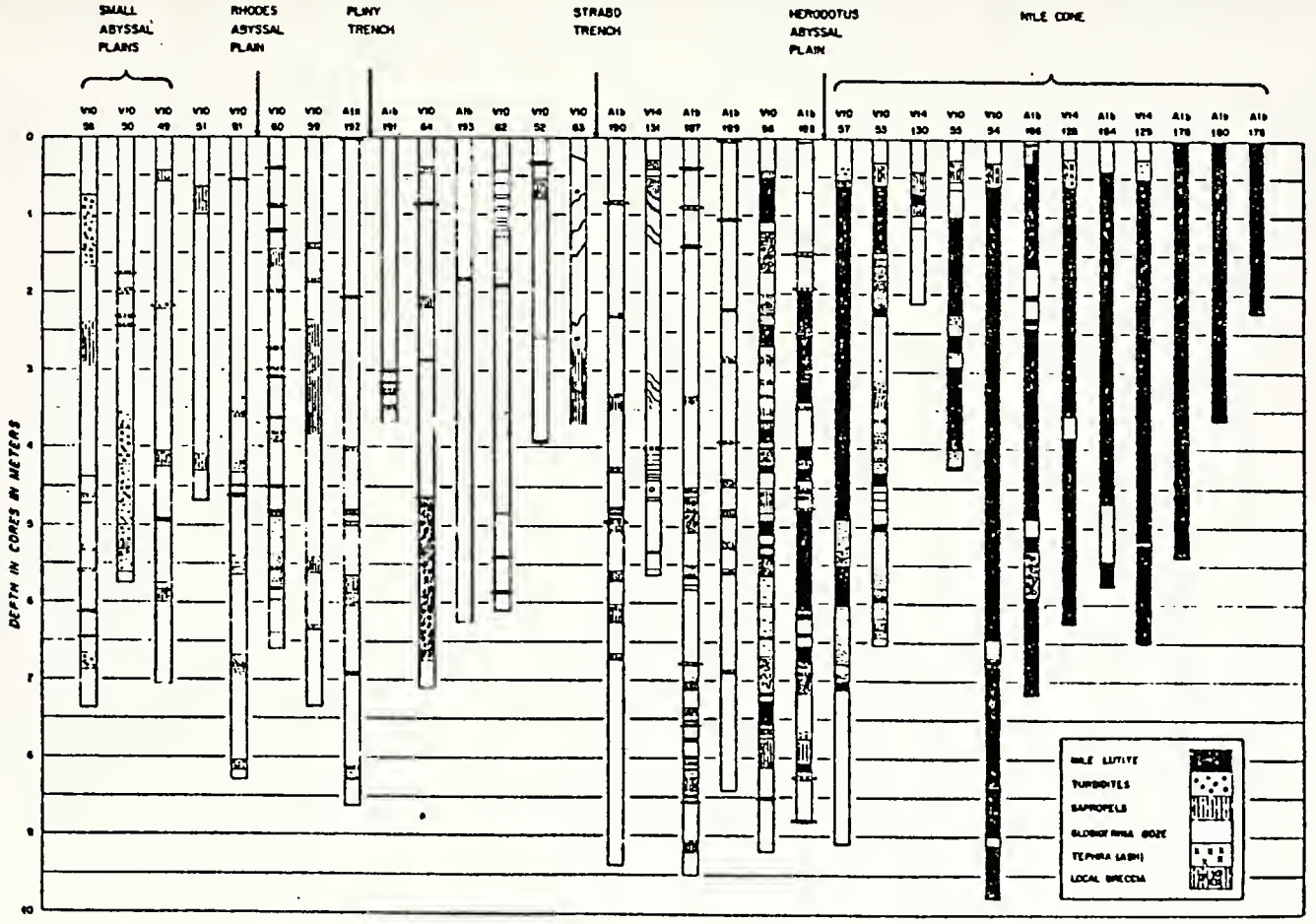

Figure 26. General stratigraphy of the 32 cores of Figure 25. The positions of the cores were projected to a line according to physiographic boundaries and depth contour (Emery et al., 1966).

The thickness of unconsolidated sediments may exceed one kilometer in some areas with sizeable local variations (Wong and Zarudzki, 1969). The thickest sections are found off the shores of Libya, Egypt, Israel, Lebanon, and Turkey.

The prevailing winds in the region are from the north, however, winds from the south and southwest do exist and are important in transporting sediments from the north African desert to some parts of the sea (Venkatarathnam and Ryan, 1971).

The main fresh-water sources for the Levantine Sea are the Nile River and the Black Sea. A major portion of the sediments carried into the Black Sea by rivers is trapped there. During periods of usually high rainfall, floods and local torrents along the rugged southern coast of Peloponnesus, Crete, and Turkey might locally contribute relatively important quantities of easily eroded surface soils.

There are four clay mineral assemblages in the Levantine Sea (Figure 27). The Nile assemblage containing very high amounts of smectite (more than 50 percent) and considerable amounts of kaolinite (15-25 percent) characterize the sediments of the eastern Levantine Basin. The second assemblage is found in the southeast Aegean Sea. Smectite is more abundant (40-60 percent) than other minerals but its concentration is not as high as in the area of Nile assemblage. Third, a relatively kaolinite-rich assemblage is present in the sediments of the Mediterranean Ridge south of Crete and its extension into the eastern Ionian Basin. Fourth, the Kithira assemblage with very high proportions of illite (50 percent) and 20-40 percent of smectite. Table III shows the total chemical composition of the upper sediment layer in the Levantine Sea.

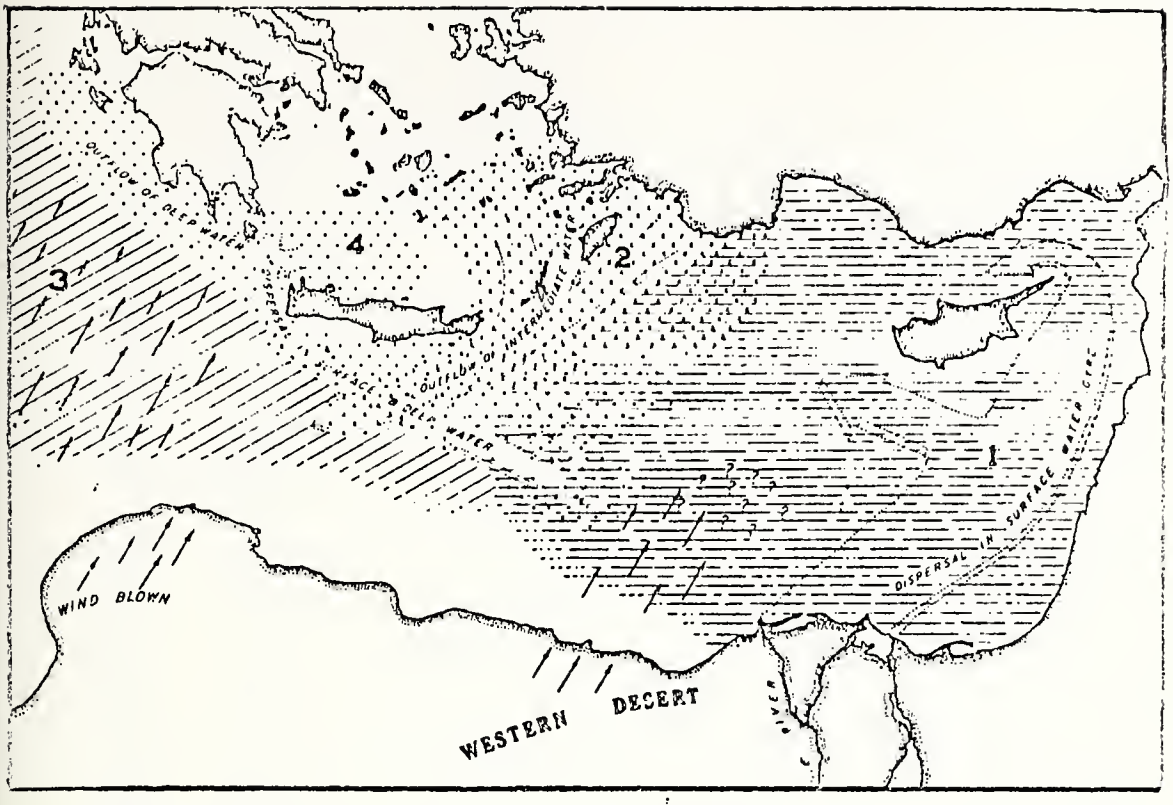

Figure 27. Distribution of the clay-mineral assemblages in the eastern Mediterranean Sea; 1=Nile assemblage; 2=southeast Aegean assemblage; 3=kaolinite-rich assemblage; 4=Kithira assemblage (Venkatarathnam and Ryan, 1971).

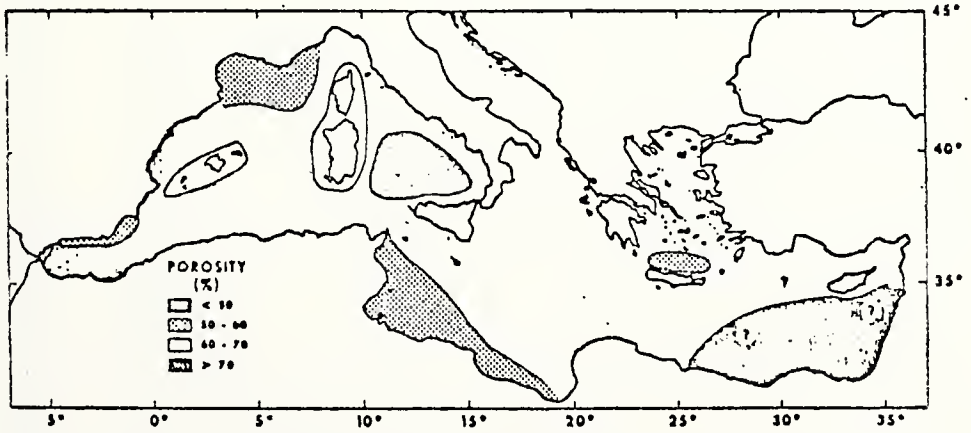

Figure 28. Porosity distribution in the Mediterranean Sea sediments (Keller and Lambert, 1972).

TABLE III

CHEMICAL COMPOSITION (IN PERCENT) OF THE UPPER SEDIMENT LAYER IN THE LEVANTINE SEA
(Emelyanov, 1972)

latitude	Longitude	Depth in m.	SiO_2	Al_2O_3	Fe_2O_3 total	TiO_2	MnO	P_2O_5	CaO	MgO	Na_2O	K_2O	Loss on ignition	Total	C_{org}	CO_2	$CaCO_3$
37 07'1	N-26 09'5 E	306	11.20	4.60	2.30	1.10	0.05	-	37.65	5.70	2.12		36.2	100.9	0.7	30.0	68.2
36 32'2	N-26 48'6 E	587	27.42	9.31	4.04	1.00	0.09	0.08	24.10	4.35	1.85	1.41	26.3	100.1	0.4	19.5	44.3
35 22'0	N-27 17'5 E	1231	30.12	10.41	5.34	0.60	0.05	0.14	23.65	1.80	1.42	1.18	25.0	99.7	0.9	15.1	34.3
36 10'3	N-28 20'4 E	2771	33.00	8.98	6.42	1.00	0.06	-	17.70	7.70	3.00	3.00	22.9	100.7	1.0	11.1	25.4
34 28'8	N-28 43'2 E	2351	18.60	7.31	3.69	trace	0.06	0.09	31.00	3.26	1.96	1.03	33.2	100.2	0.5	24.9	56.6
34 39'4	N-31 58'5 E	2295	26.80	9.02	5.08	1.00	-	0.09	24.20	3.45	1.87	0.98	27.1	99.4	0.4	24.0	54.6
36 11'0	N-31 59'3 E	2203	36.12	10.50	6.70	0.60	0.08	-	19.00	3.90	1.99	1.79	20.6	101.2	1.2	10.5	23.9
36 00'0	N-32 31'2 E	1063	33.60	12.14	5.86	0.80	0.04	-	19.00	4.26	2.92	2.92	22.2	101.0	0.4	19.5	44.3
34 54'4	N-34 26'6 E	820	27.34	10.56	5.94	0.50	0.15	-	23.90	3.20	1.91	1.10	26.2	100.8	1.2	10.5	23.9
35 47'8	N-34 55'4 E	698	29.86	10.69	6.81	0.50	0.06	0.12	21.30	4.05	1.97	1.13	25.0	101.5	0.5	15.8	35.9
35 57'0	N-35 04'8 E	1150	12.18	4.11	2.04	0.60	-	-	36.90	5.73	2.80	2.80	36.0	100.5	-	-	-
36 13'7	N-35 33'8 E	175	28.48	10.99	6.04	0.60	0.04	0.10	20.90	5.40	2.00	1.17	25.0	100.7	0.6	16.2	36.8

Porosity of the Levantine Basin sediments is shown in Figure 28. The relatively low porosities found north of Crete are associated with fine-grained ash and pumice deposits. Highest porosities are associated with the lutites of the Nile-contributed sediments.

VI. CORRELATION BETWEEN SOUND VELOCITY AND OTHER PHYSICAL PROPERTIES OF THE BOTTOM SEDIMENTS

Low frequency propagation models employ the environmental parameters of both the water column and the ocean bottom. The sea bottom is a reflecting and scattering boundary of the sea having some characteristics similar to the sea surface. Sound velocity in the Mediterranean Sea sediments has been intensively examined and is reviewed here. Relevant physical properties of marine sediments include grain size, porosity, void ratio, and moisture content.

Sound velocity is positively correlated to the mean grain size as shown in Figure 29. There is an over-all increase in sound velocity as the skewness values change from negative to positive. In fine-grained sediments, if coarse mud is dominant and clay is secondary, the size distribution is negatively skewed (Horn, Horn, and Delach, 1968).

Porosity is defined by $n = \frac{V_v}{V}$, and void ratio by $e = \frac{V_v}{V_s}$, where

n = porosity

e = void ratio

V_v = volume of voids

V = volume of total mass, including solids, water, and air

V_s = volume of the solids

A study of 14 Mediterranean Sea cores by Horn et al.(1968) correlated sound speed with measurable physical sediment properties (Figures 29-34). Porosity is the prime factor affecting compressional sound velocity in the unconsolidated sediments (Figure 30). The sound velocity was found to increase as sediment porosity decreases; the highest sound velocity

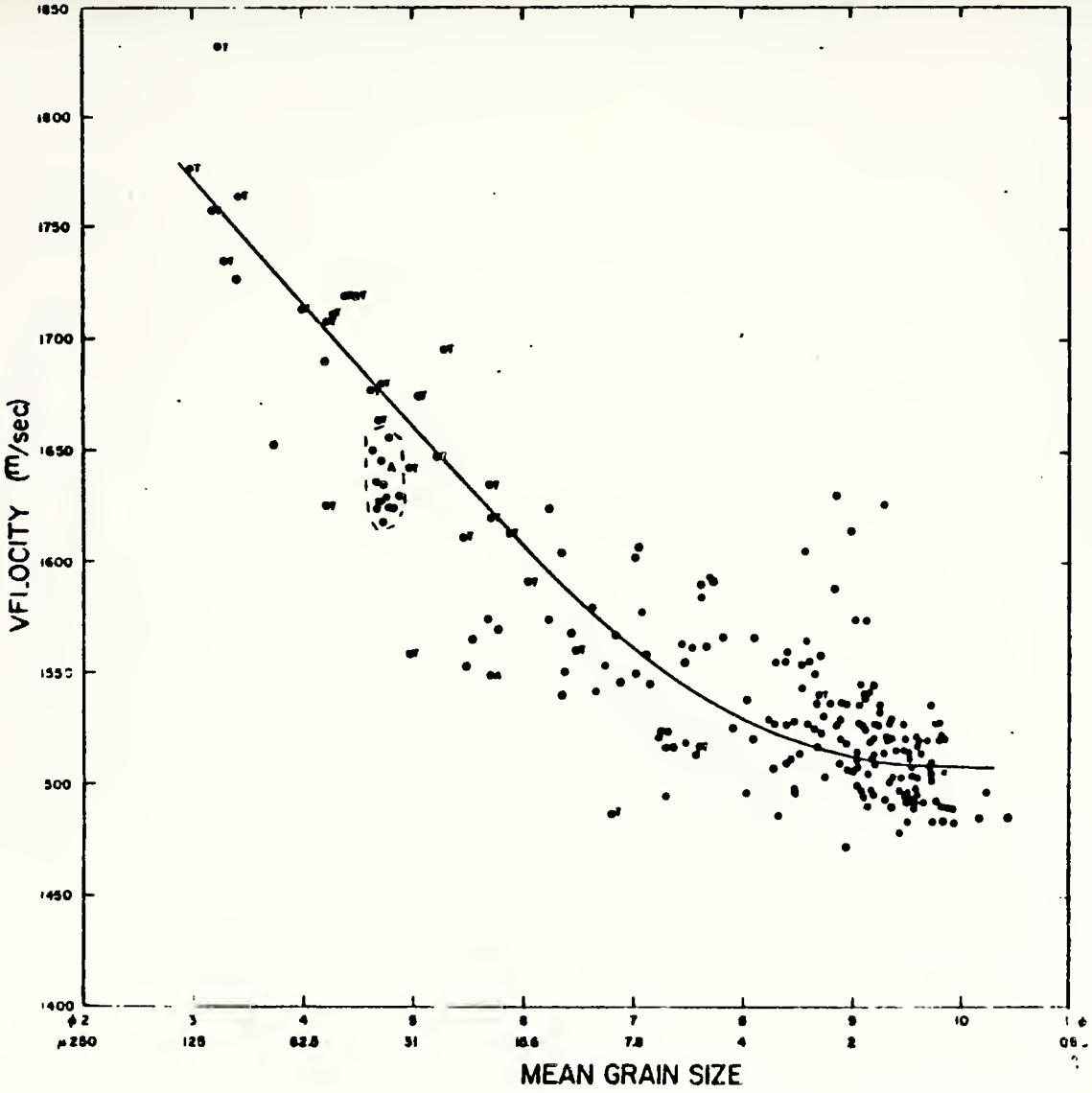

Figure 29. Relationship between mean grain size and sound velocity (Horn et al., 1968).

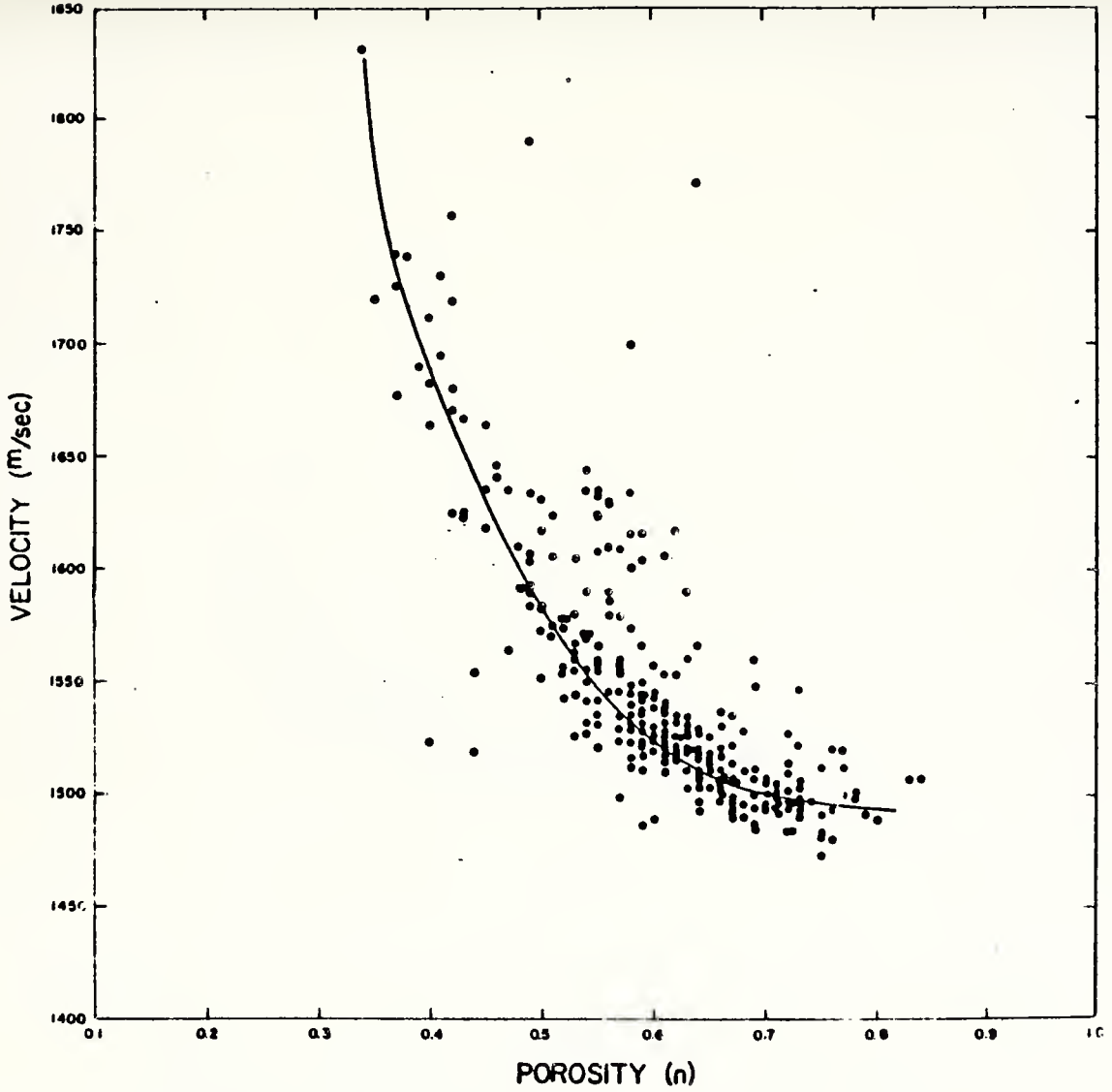

Figure 30. Relationship between porosity and sound velocity (Horn et al., 1968).

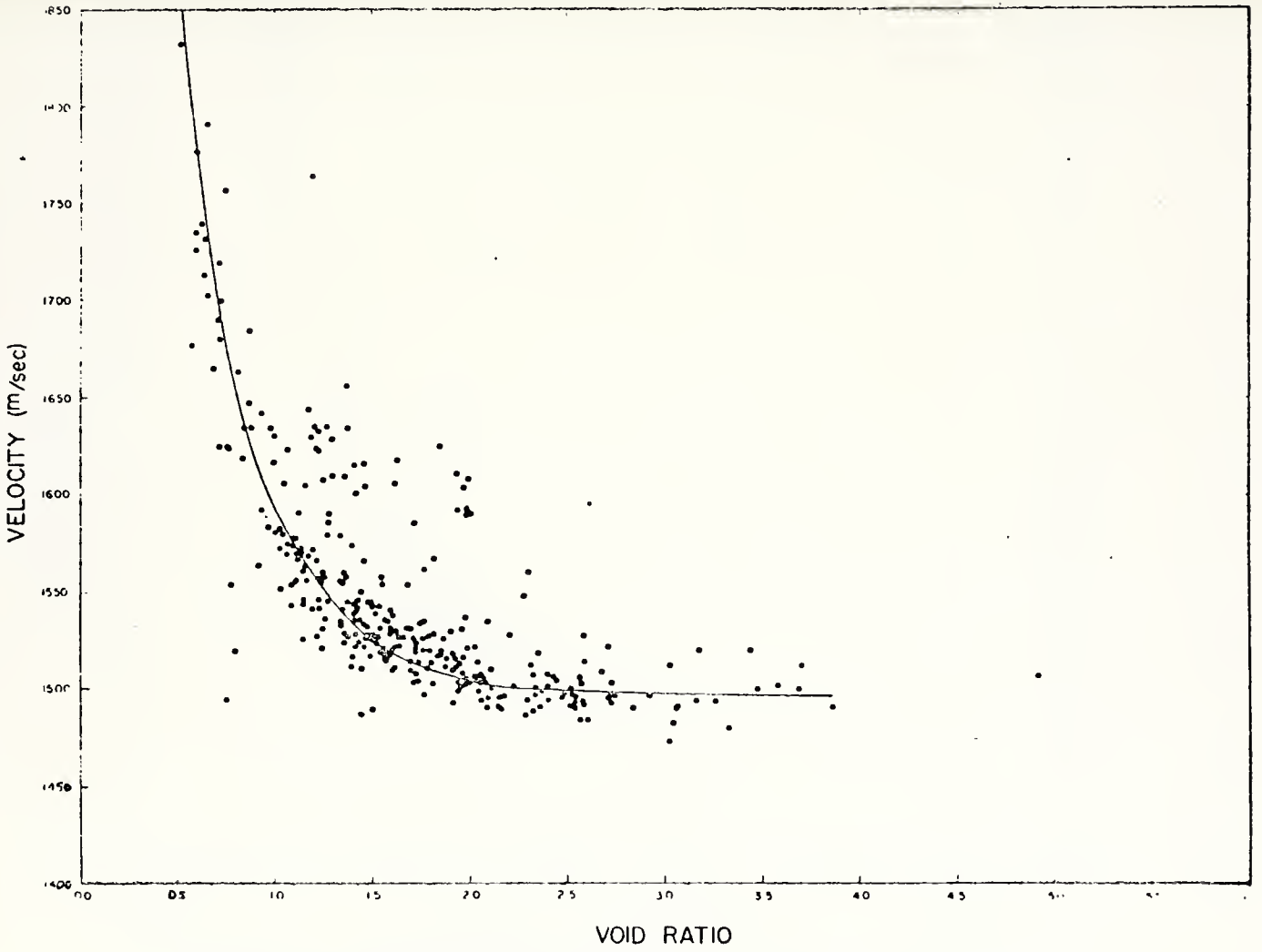

Figure 31. Relationship between void ratio and sound velocity (Horn et al., 1968).

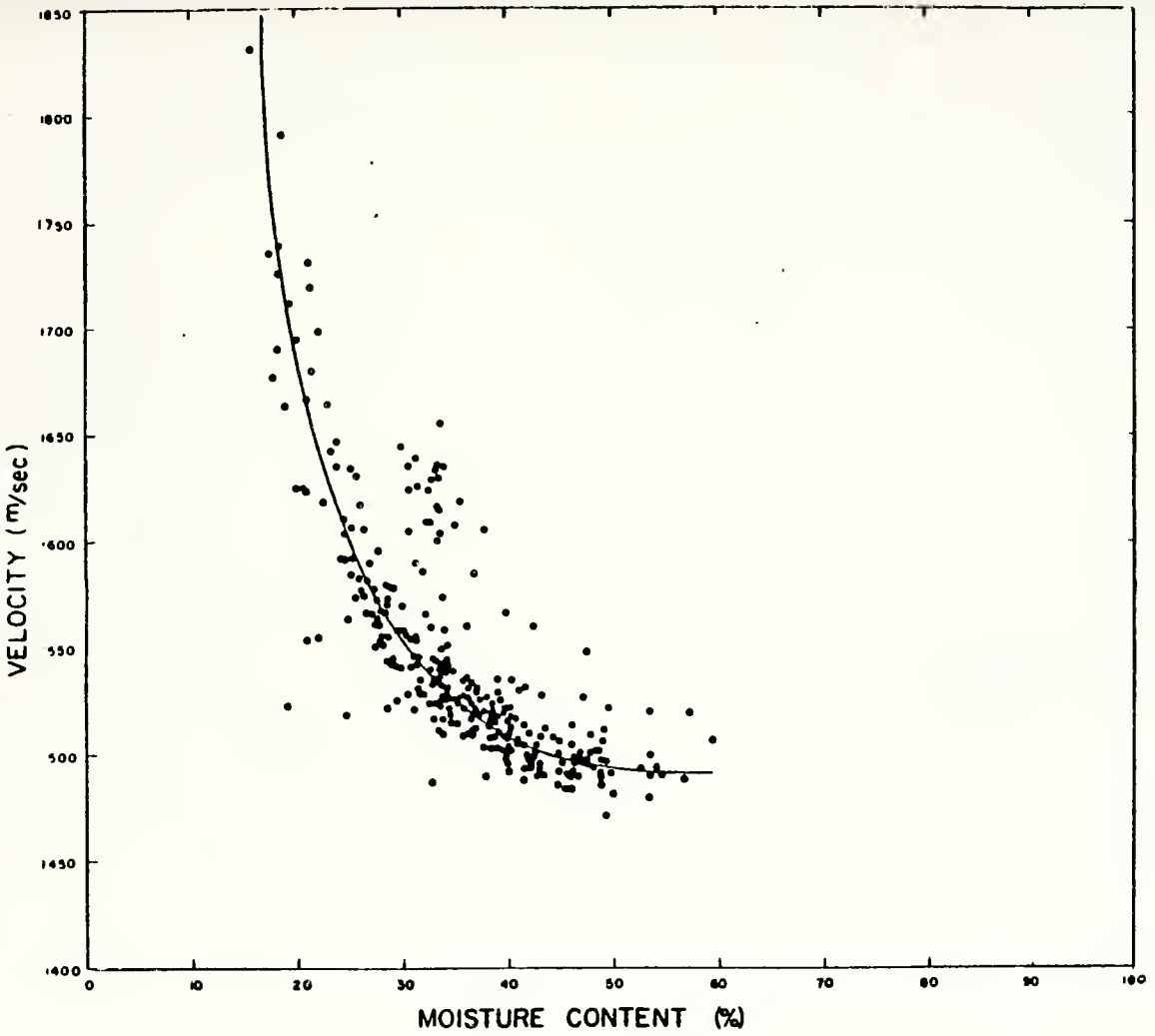

Figure 32. Relationship between moisture content and sound velocity (Horn et al., 1968).

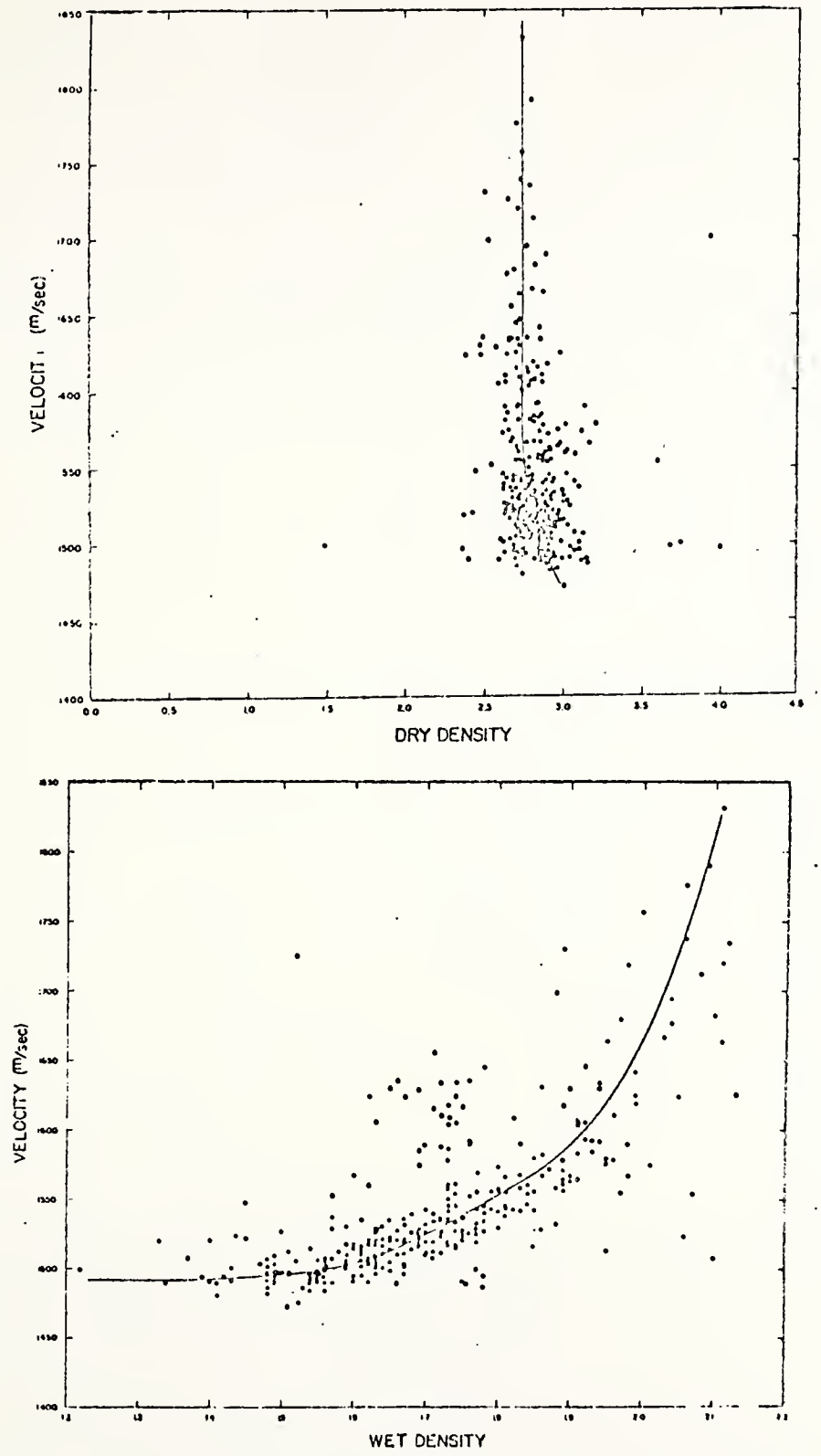

Figure 33. Relationship between density and sound velocity (Horn et al., 1968).

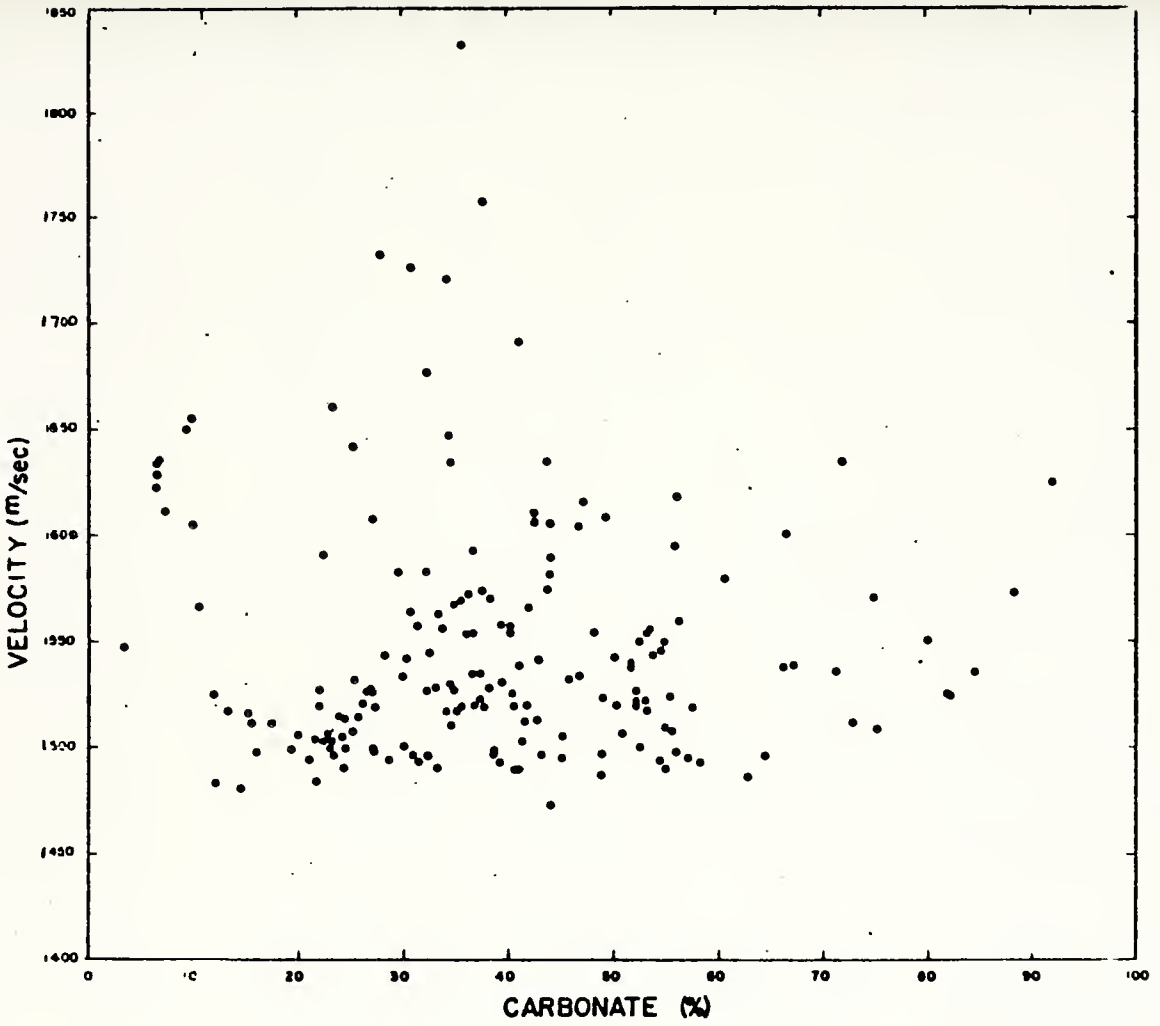

Figure 34. Relationship between carbonate content and sound velocity (Horn et al., 1968).

(1832 m/s) was in a layer of fine-grained sand that had a porosity of 0.34. Void ratio and moisture content are also inversely proportional to sound velocity. Figures 31 and 32 show these relationships. The highest velocity of 1832 m/s coincided with a moisture content of 16 percent.

Density and sound velocity are directly proportional (see Figure 33). The lowest sound velocity, 1478 m/s, was in a sandy mud with a wet density of 1.44 grams/cubic centimeter. Since this approaches the sound velocity of the adjacent sea water much of the impinging energy would penetrate the bottom rather than being reflected back into the water column.

The highest velocity 1753 m/s in coarse sand occurred in a sample having a wet density of 2.08 gm/cm^3. The sediments tested from the Mediterranean Sea had wet densities that range from 1.22 to 2.14 gm/cm^3. Little relationship was found between carbonate content and sound velocity (Figure 34).

Urick (1967, page 130) shows the relation between porosity and bottom reflection loss. The data presented by Horn et al. (1968) shows that the sampled areas of the Levantine Sea represent a nearly mean value of bottom loss. On this basis a bottom type of four out of nine was selected for acoustic modelling purposes. A value of eight was chosen for Location A due to the irregular bathymetry of that area.

VII. SOUND PROPAGATION FOR ANTISUBMARINE WARFARE

Four specific sites (see Figure 1) were chosen for computing the acoustical transmission loss (TL) for the Levantine Sea, as follows

Site	Latitude	Longitude
A	35^{o} 00'N	23^{o} 10'E
B	33^{o} 00'N	27^{o} 00'E
C	35^{o} 00'N	31^{o} 00'E
D	34^{o} 00'N	34^{o} 00'E

The Integrated Carrier Acoustic Prediction System (ICAPS), for passive sonar, was used to calculate TL. Inputs to ICAPS consisted of BT data from Fleet Numerical Weather Central's hydroclimatology file, wave height from atlas data (Oceanographic Atlas of the North Atlantic Ocean, 1963), source and receiver depths, acoustic frequency, bottom depth, and bottom-loss type.

A target depth of 50 feet was assumed for a submarine at periscope depth, and a receiver (sonar) depth of 21 feet was taken to simulate a surface ship hull-mounted sonar. At Location C additional target and receiver depth combinations were examined in order to simulate variable depth sonar and submarine sonar. BT data were selected from February, July, November, and December for all four sites to show seasonal effects; BT data for all months of the year are tabulated in Appendix B. All TL curves are shown in Appendix A. In order to cover a broad frequency range and simulate a submarine source, 50 Hz, 300 Hz, 850 Hz, and 5000 Hz frequencies were chosen.

Location A is the deepest of the four locations. Figures 35-42 and Table IV show the sound propagation and TL properties at the Location A for the four different months. The 50 Hz frequency showed no convergence zone (CZ) at any time of year. The higher frequencies demonstrate CZ propagation. Maximum CZ range occurs in summer.

Location B has TL characteristics similar to that of Location A. Figures 43-50 and Table V show the sound propagation and TL properties at the Location B for the four different months. The 50 Hz frequency does not show a CZ. The 5000 Hz transmission has the maximum TL. The 300 Hz and 850 Hz TL patterns are parallel and have the same CZ range. Maximum CZ range occurs in summer.

Location C sound propagation and TL properties are shown in Figures 51-82 and Tables VI-X. The longest CZR of 58 kyds appears for 300 Hz and 850 Hz in summer. The 50 Hz frequency showed no CZ again except in November and 5000 Hz has the longest TL. In February, various target-sonar depth combinations demonstrate only minimal differences in propagation loss and CZ range. In July and December, the deeper combinations show shorter CZ range and TL is a minimum for the sonar and target at the same depth. The advantage of locating the hydrophone at target depth is a reduction of TL of about 5-10 Hz. In November using 100 ft as the sonar depth the possibility of detection of a submarine near the surface is high with low TL in low frequencies. Using deep sonar, then, the possibility of detection of a submarine in deeper water increases.

Location D shows a CZ for 50 Hz propagation in July and November, as may be seen in Figures 83-90 and Table XI. But TL is also high at both times. The 300 Hz and 850 Hz frequencies show longer ranges to CZ than the other points. Once again, seasonal variation in CZ range is significant.

Sound propagation conditions, as mostly dependent on the temperature changes, show unique differences between winter and summer. Maximum sound velocity occurs simultaneously with maximum surface temperature in August. The Levantine Sea has the highest sound velocity in the Mediterranean Sea. According to Urick (1967), a shallow summertime channel exists in the Mediterranean Sea. However, in the Levantine Sea this "summertime channel" lasts from spring to fall. It is most intense in summer.

Reflection from the ocean bottom can extend propagation ranges; this is known as bottom-bounce. Major factors affecting bottom-bounce transmission include water depth, angle of incidence, frequency, bottom composition, and bottom roughness. A flat bottom allows maximum accuracy in estimating range. Because of the rough topography and generally shallow depths, bottom-bounce path prediction in the Levantine Sea is difficult. The sediments consist of mud in the deeper portions of the sea. In the coastal areas sediment composition is either a mixture of mud-sand-rock or mud-rock. They are all poor reflectors. Therefore bottom-bounce propagation is expected to be weak. Duct propagation in the surface layer is limited in winter, because the mixed layer depth in the Levantine Sea is very shallow.

TABLE IV. Convergence Zone Range and Transmission Loss values for Location A in specific months (CZR is in kyds and TL is in dB).

Frequency	February		July		November		December	
	CZR	TL	CZR	TL	CZR	TL	CZR	TL
50 Hz	-	90(Ave.)	-	95(Ave.)	-	97(Ave.)	-	85(Ave.)
300 Hz	26 52 77	72.3 85.9 80.9	43 85	72.9 80.3	38 75	73.5 78.8	34 67	72.9 78.9
850 Hz	26 51 76	72.7 77.8 84.3	42 83	72.1 76.3	37 74	70.2 77.6	34	71.7
5000 Hz	25	78.9	41	78.6	37	83.5	-	Duct

TABLE V. Convergence Zone Range and Transmission Loss values for Location B in specific months.

Frequency	February		July		November		December	
	CZR	TL	CZR	TL	CZR	TL	CZR	TL
50 Hz	-	92(Ave.)	-	90(Ave.)	-	85(Ave.)	-	90 (Ave.)
300 Hz	32 64 96	71.7 77.1 79.6	42 84	77.5 86.6	39 78	71.2 76.9	36 72	70.9 76.6
850 Hz	32 64 96	68.9 75.2 79.2	42 85	69.3 77.8	39 78	70.9 77.9	36 72	72.2 78.3
5000 Hz	32	83.6	42	77.4	39	85.5	36	85.3

TABLE VI. Convergence Zone Range and Transmission Loss values for Location C in specified months.

Frequency	February		July		November		December	
	CZR	TL	CZR	TL	CZR	TL	CZR	TL
50 Hz	-	90(Ave.)	-	92(Ave.)	43	72.8	-	85(Ave.)
300 Hz	30 61	72.5 77.2	58	75.8	41 82	71.4 75.5	36 72	71.6 78.2
850 Hz	30 60	69.4 76.2	58	76.8	41 81	72.3 78.5	36 71	72 76.2
5000 Hz	30	82.7	44	92.4	41	83.2	-	Duct

TABLE VII. February Convergence Zone Range and Transmission Loss at Location C for various source depths (TD) and receiver depths (SD).

Frequency	TD: 50 ft SD: 100 ft		TD: 100 ft SD: 100 ft		TD: 300 ft SD: 100 ft		TD: 50 ft SD: 300 ft		TD: 100 ft SD: 300 ft		TD: 300 ft SD: 300 ft	
	CZR	TL	CZR	TL	CZR	TL	CZR	TL	CZR	TL	CZR	TL
50 Hz	-	85(Ave.)	-	80(Ave.)	-	82(Ave.)	-	85(Ave.)	-	80(Ave.)	-	80(Ave.)
300 Hz	30 60	71.0 76.9	30 59	72.9 76.7	29	75.2	32 63	71.9 76.6	32 62	73.9 79.5	31 61	73.7 78.5
850 Hz	30 60	75.4 78.2	29 59	71.1 79.2	28	73.6	32	74.3	28	73.6	27 57	75.7 82.5
5000 Hz	30	84.3	29	82.3	28	84.1	28	83.6	28	84.1	30	80.6

TABLE VIII. July Convergence Zone Range and Transmission Loss at Location C for various source depths (TD) and receiver depths (SD).

Frequency	TD: 50 ft SD: 100 ft		TD: 100 ft SD: 100 ft		TD: 300 ft SD: 100 ft		TD: 50 ft SD: 300 ft		TD: 100 ft SD: 300 ft		TD: 300 ft SD: 300 ft	
	CZR	TL	CZR	TL	CZR	TL	CZR	TL	CZR	TL	CZR	TL
50 Hz	-	85(Ave.)	-	80(Ave.)	-	81(Ave.)	-	88(Ave.)	-	81(Ave.)	-	80(Ave.)
300 Hz	43 57	79.5 75.7	37 55	70.4 78.1	40	77.2	57	76.7	-	-	33 65	69.7 74.5
850 Hz	43	81.1	37	70.1	-	-	57	80.4	-	-	32 64	70.3 75.4
5000 Hz	43	93.9	36	78.3	35	87.5	42	96.2	35	87.5	32	74.3

TABLE IX. November Convergence Zone Range and Transmission Loss at Location C for various source depths (TD) and receiver depths (SD).

Frequency	TD: 50 ft SD: 100 ft		TD: 100 ft SD: 100 ft		TD: 300 ft SD: 100 ft		TD: 50 ft SD: 300 ft		TD: 100 ft SD: 300 ft		TD: 300 ft SD: 300 ft	
	CZR	TL	CZR	TL	CZR	TL	CZR	TL	CZR	TL	CZR	TL
50 Hz	43	72.9	42	73.6	-	80(Ave.)	-	82(Ave.)	-	80(Ave.)	33	72.2
300 Hz	41 82	72.4 77.0	41	72.9	42	78.2	42	77.9	42	78.2	31 62	69.6 74.7
850 Hz	41 82	74.1 80.5	41	74	40	79.8	42	78.7	40	79.8	30 62	70.9 74.8
5000 Hz	41	86.6	39	86.4	43	93.4	39	93.3	43	93.4	31	78.8

TABLE X. December Convergence Zone Range and Transmission Loss at Location C for various source depth (TD) and receiver depths (SD).

Frequency	TD: 50 ft SD: 100 ft		TD: 100 ft SD: 100 ft		TD: 300 ft SD: 100 ft		TD: 50 ft SD: 300 ft		TD: 100 ft SD: 300 ft		TD: 300 ft SD: 300 ft	
	CZR	TL	CZR	TL	CZR	TL	CZR	TL	CZR	TL	CZR	TL
50 Hz	-	81(Ave.)	-	80(Ave.)	-	81(Ave.)	-	81(Ave.)	-	80(Ave.)	32	73.9
300 Hz	35 71	69.6 74.3	35 71	68.0 72.7	37 70	74.9 80.1	37 73	73.2 78.0	37 70	74.9 80.1	31 62	70.3 74.4
850 Hz	35 71	70.3 79.7	35 70	71.4 78.1	33 72	77.5 79.9	37 73	75.0 83.3	33 72	77.5 79.9	31 61	68.6 75.1
5000 Hz	35	82.9	35	83.9	33	82.8	34	89.3	33	82.8	30	78.3

TABLE XI. Convergence Zone Range and Transmission Loss for Location D in specified months.

Frequency	February		July		November		December	
	CZR	TL	CZR	TL	CZR	TL	CZR	TL
50 Hz	-	95 (Ave.)	-	92 (Ave.)	-	90(Ave.)	-	90(Ave.)
300 Hz	31 61 92	71.7 77.2 80.0	47 94	77.7 78.6	45	81.4	37 74.	7.17 77.2
850 Hz	30 61 91	73.5 76.5 81.1	47 94	70.6 76.3	45	77	37 74	71.9 78.8
5000 Hz	30	80.0	46	82.1	42	92.1	37	85.7

VIII. CONCLUSION

Sound propagation patterns are created by sound speed gradients. Sound rays propagate away from any layer that has a sound velocity maxima. In the upper layers of the Levantine Sea, heating by the sun together with the absence of the surface mixing by the wind, creates a sound channel. This channel occurs all year long except in winter when the isothermal water and a positive velocity gradient extend throughout the water column from bottom to surface. The sound channel becomes stronger in summer, with a maximum sound channel axis depth of 1000 m in August, and weaker in spring and fall. When the sound channel is strong, a near-surface negative gradient and resulting downward refraction greatly limit the surface duct range of ship sonars. Long ranges then become possible via the CZ path. In a weak mixed layer, high frequencies are ducted in the surface layer. Low frequencies leak from the surface layer and propagate along other paths.

Seasonal temperature variation affects only the upper 125-150 m (surface layer) of water. The rest of the water column has nearly the same temperature all year long. At the surface, maximum and minimum temperatures occur during the months of August and February. The sea surface temperature difference between these two months is 9-10 ^{o}C. Seasonal salinity changes are small; therefore the sound speed profile is mainly influenced by the temperature in the upper layers. Temperature changes cause a 25-30 m/sec sound velocity variation in the surface layer.

Bottom reflectivity depends on the bathymetry and the composition of the bottom sediments. Rough topography and mud sized sediment causes poor reflectivity in the basin.

Finally, in one-way sound propagation, high frequencies have the highest TL as usual. The lowest transmission losses occur for the 300 and 850 Hz signals. Optimum passive detection of submarine targets was found to occur when source and receiver were at the same depth. This could be achieved with the sonar either on a submarine or lowered below a surface ship.

APPENDIX A

SOUND VELOCITY AND TRANSMISSION LOSS CURVES

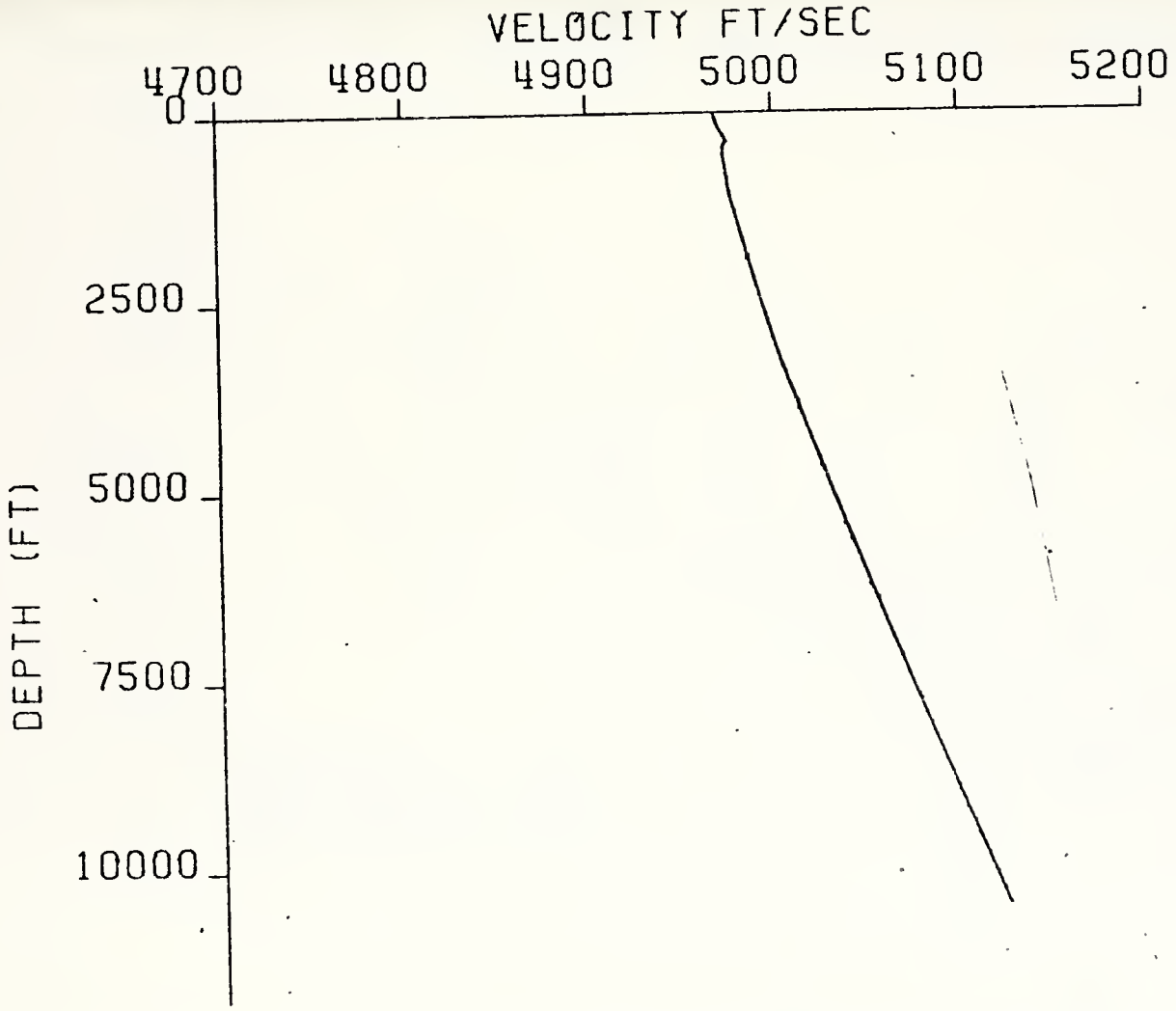

Figure 35. Sound velocity profile at point A in February.

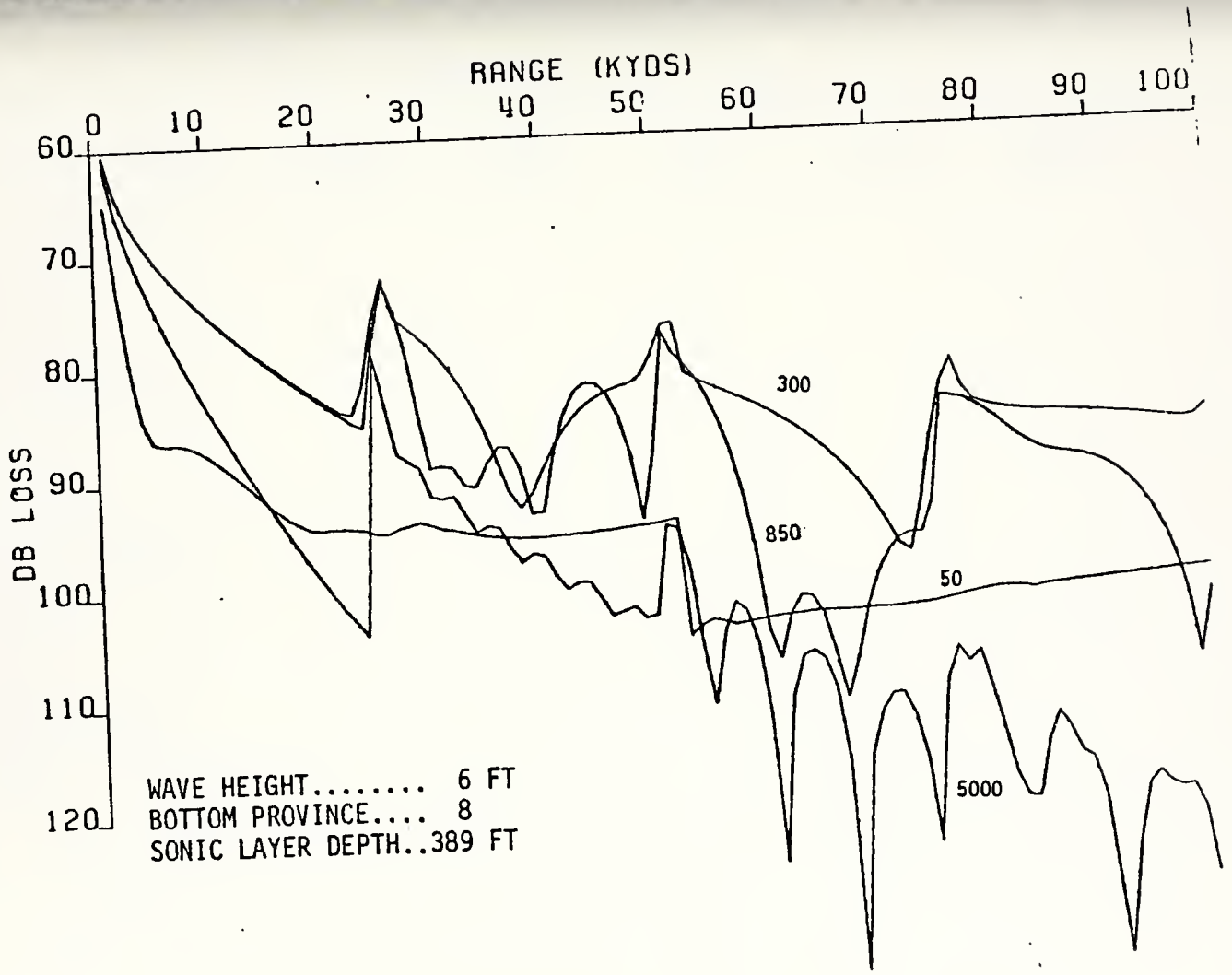

Figure 36. Transmission loss at point A in February. Curves labelled with frequency (Hz).

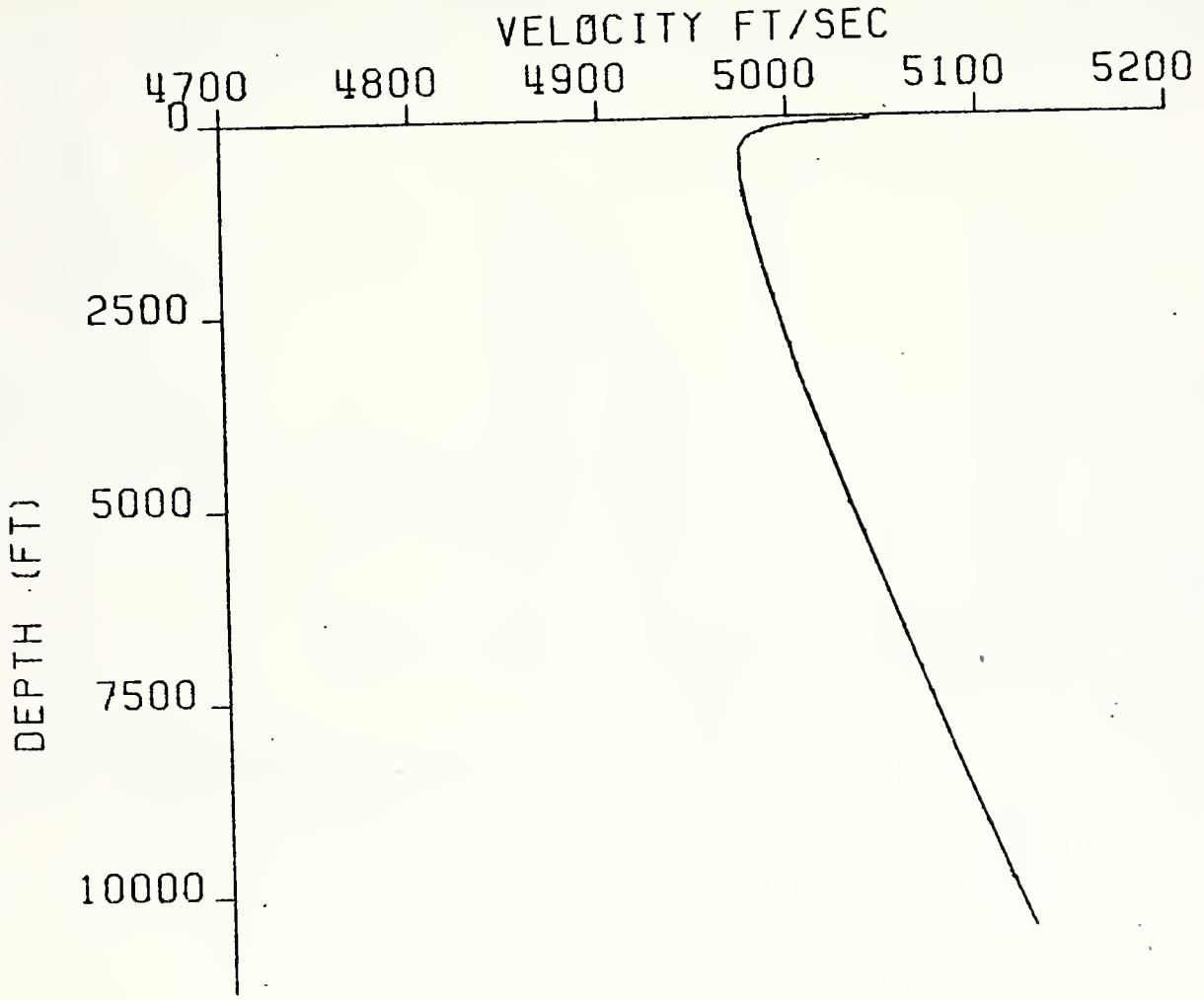

Figure 37. Sound velocity profile at point A in July.

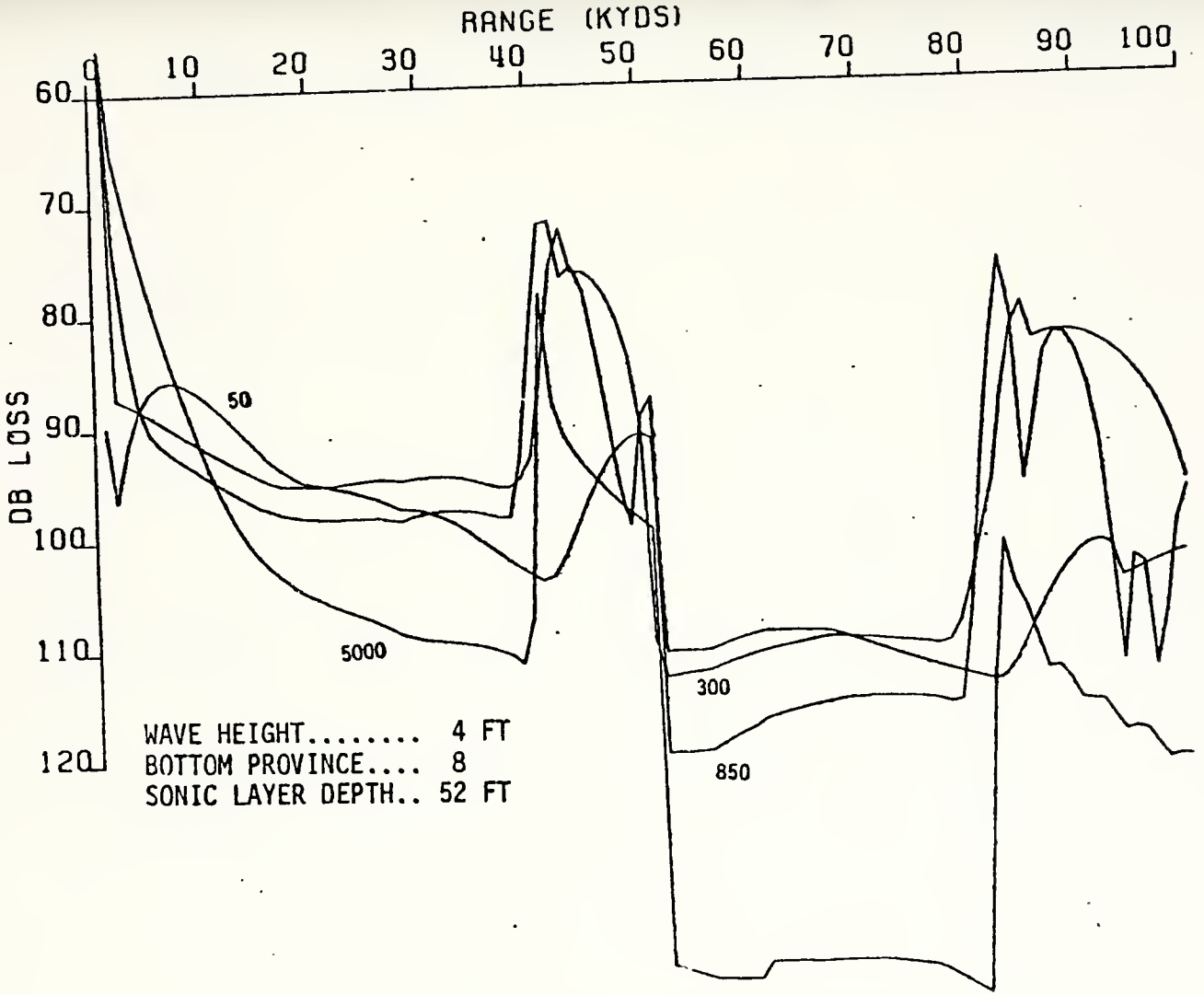

Figure 38. Transmission loss at point A in July.

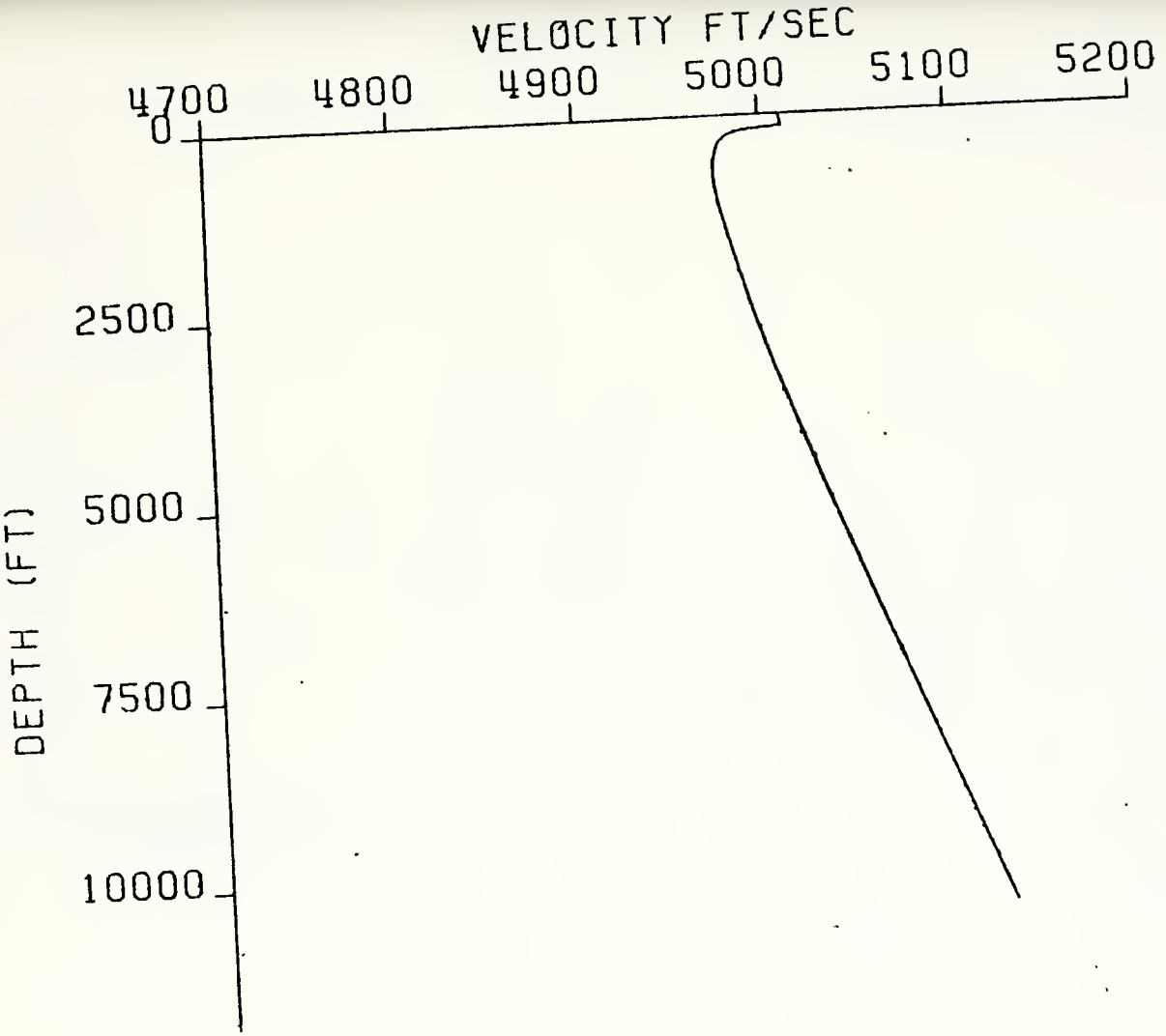

Figure 39. Sound velocity profile at point A in November.

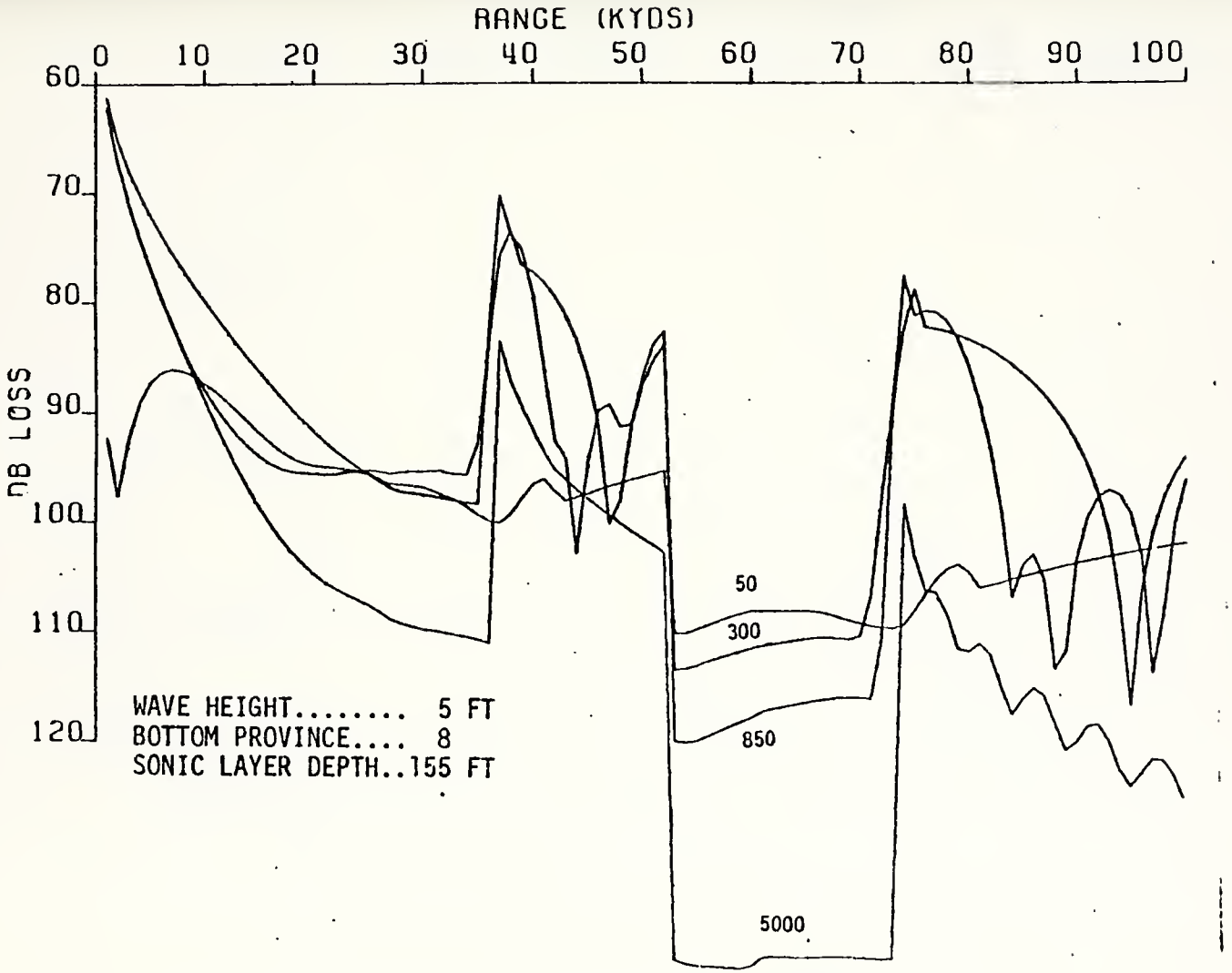

Figure 40. Transmission loss at point A in November.

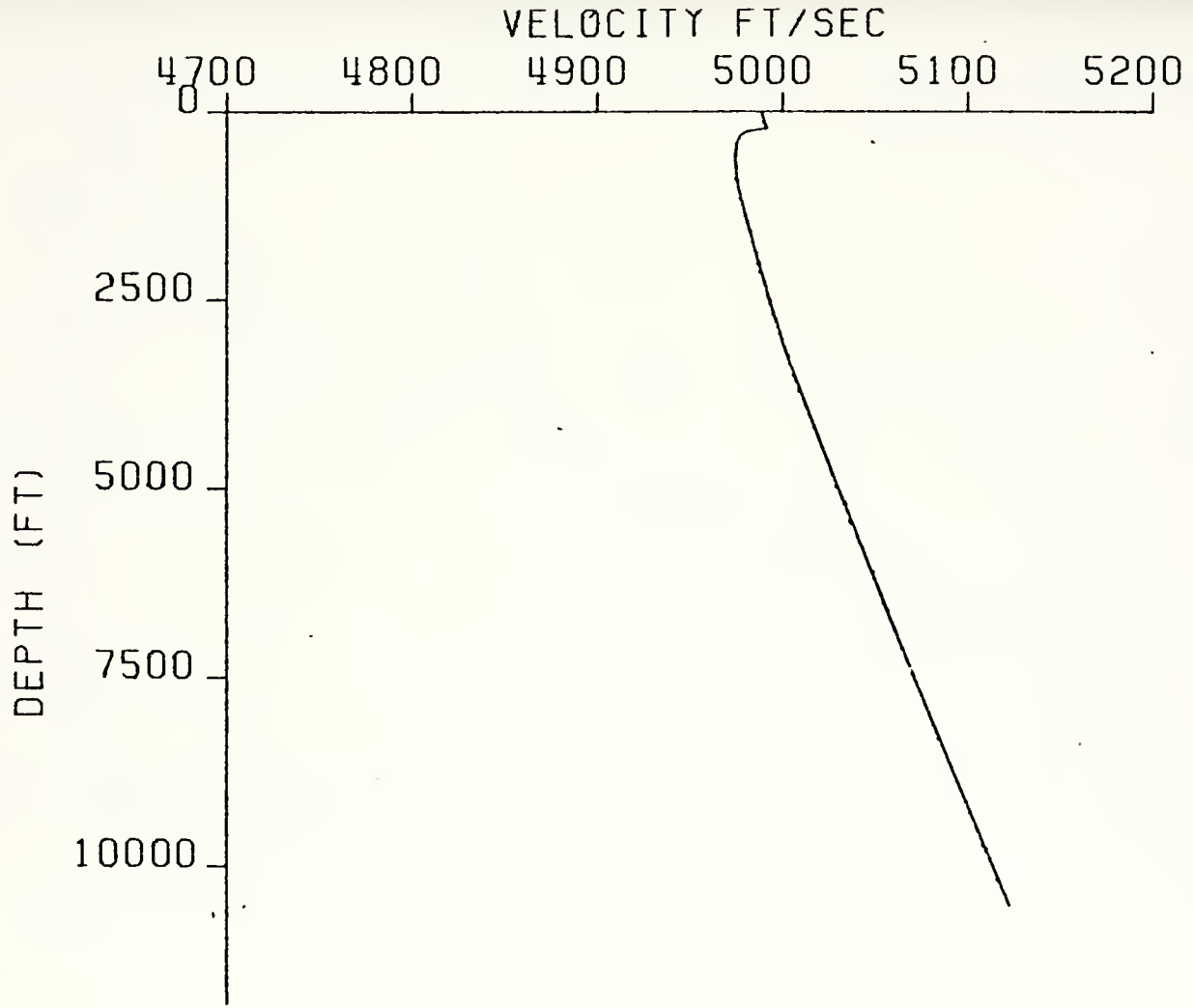

Figure 41. Sound velocity profile at point A in December.

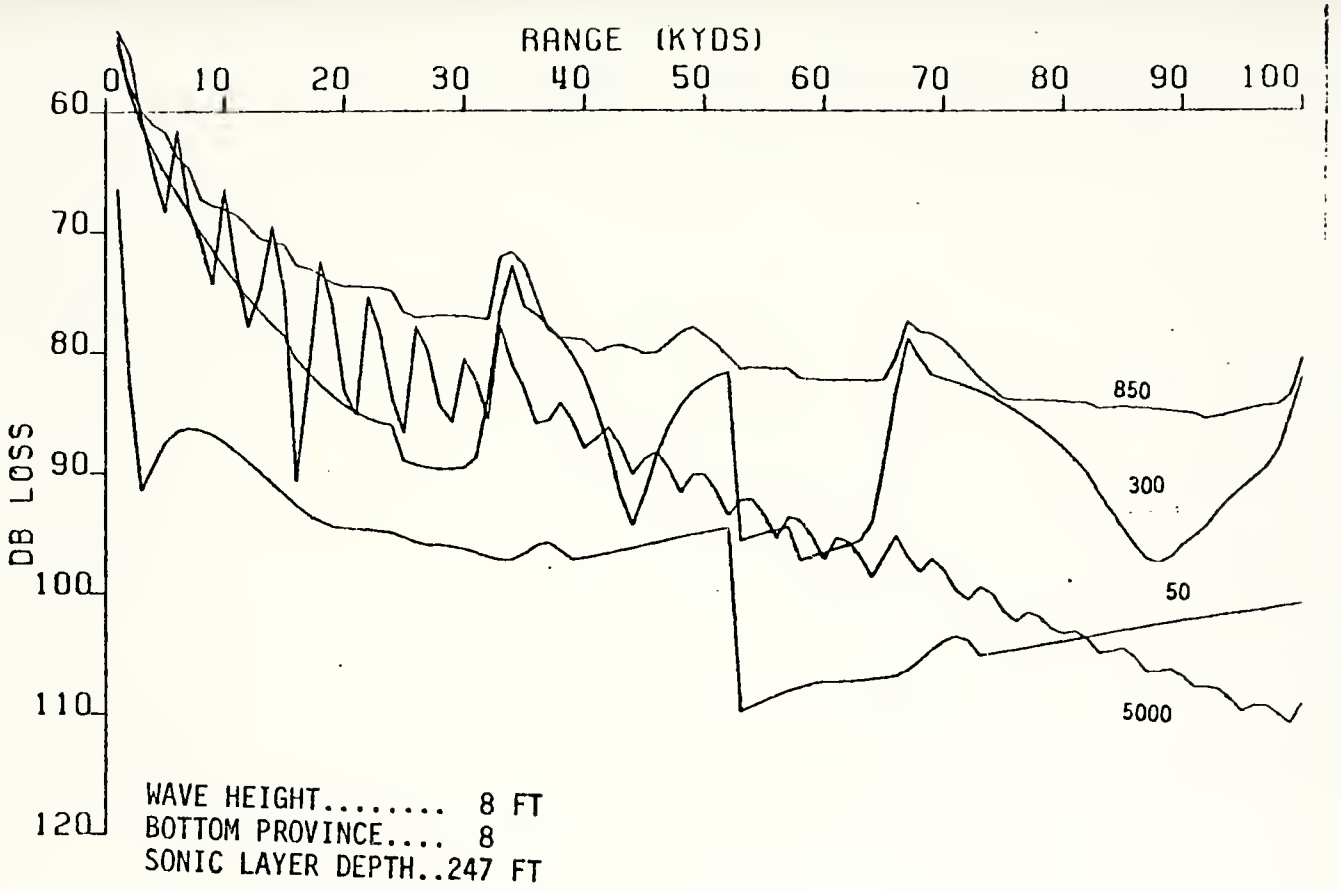

Figure 42. Transmission loss at point A in December.

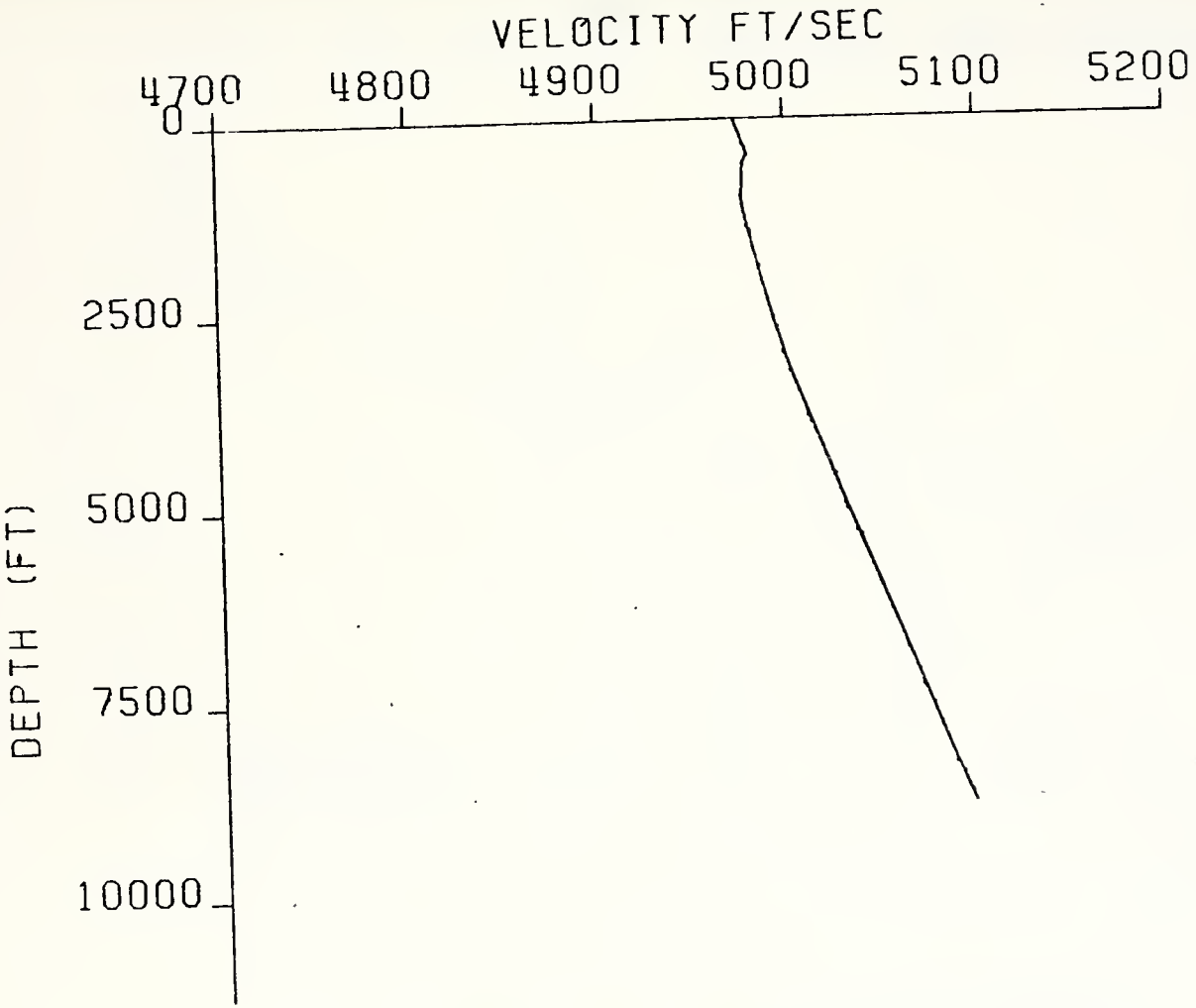

Figure 43. Sound velocity profile at point B in February.

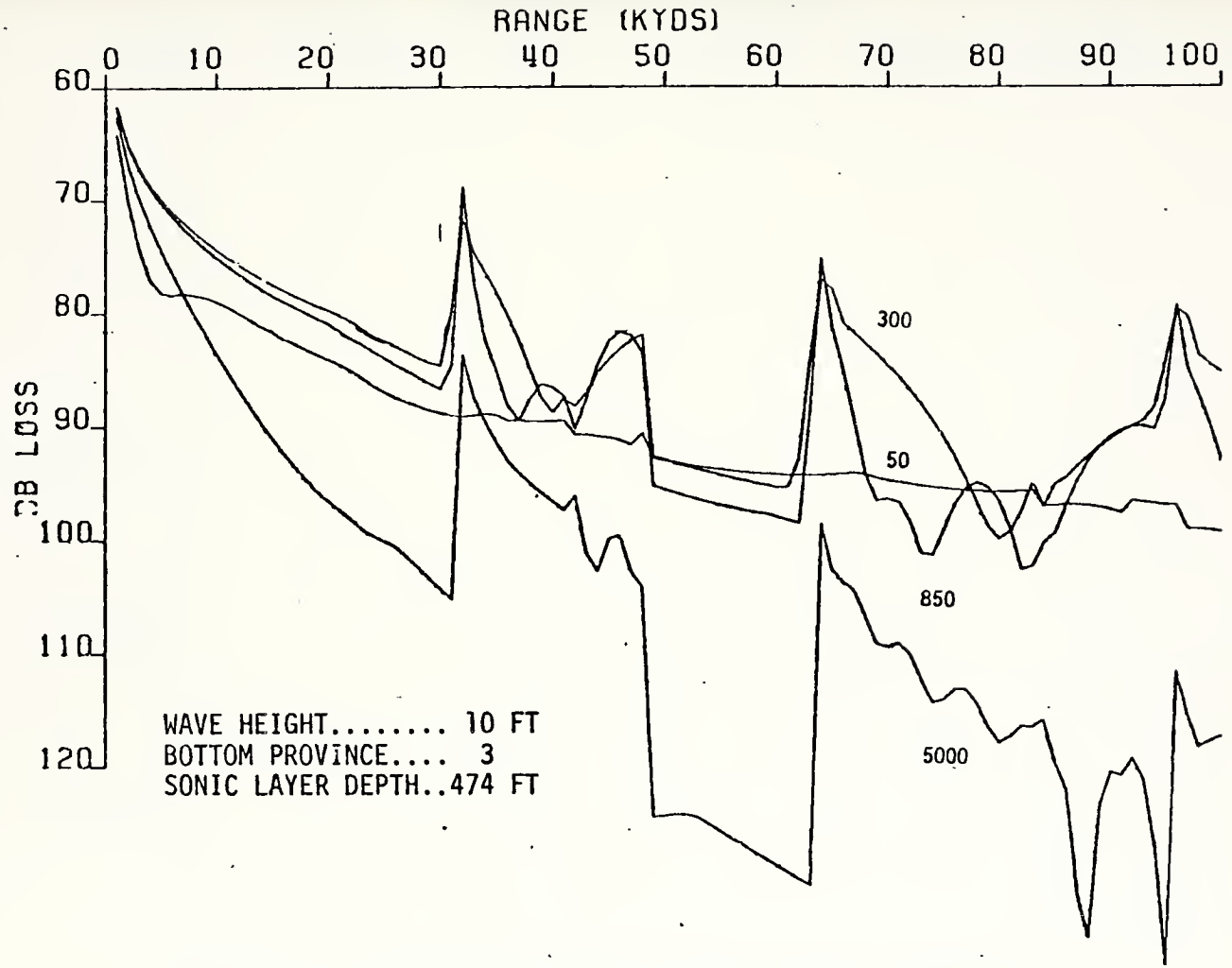

Figure 44. Transmission loss at point B in February.

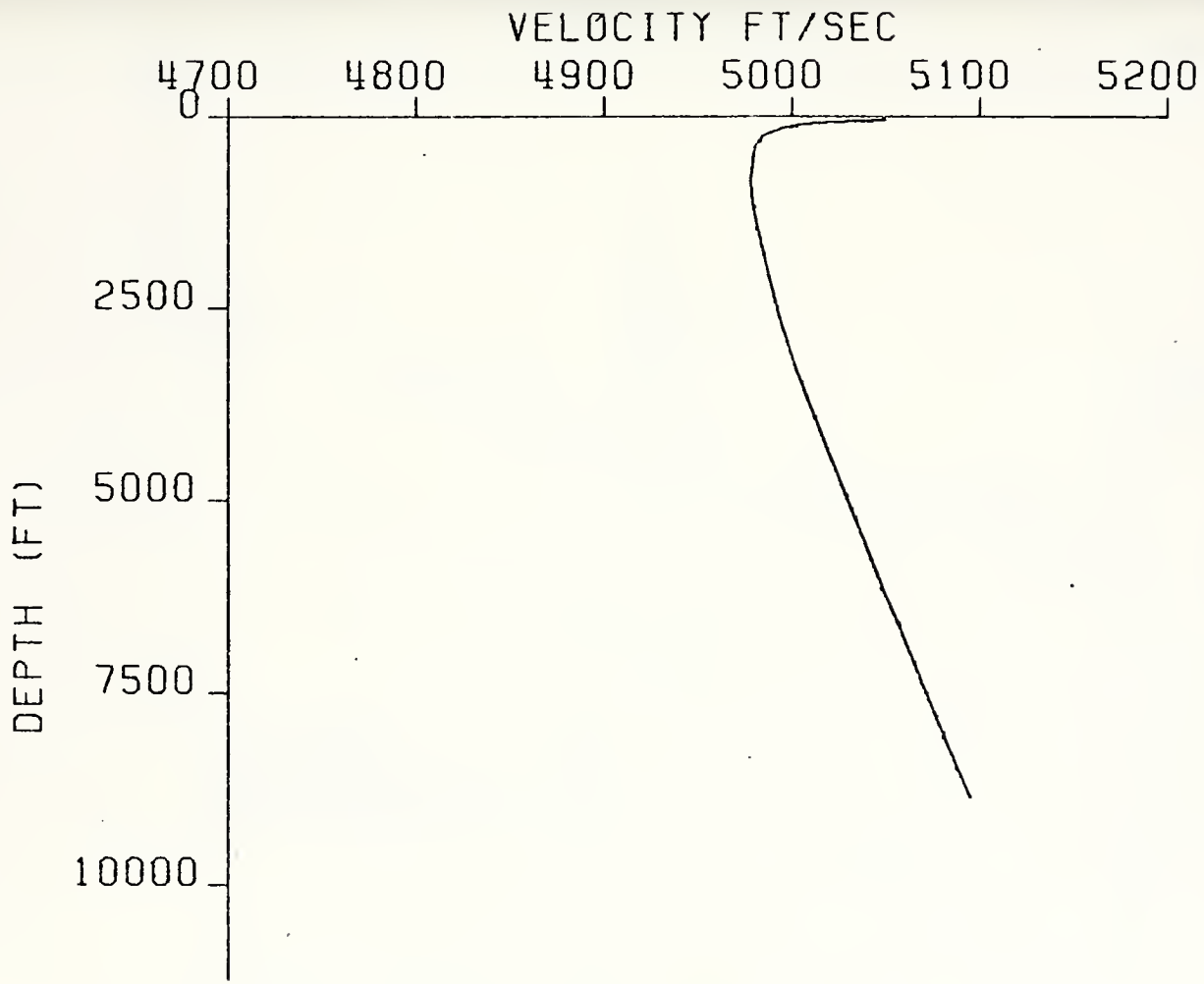

Figure 45. Sound velocity profile at point B in July.

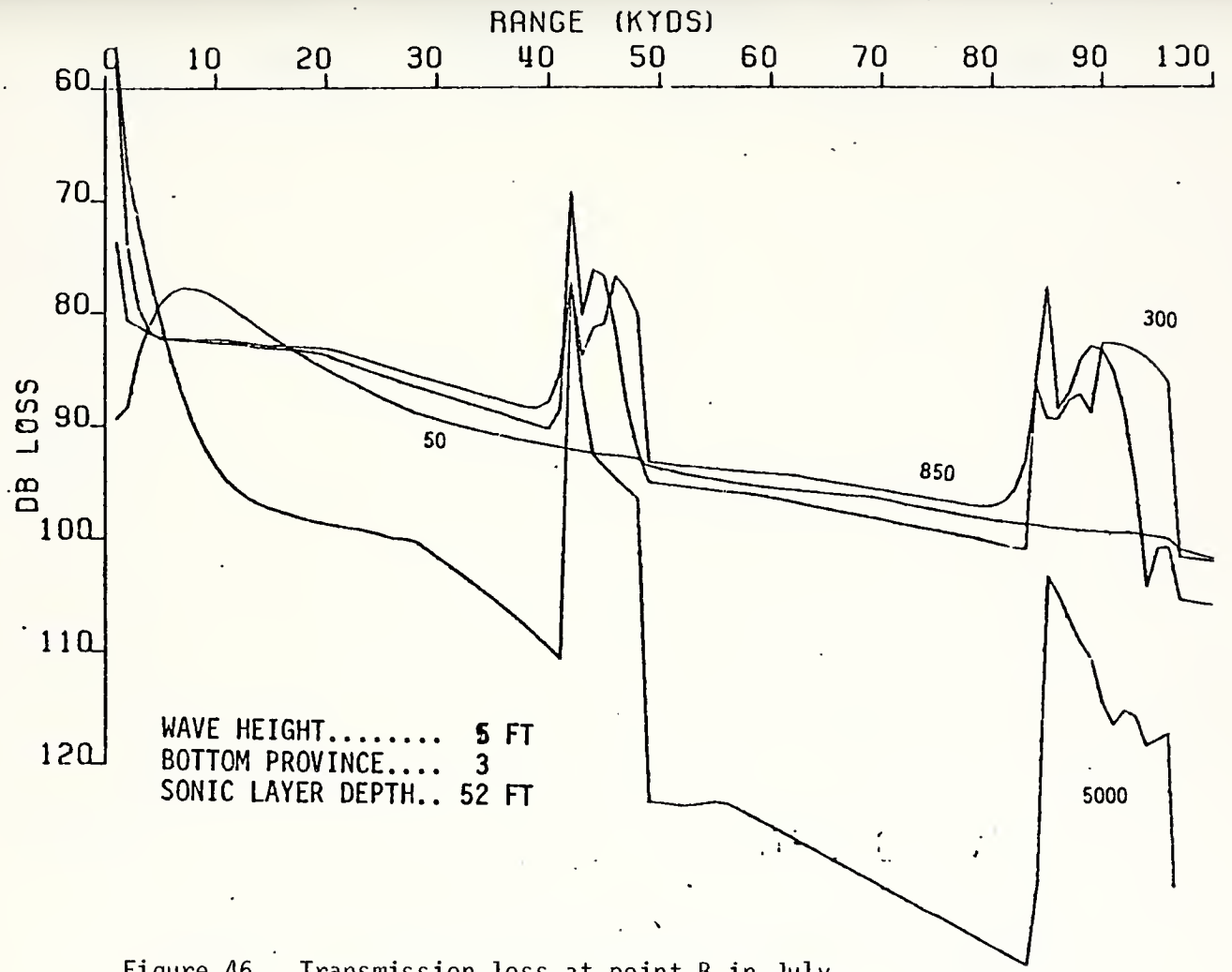

Figure 46. Transmission loss at point B in July.

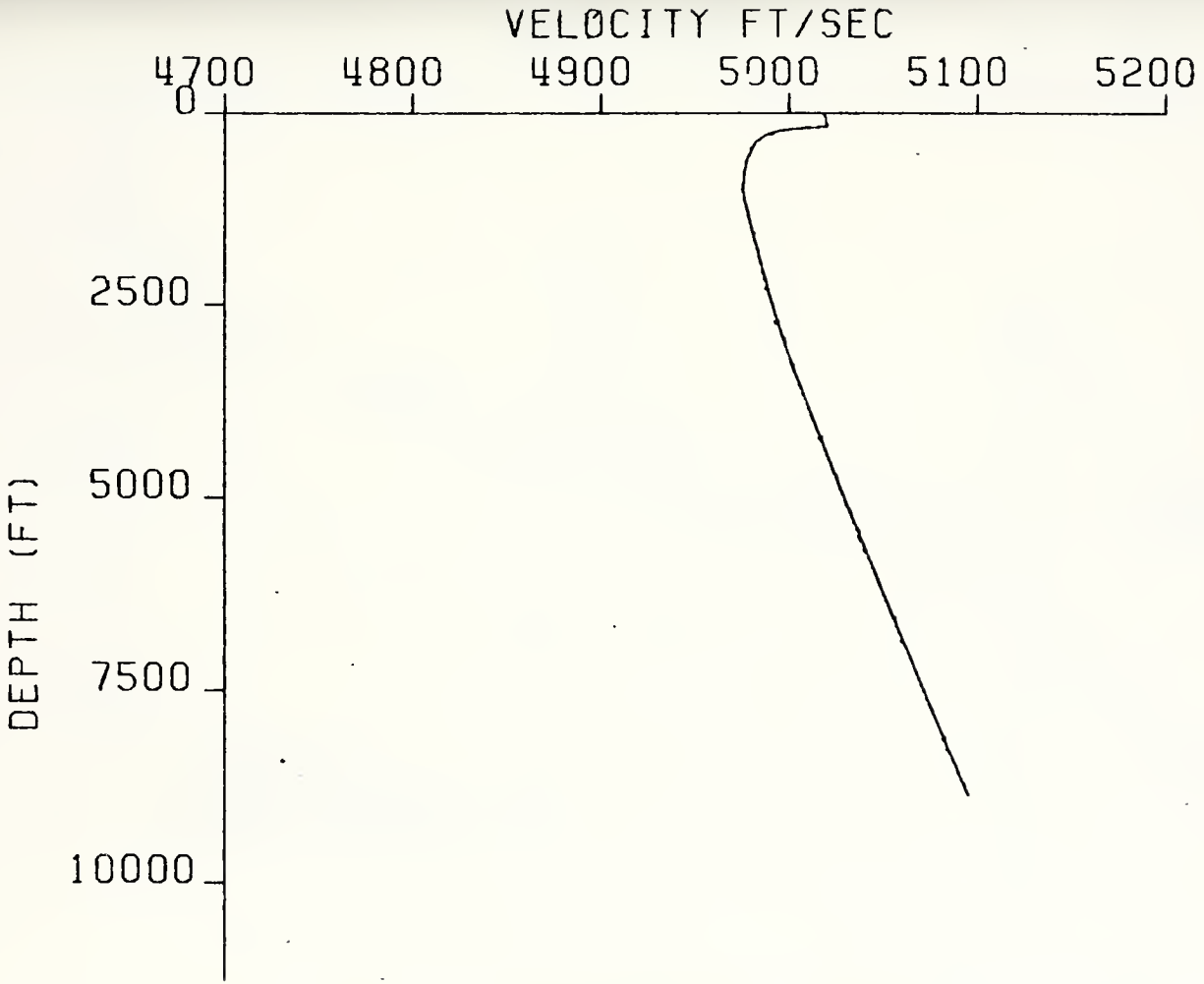

Figure 47. Sound velocity profile at point B in November.

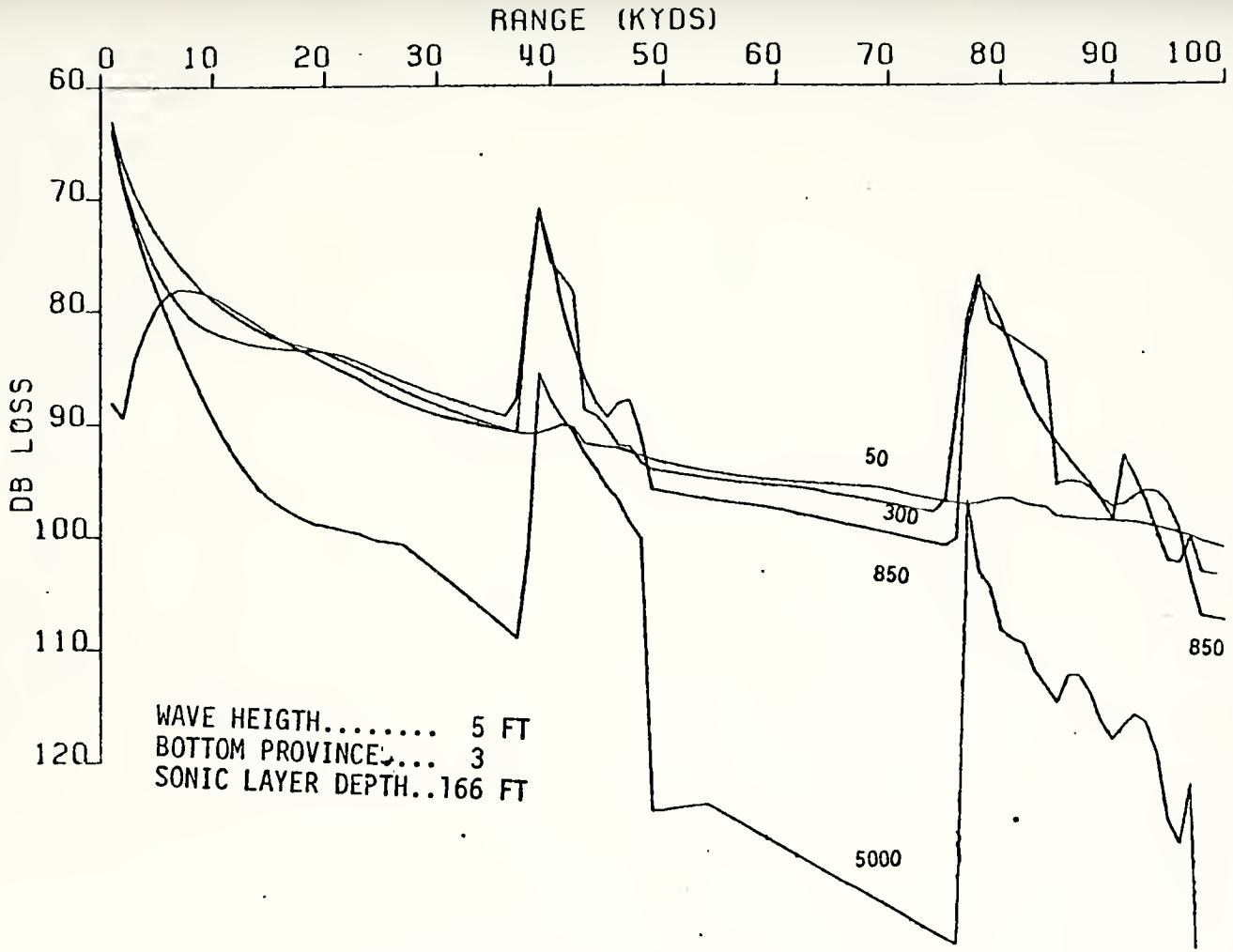

Figure 48. Transmission loss at point B in November.

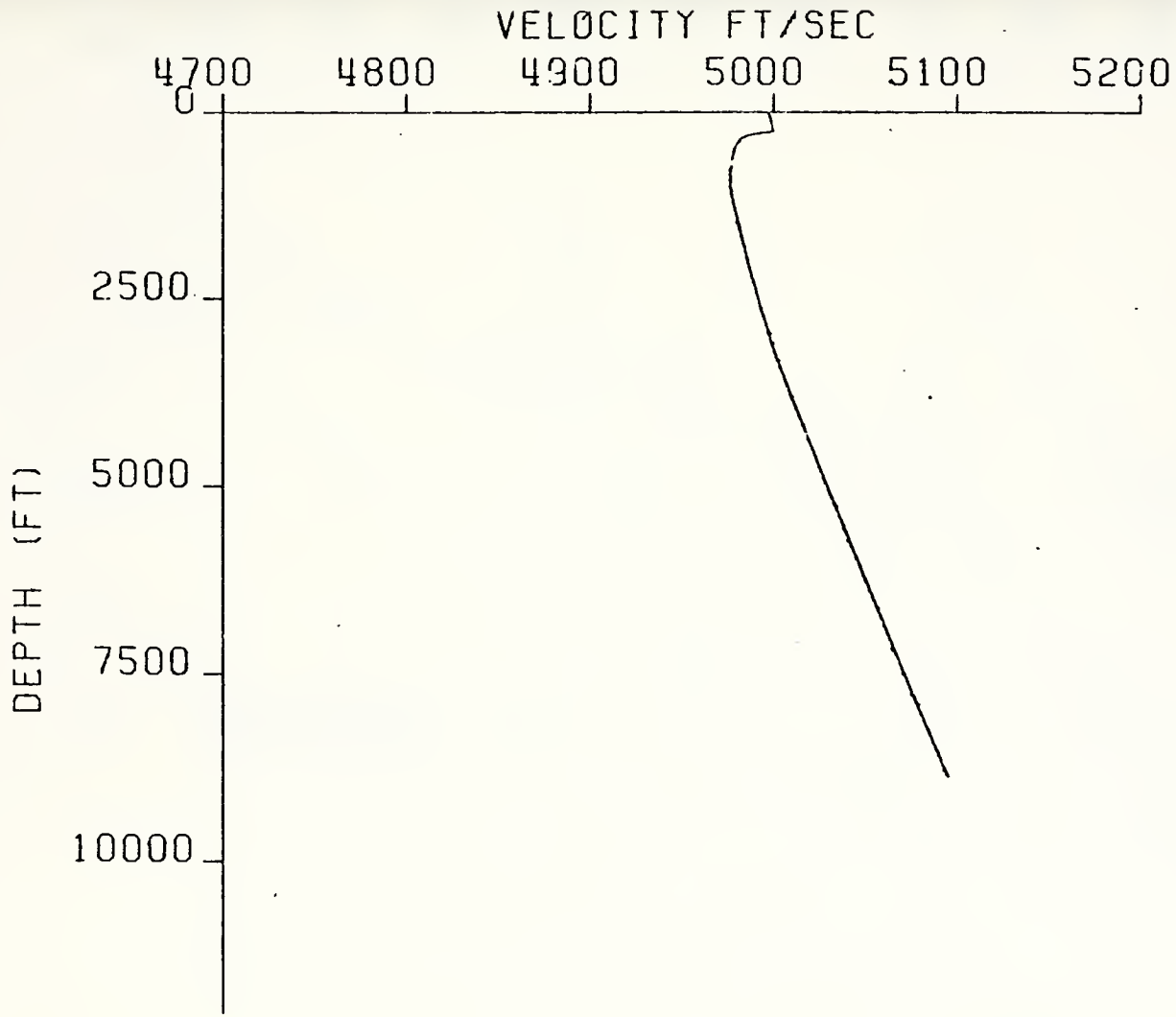

Figure 49. Sound velocity profile at point B in December.

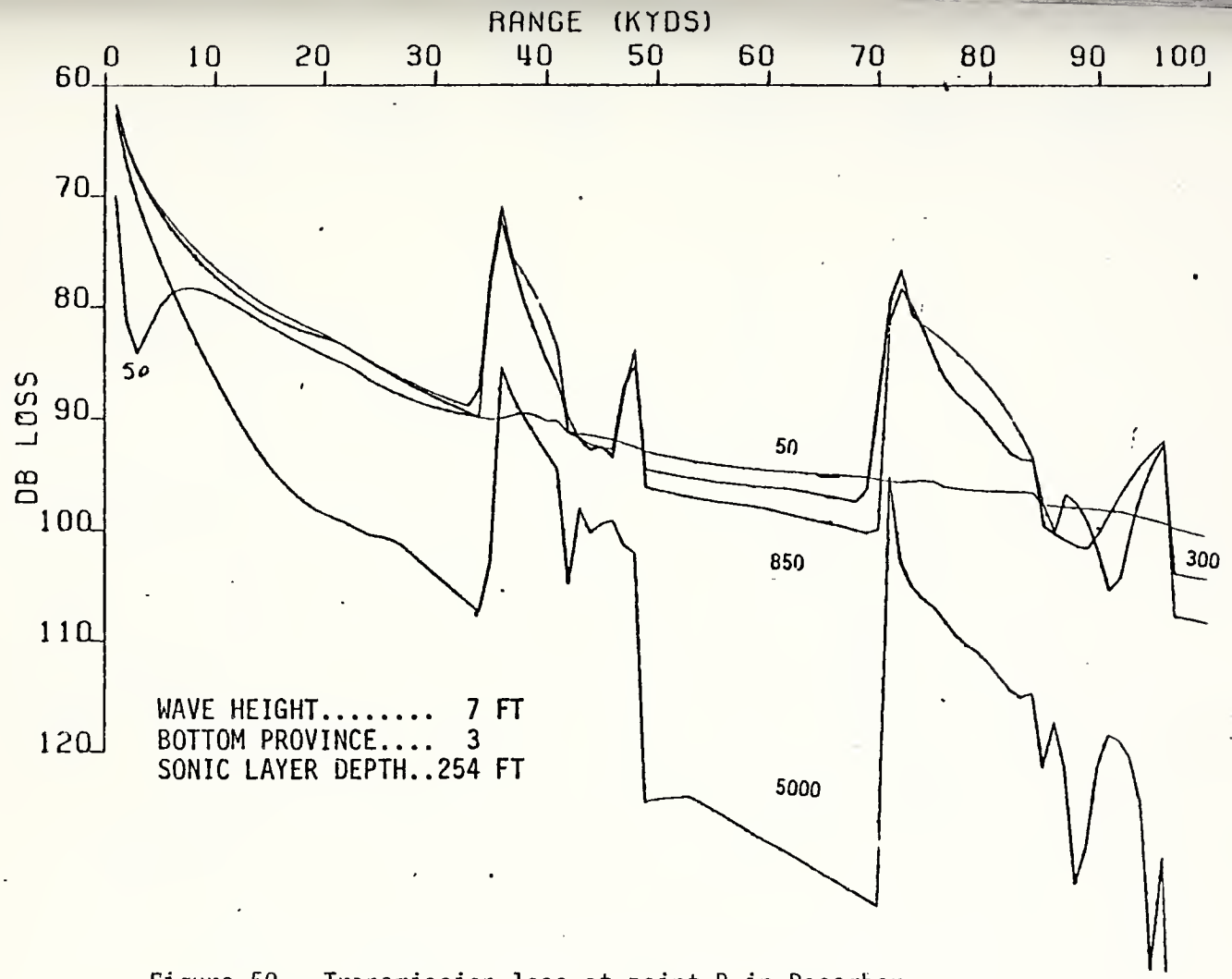

Figure 50. Transmission loss at point B in December.

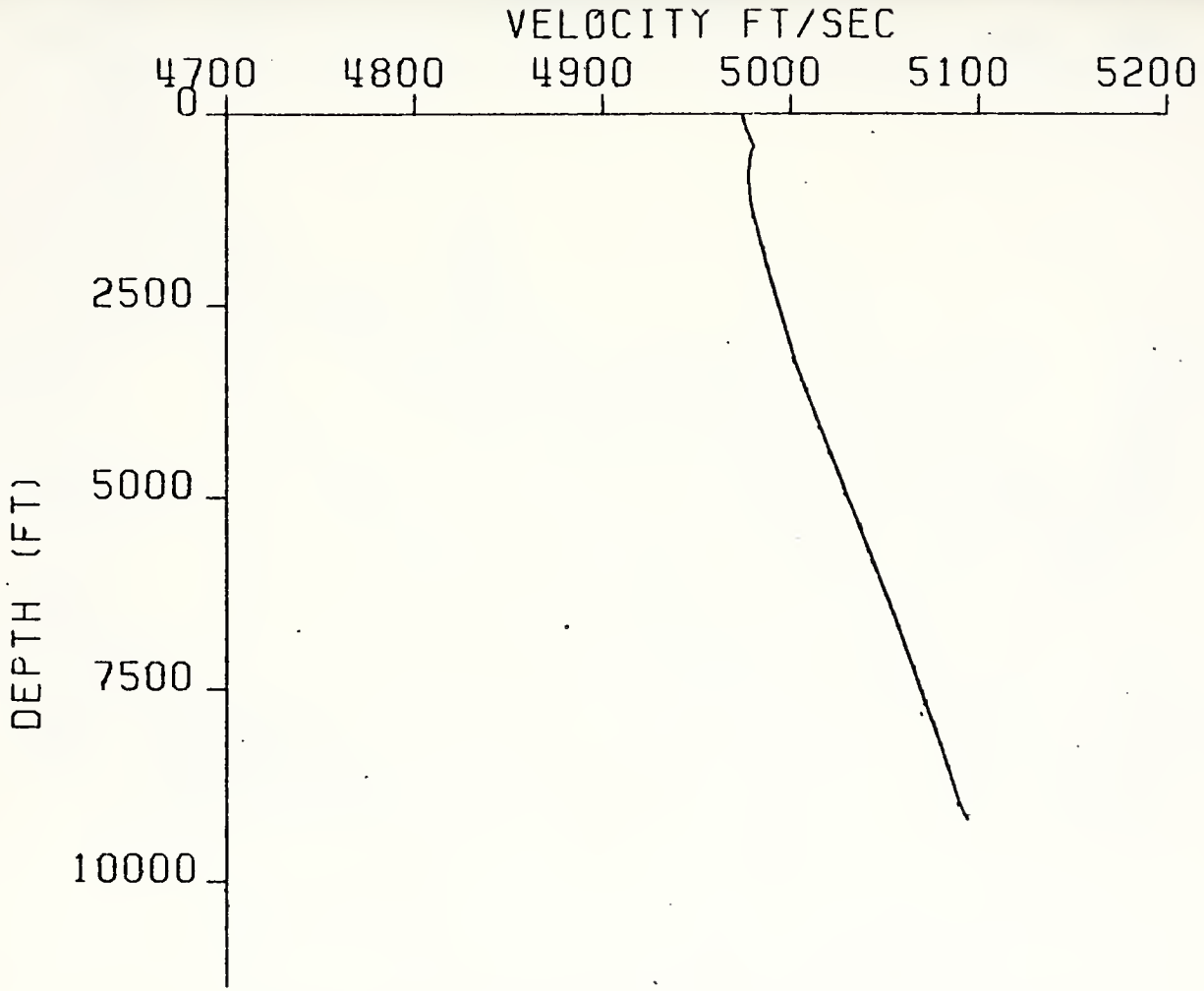

Figure 51. Sound velocity profile at point C in February.

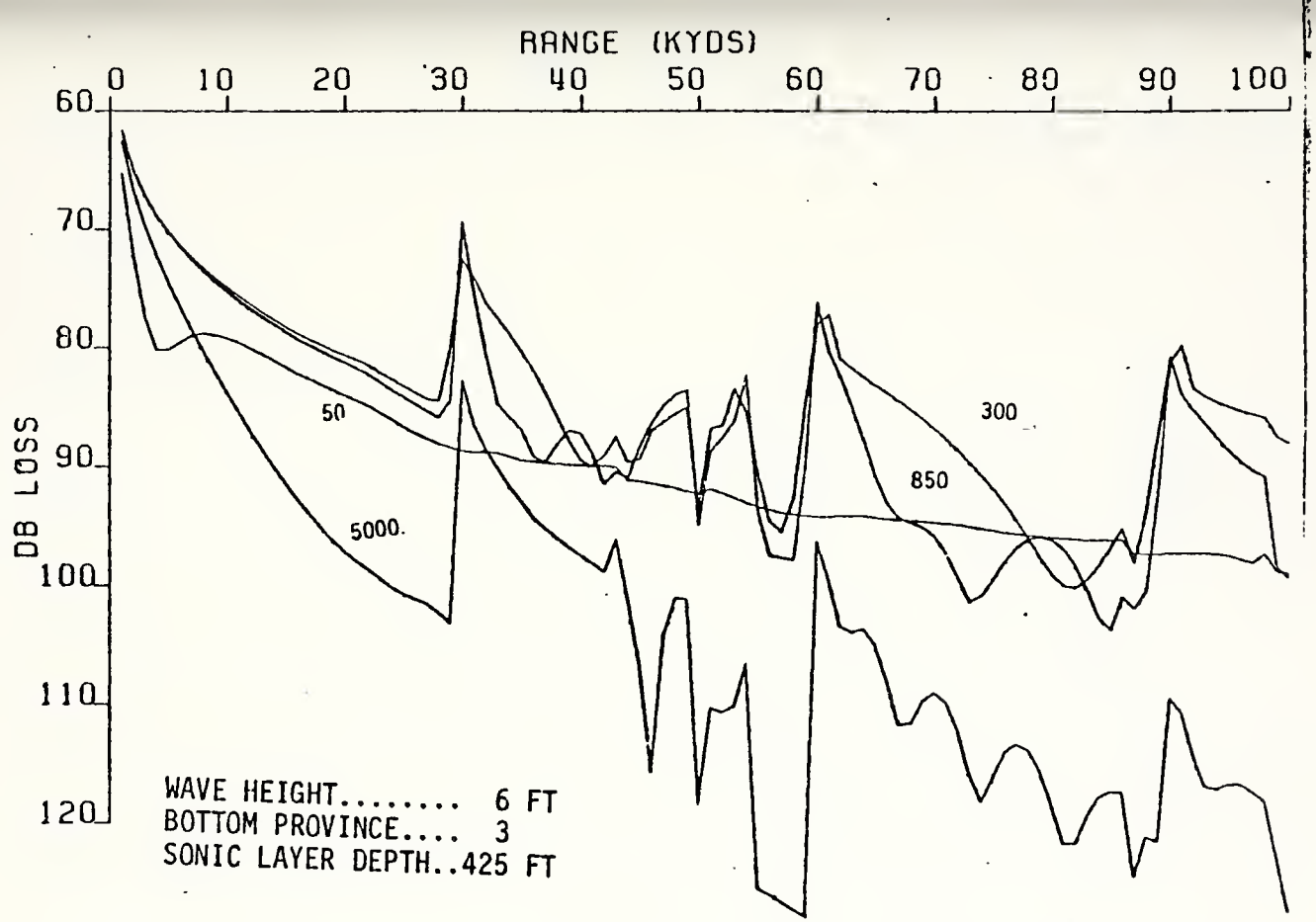

Figure 52. Transmission loss at point C in February.

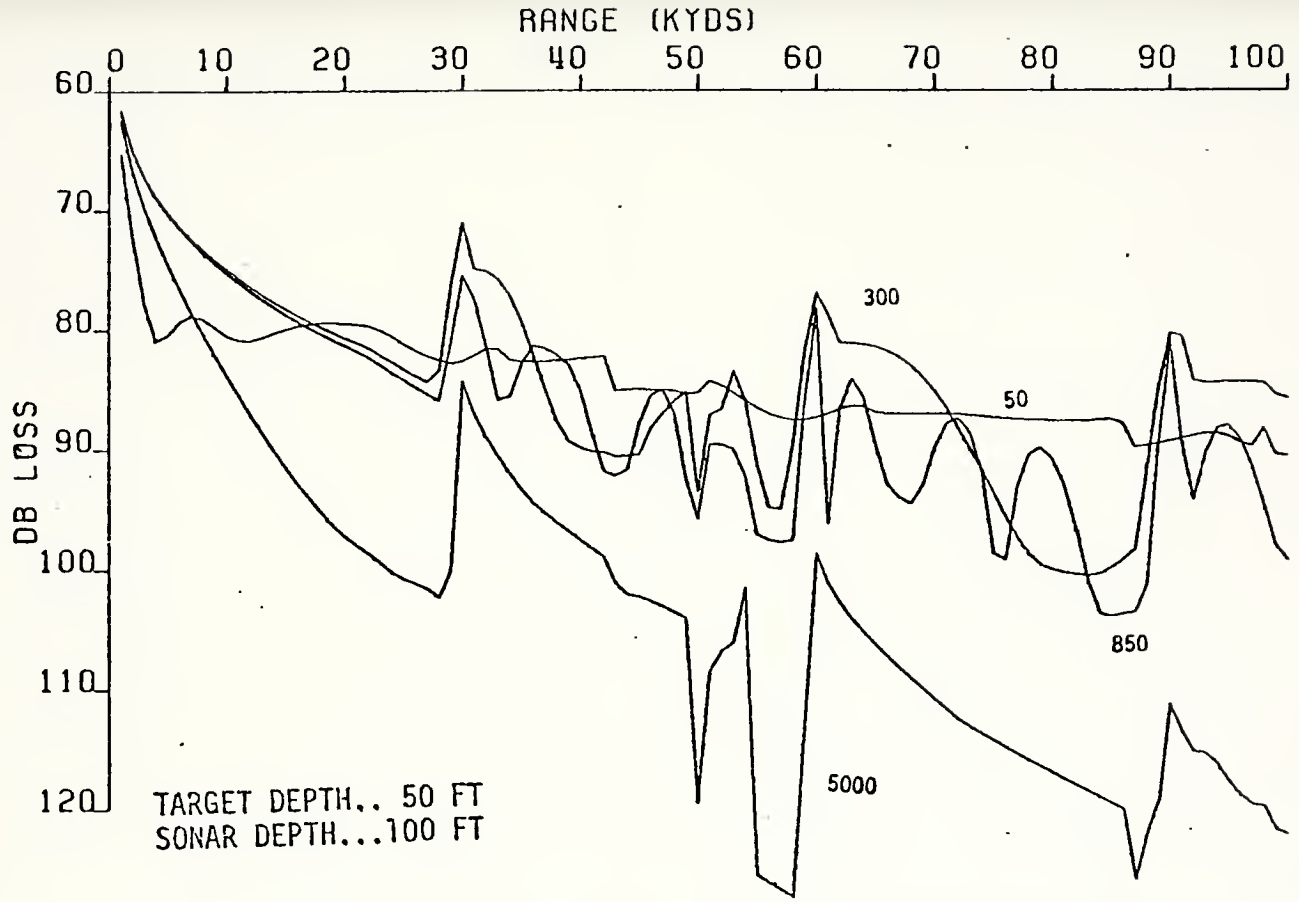

Figure 53. Transmission loss at point C in February with shown depths above.

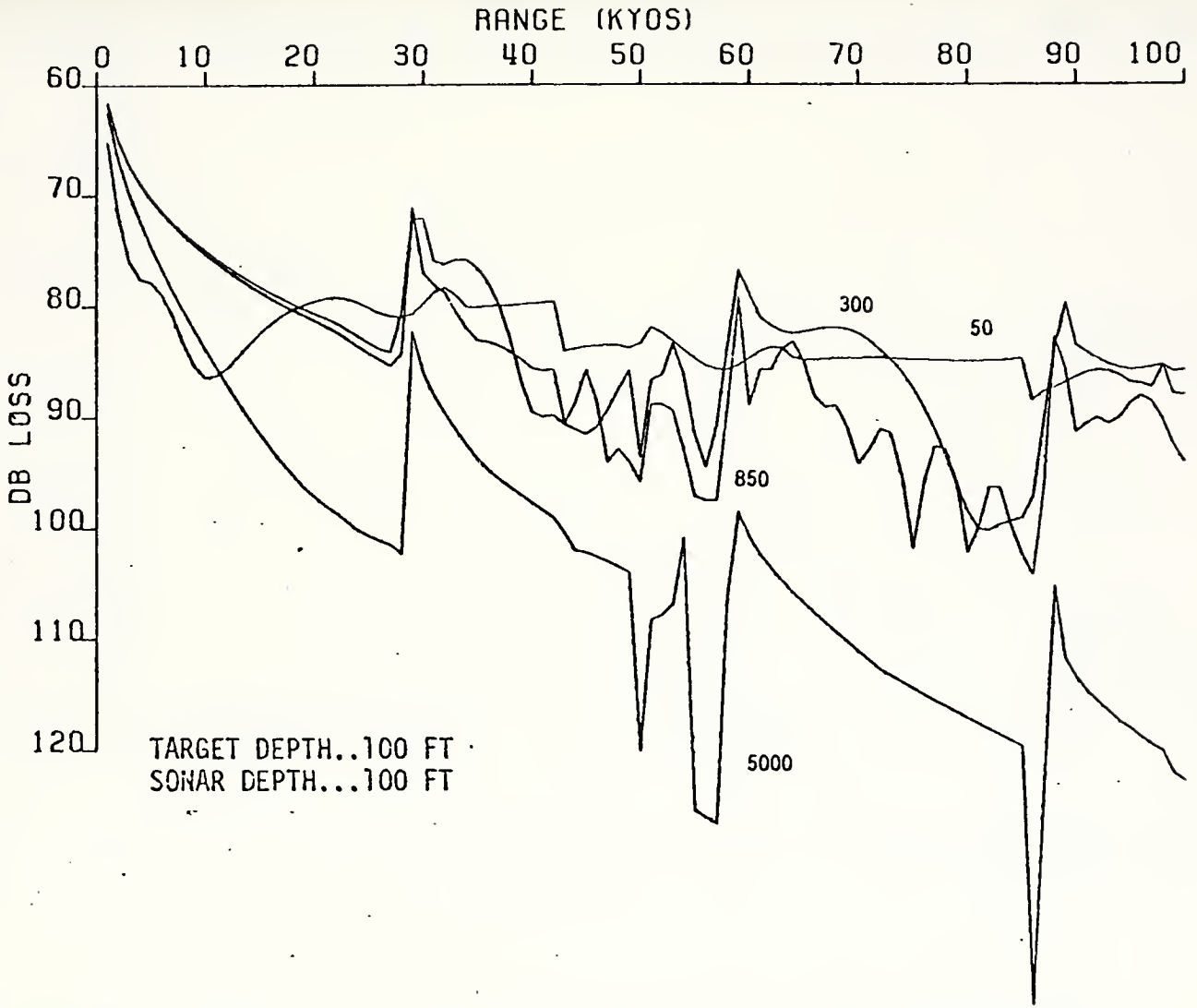

Figure 54. Transmission loss at point C in February with shown depths above.

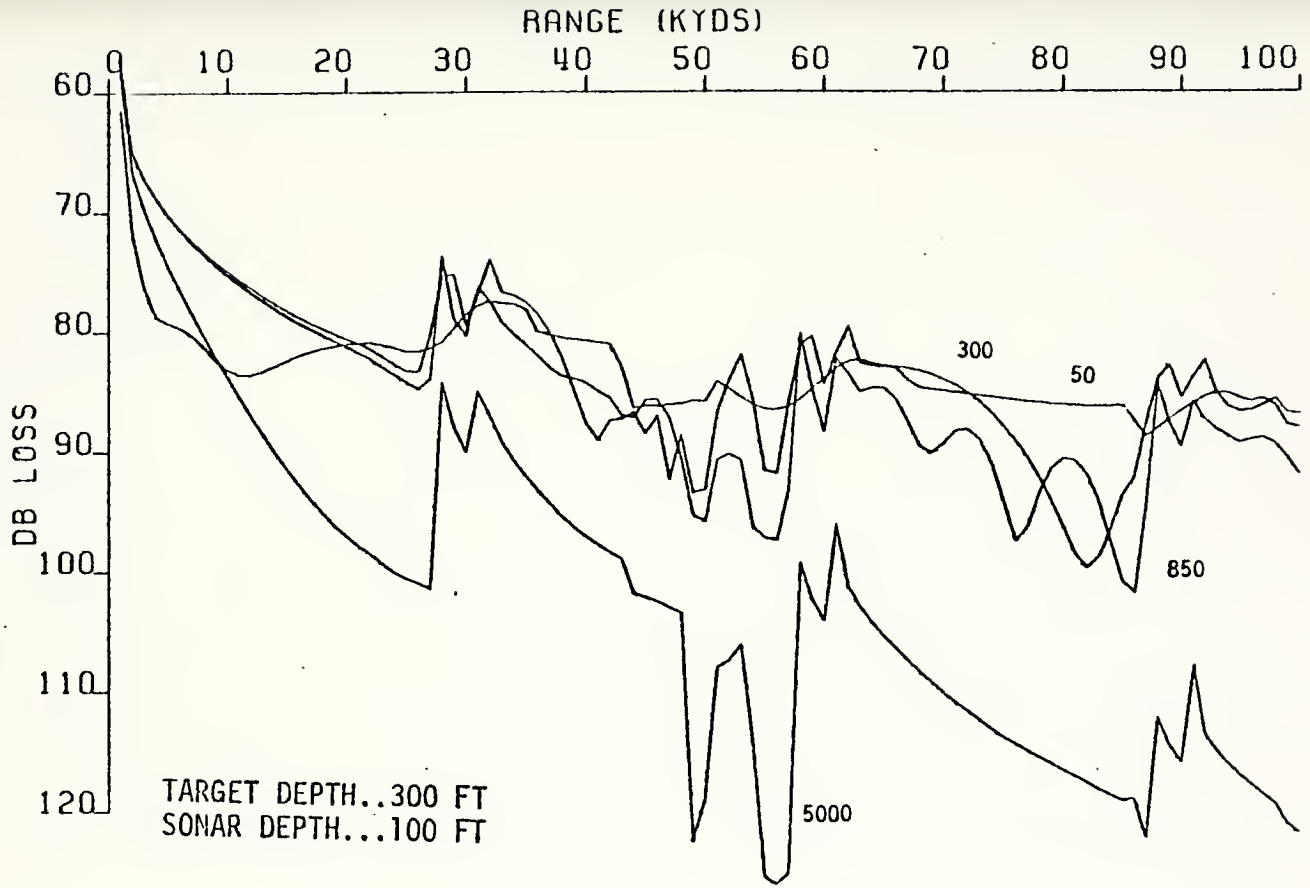

Figure 55. Transmission loss at point C in February with shown depths above.

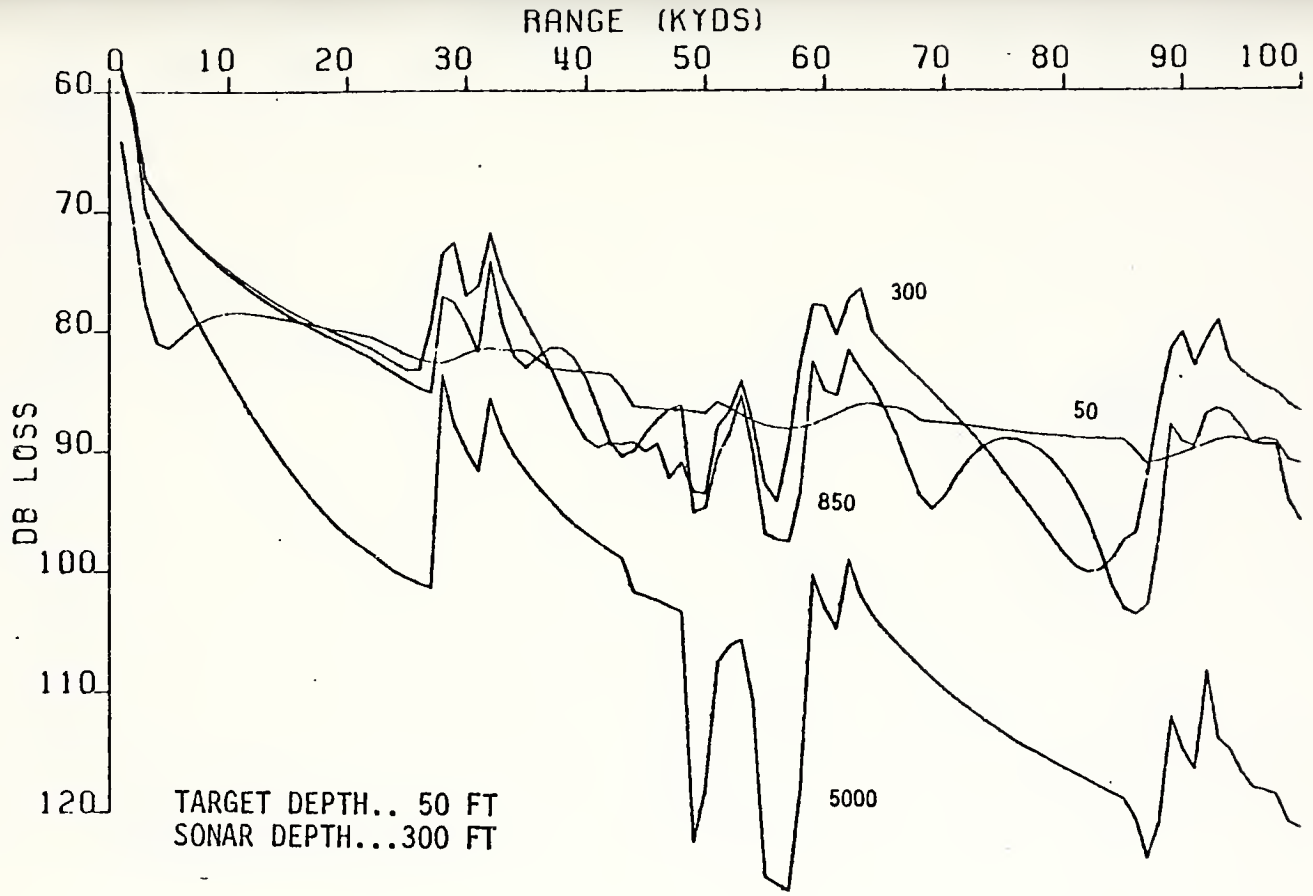

Figure 56. Transmission loss at point C in February with shown depths above.

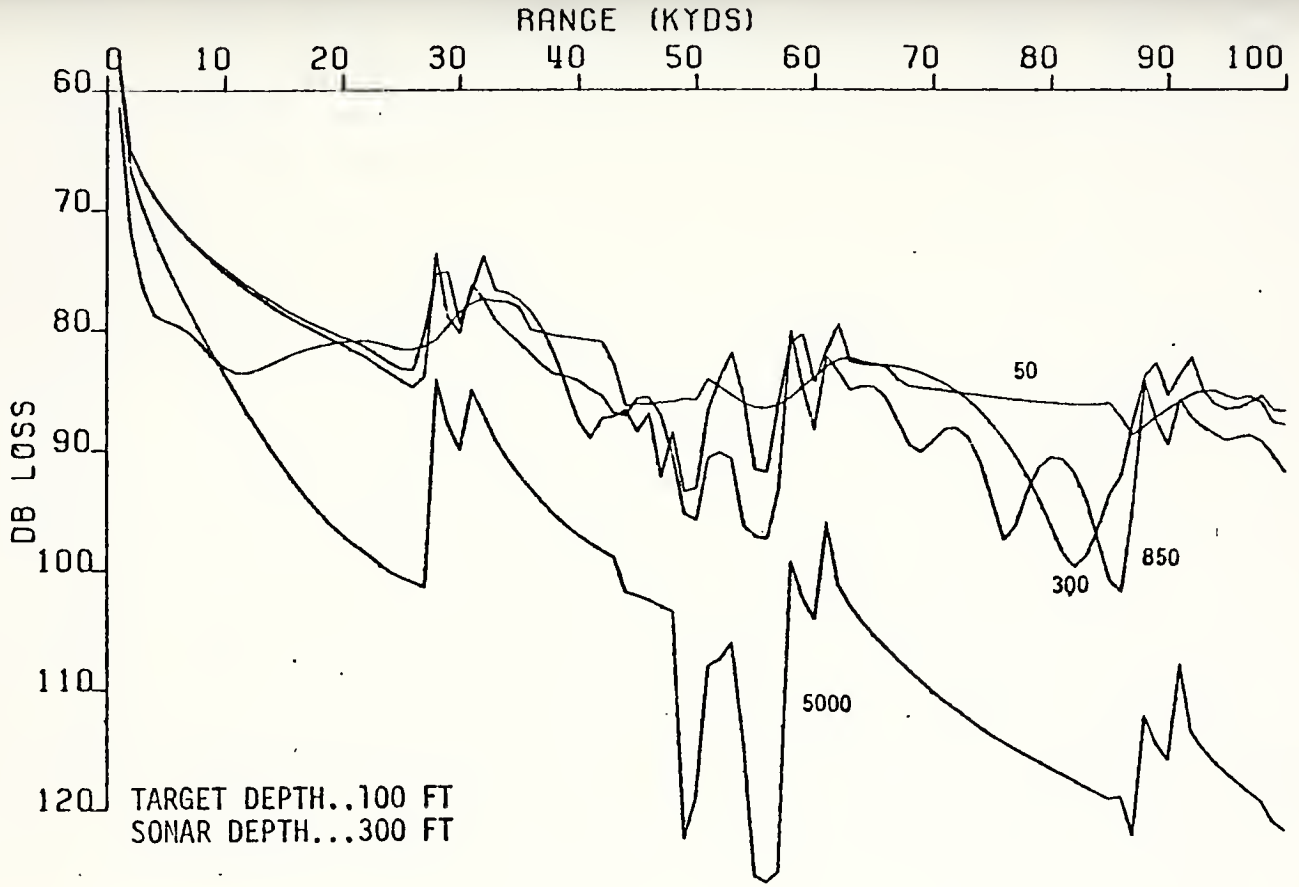

Figure 57. Transmission loss at point C in February with shown depths above.

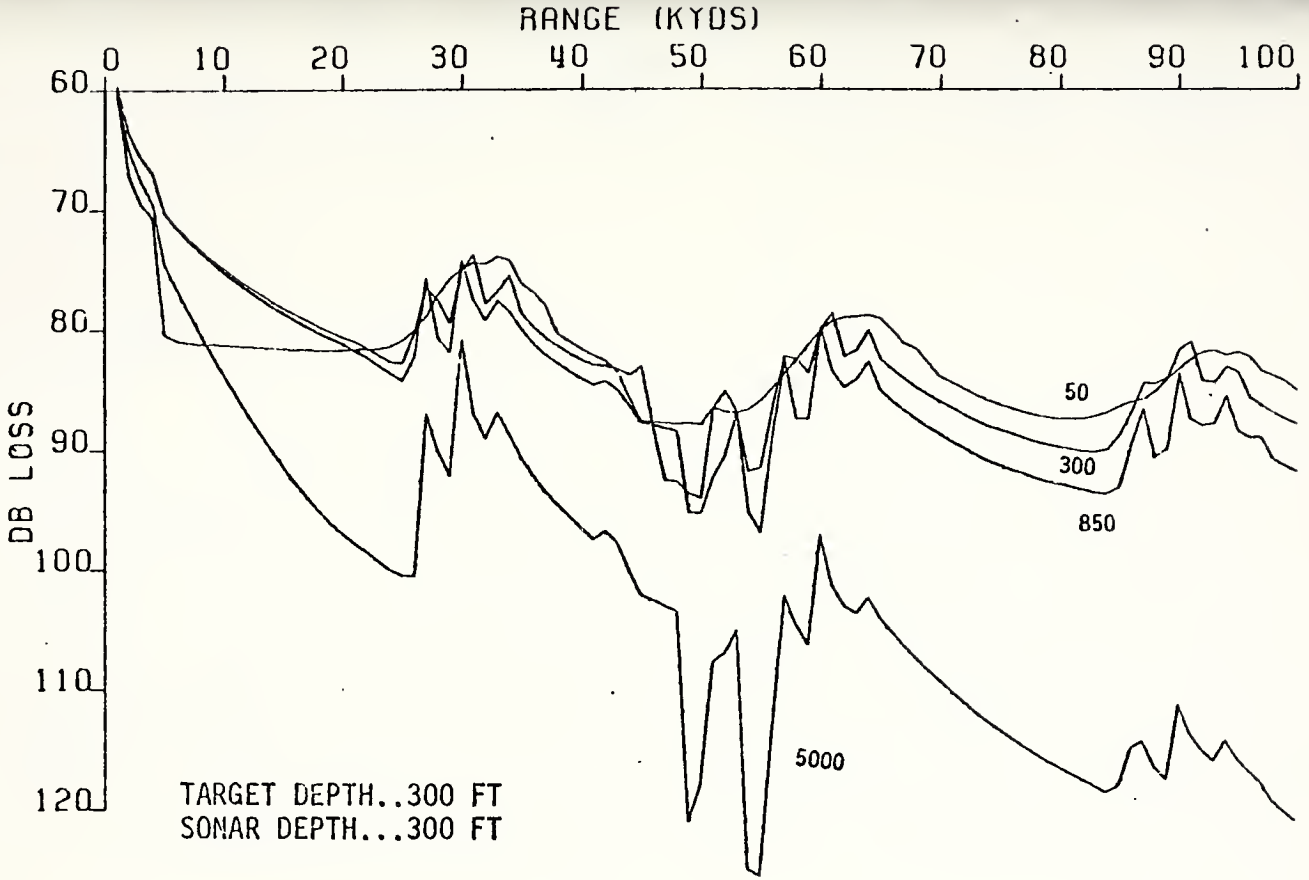

Figure 58. Transmission loss at point C in February with shown depths above.

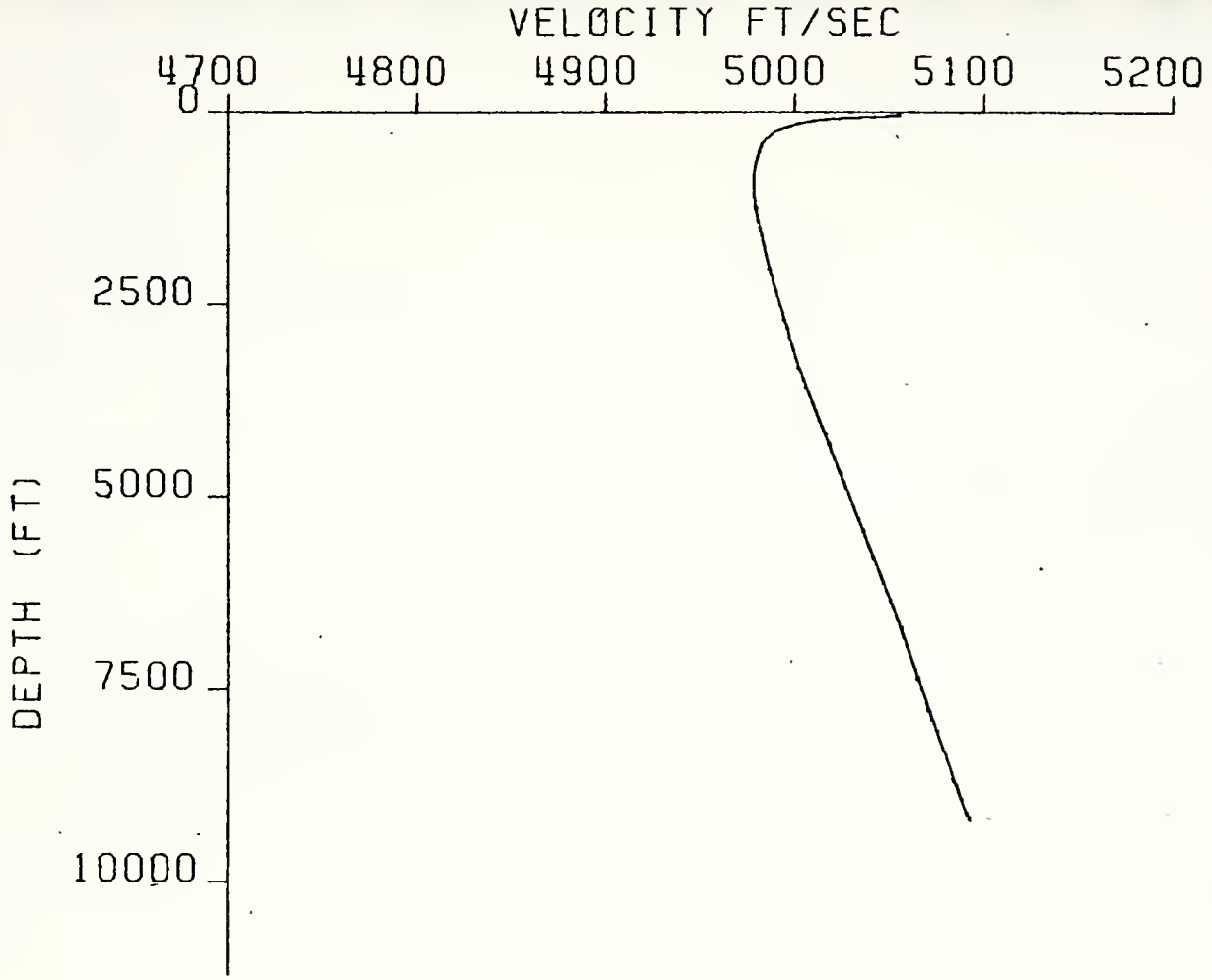

Figure 59. Sound velocity profile at point C in July.

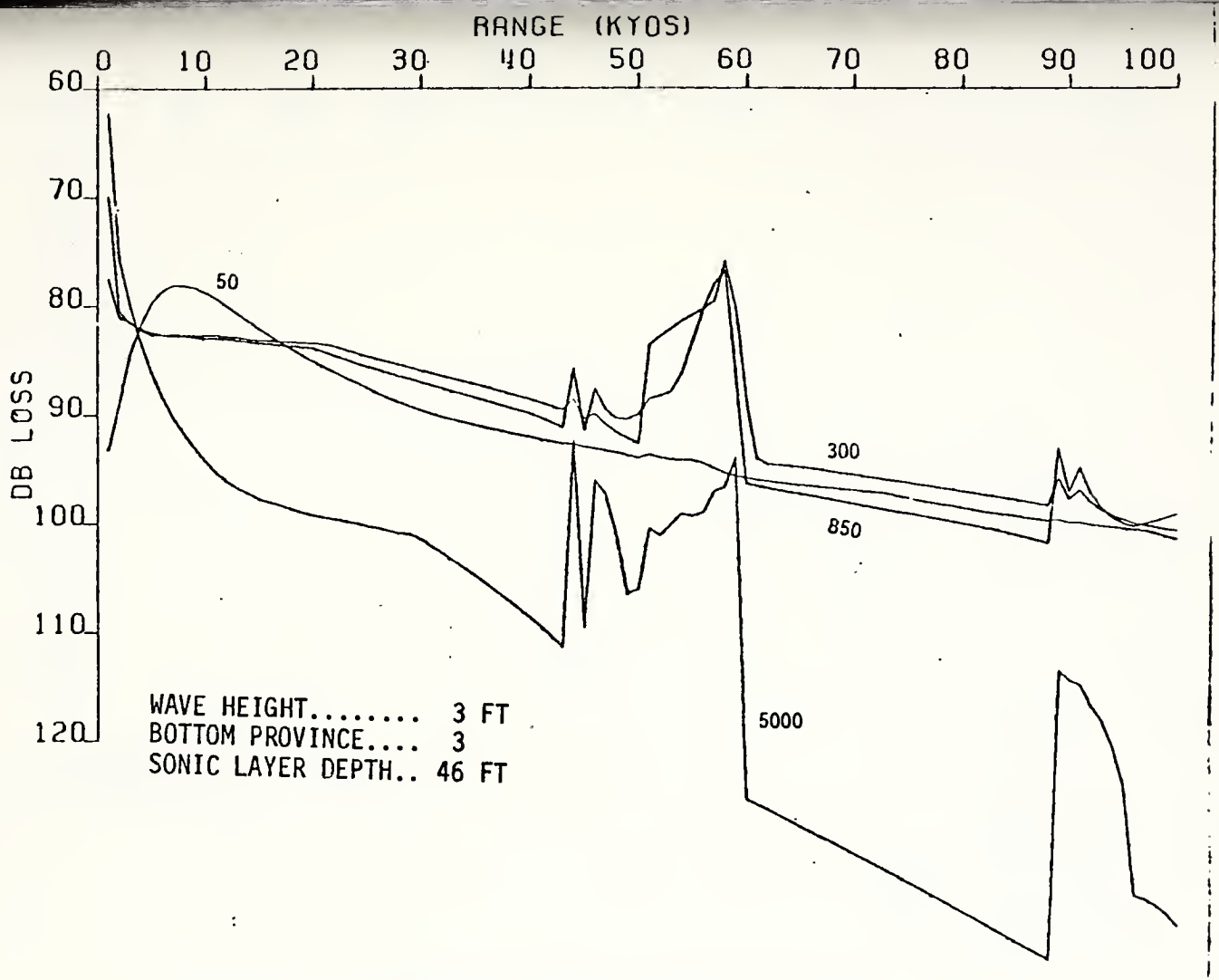

Figure 60. Transmission loss at point C in July.

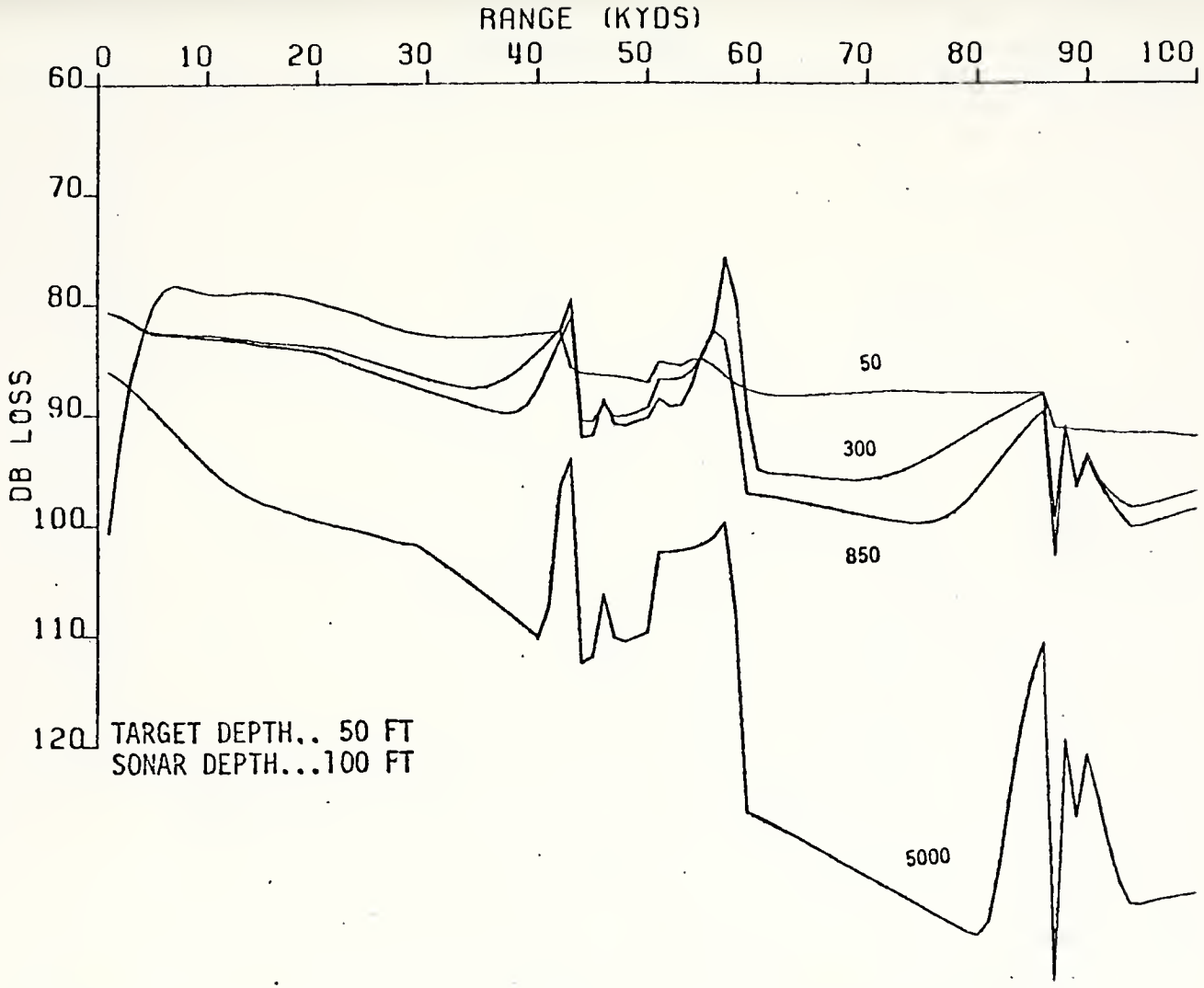

Figure 61. Transmission loss at point C in July with shown depths above.

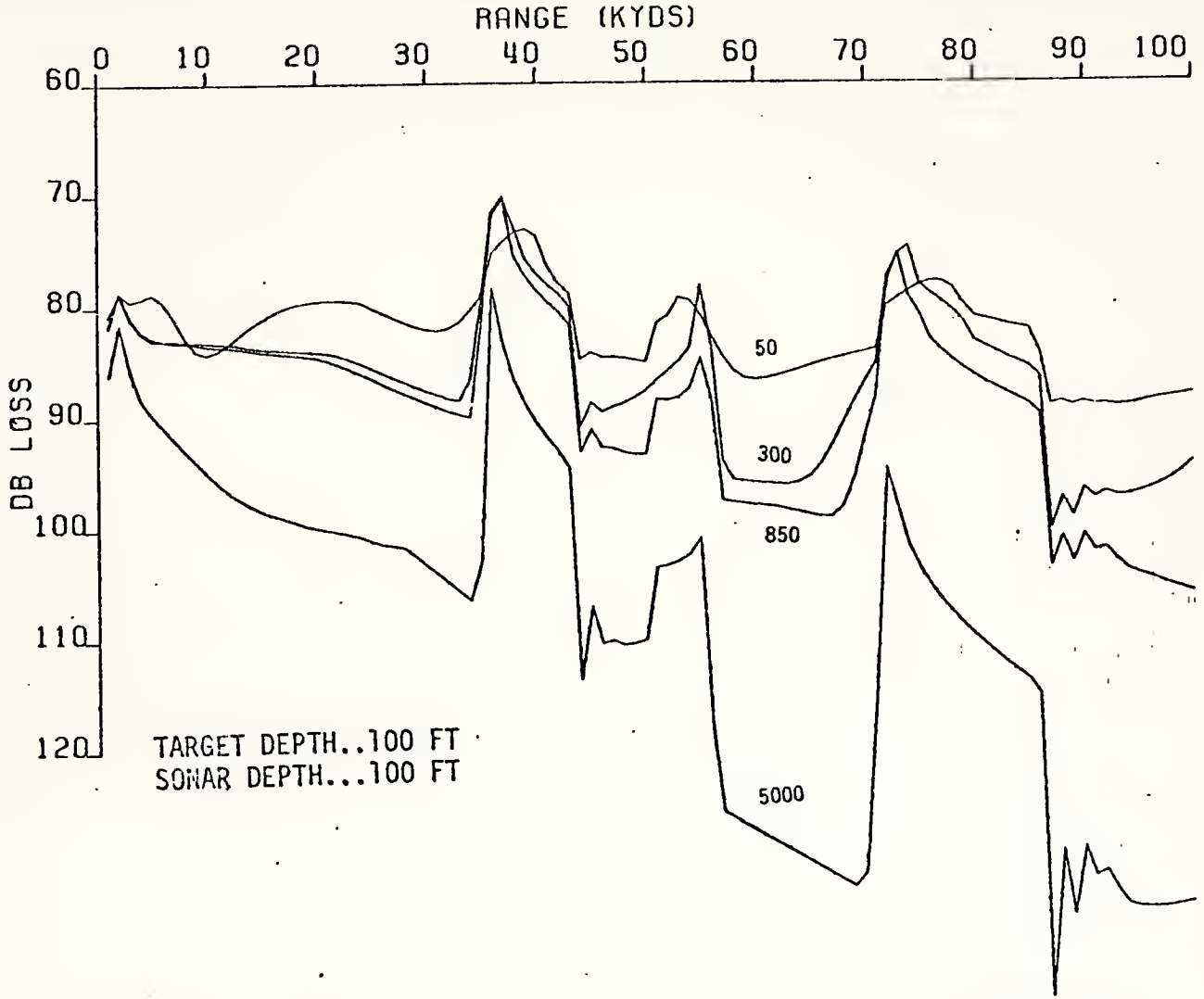

Figure 62. Transmission loss at point C in July with shown depths above.

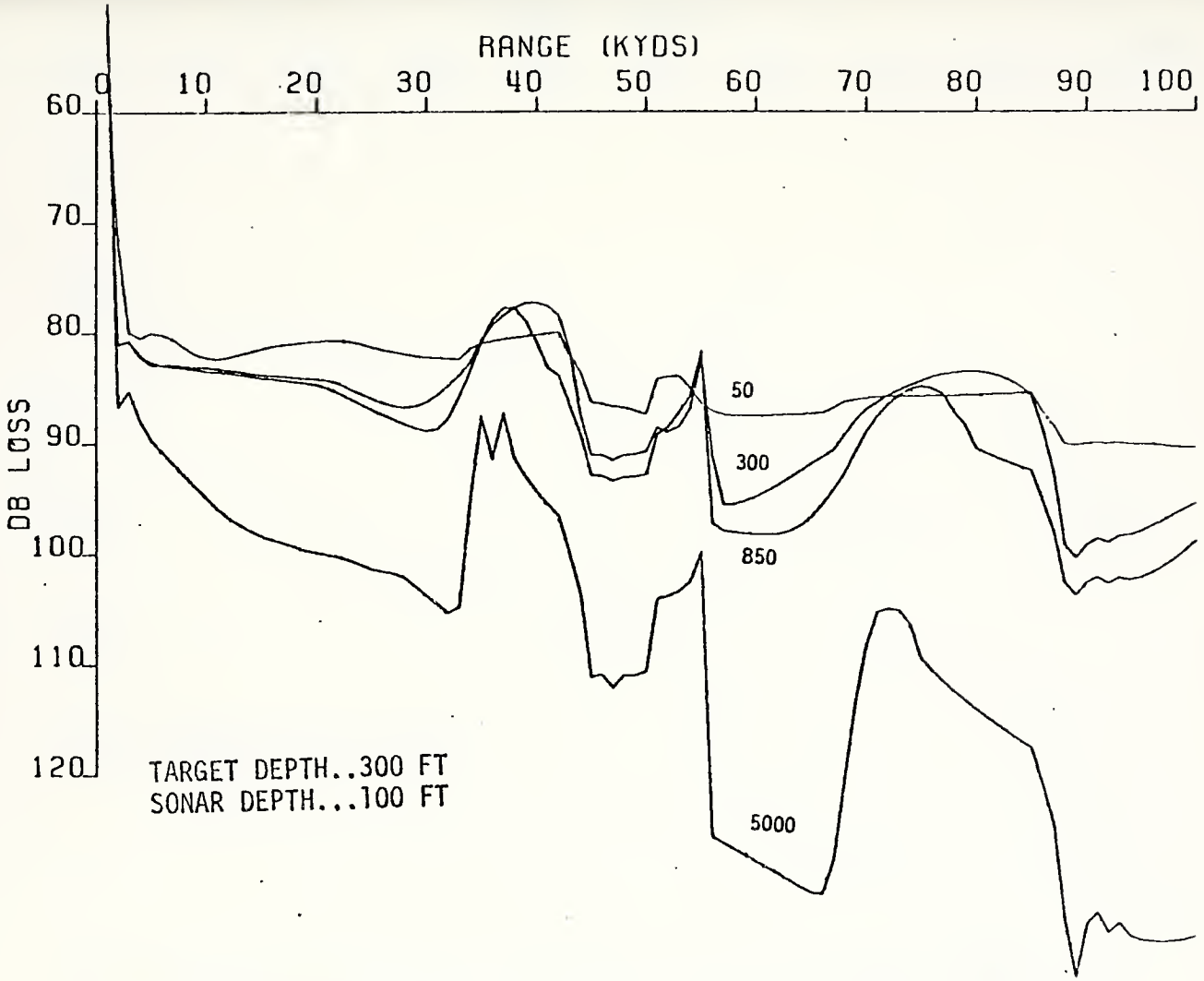

Figure 63. Transmission loss at point C in July with shown depths above.

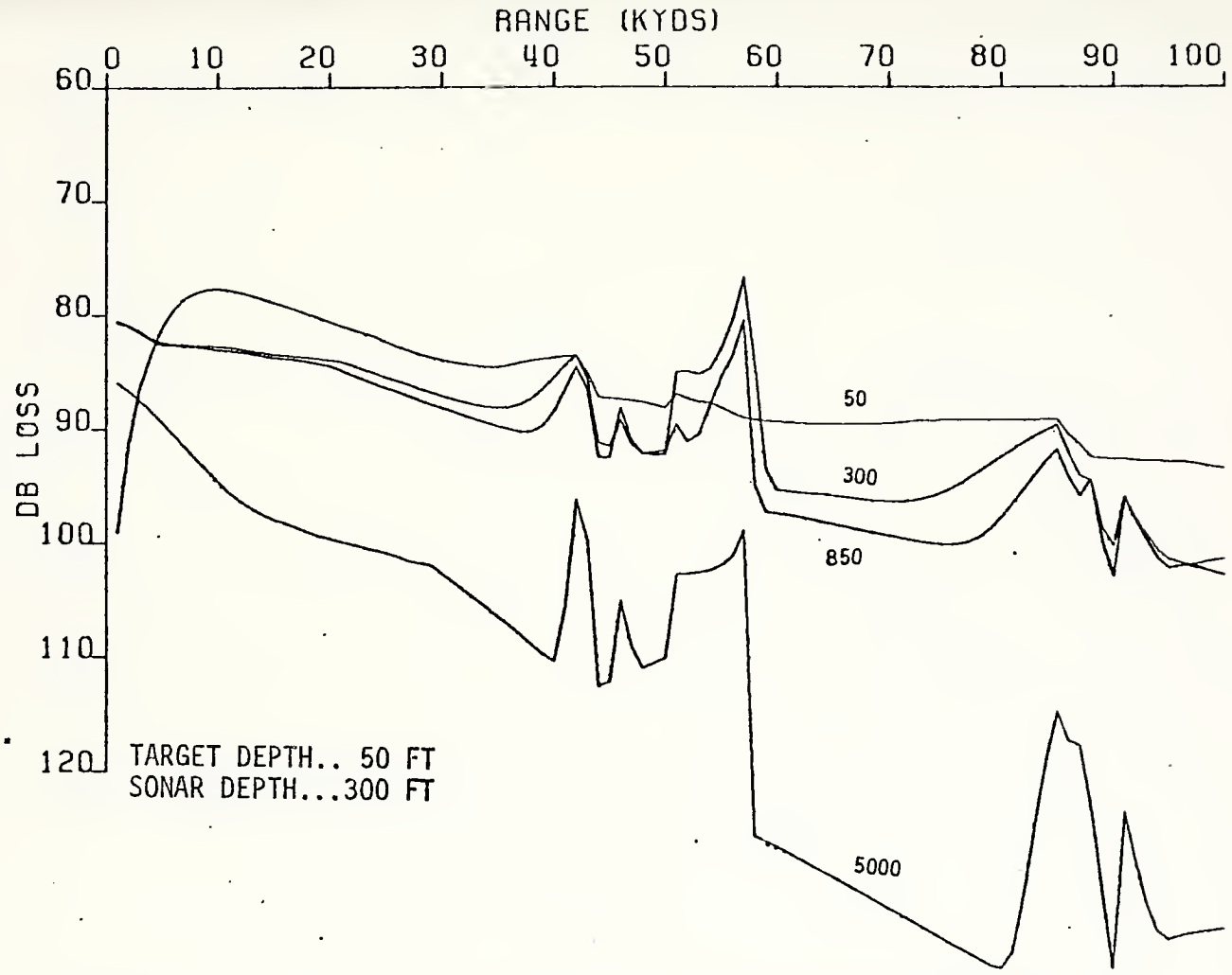

Figure 64. Transmission loss at point C in July with shown depths above.

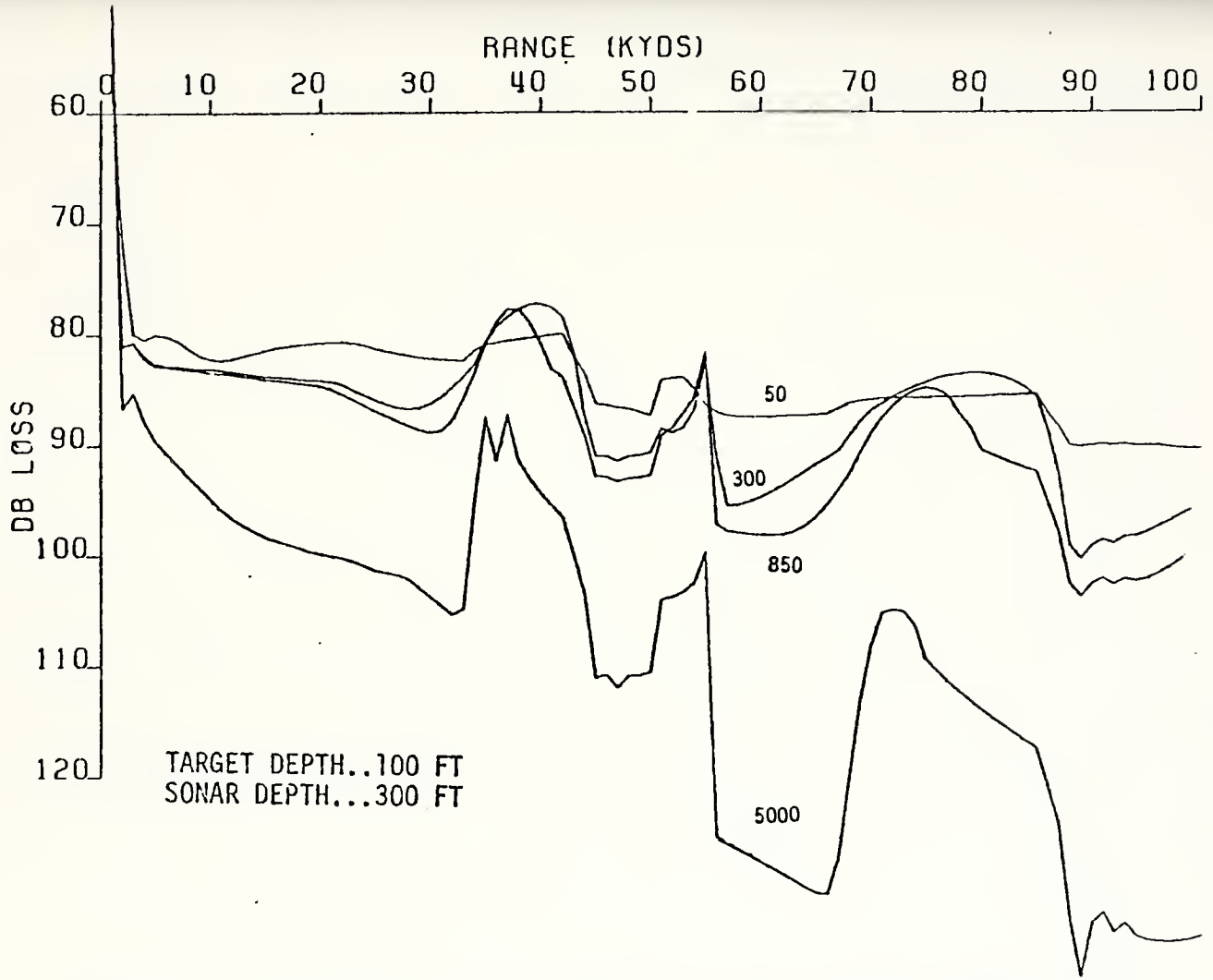

Figure 65. Transmission loss at point C in July with shown depths above.

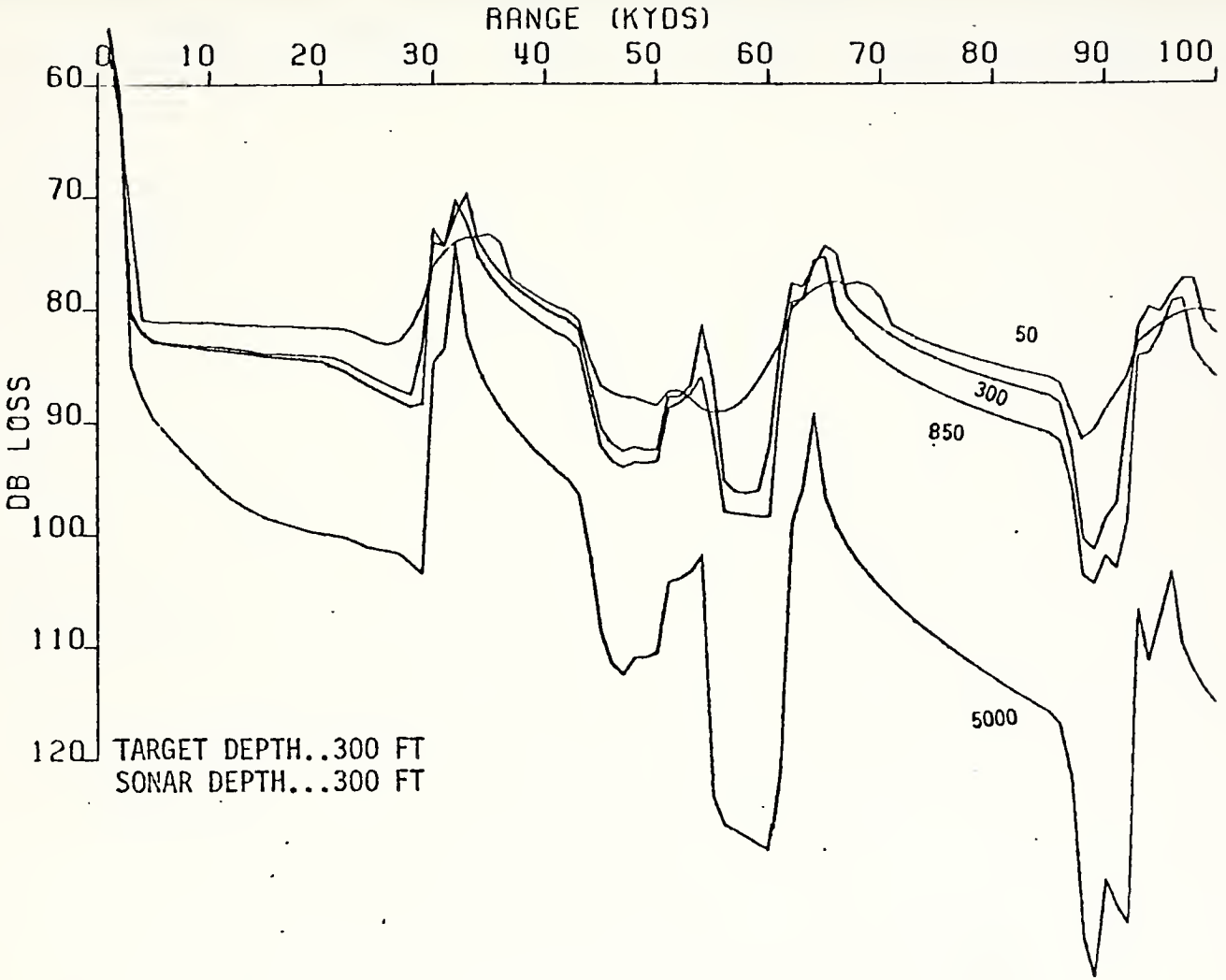

Figure 66. Transmission loss at point C in July with shown depths above.

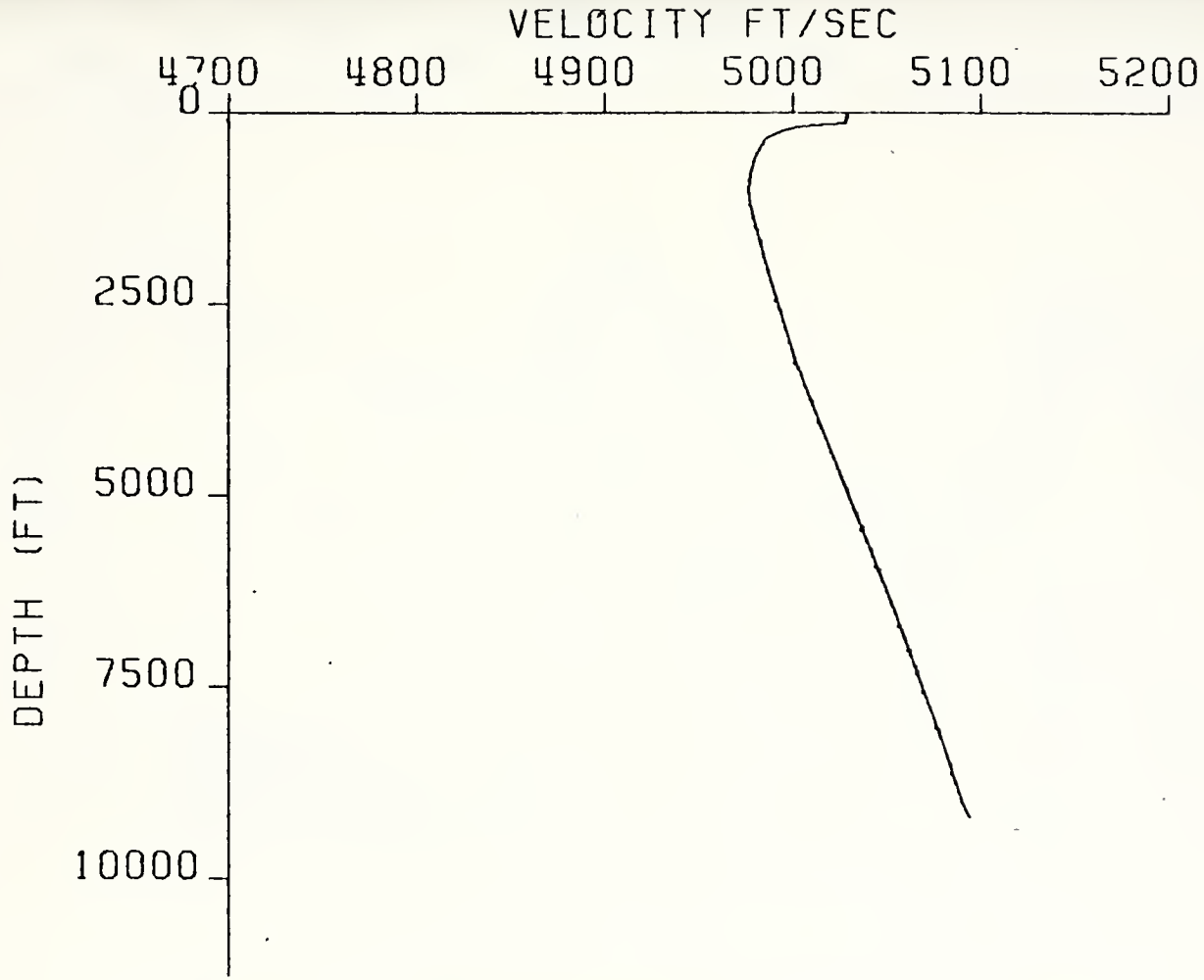

Figure 67. Sound velocity profile at point C in November.

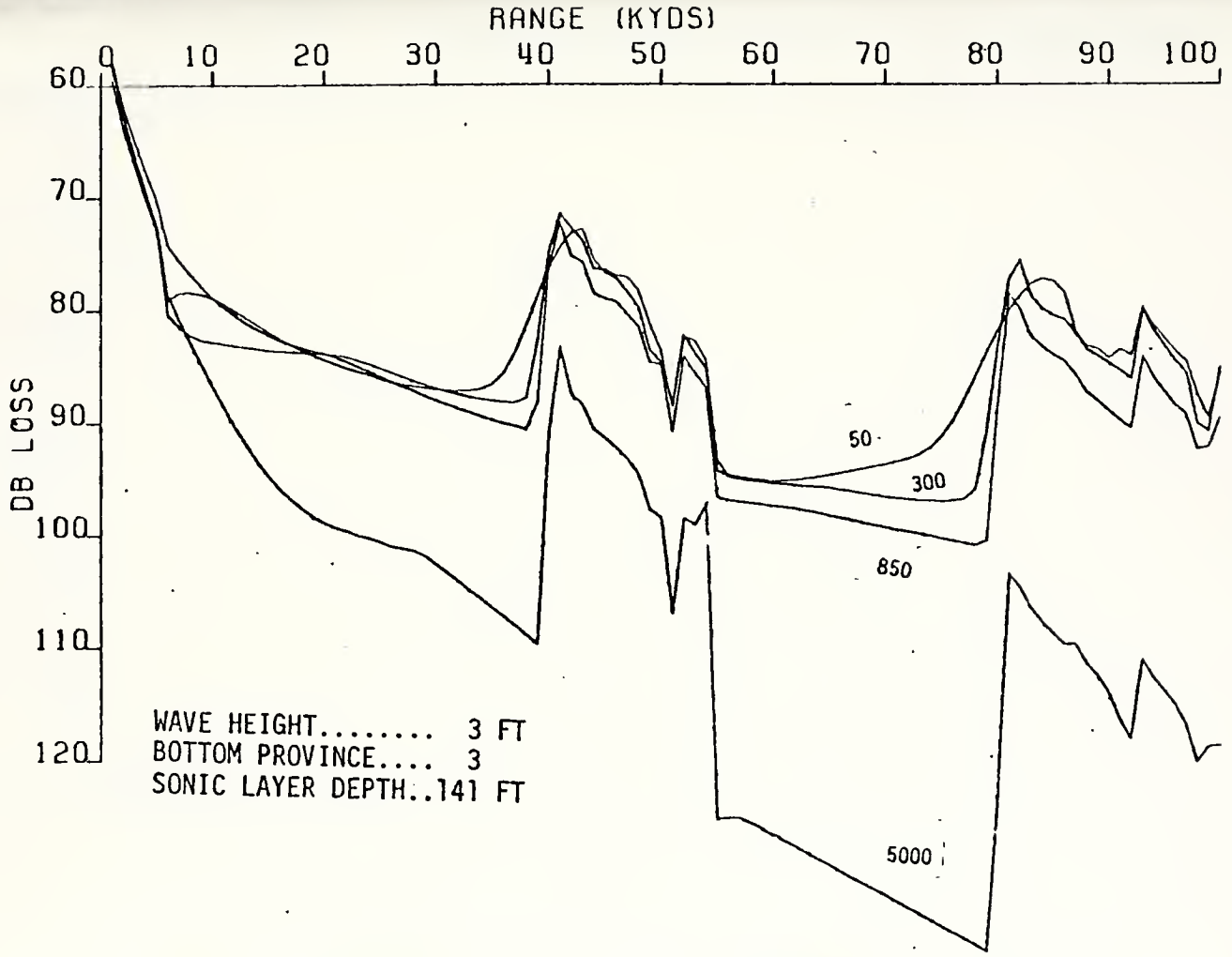

Figure 68. Transmission loss at point C in November.

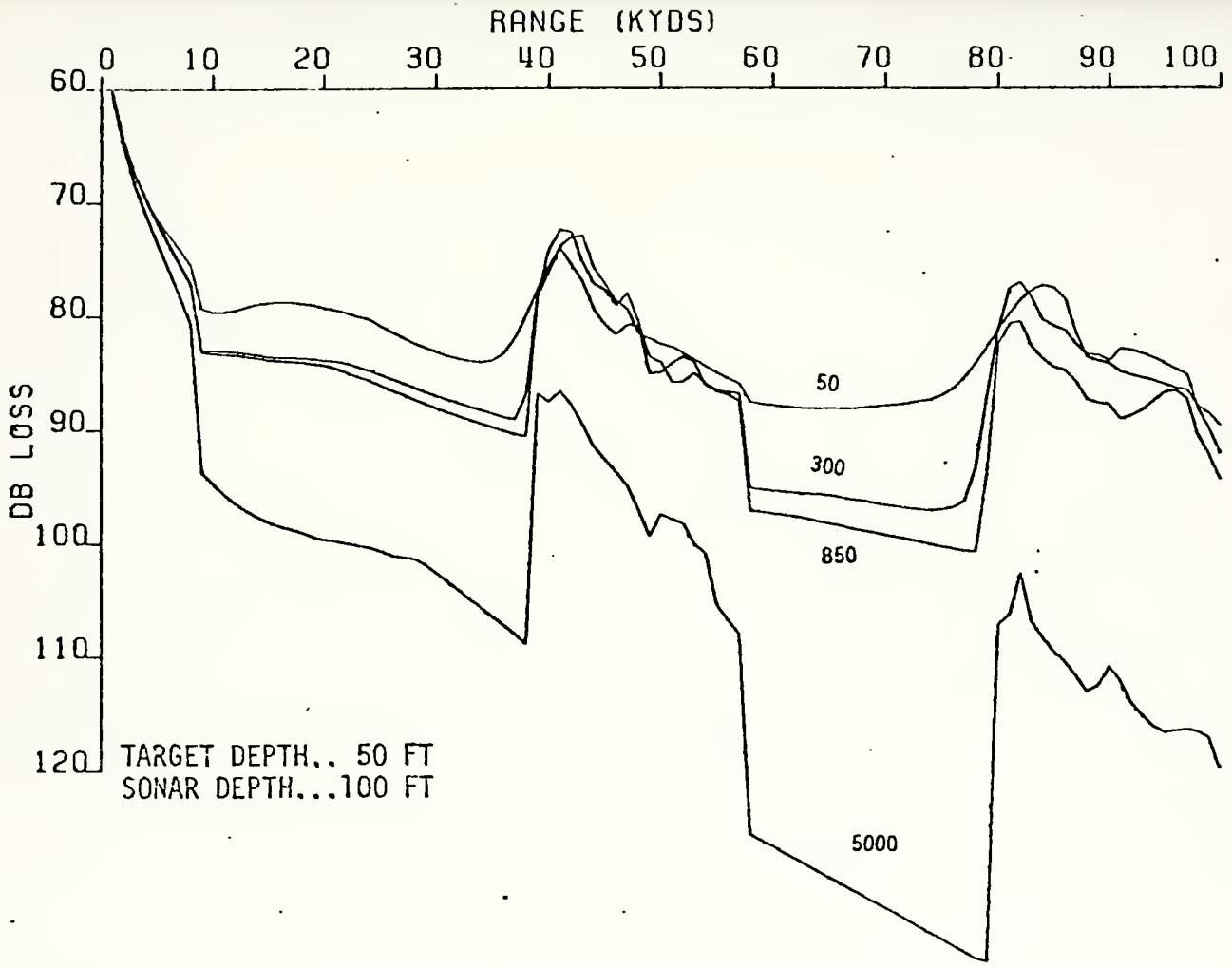

Figure 69. Transmission loss at point C in November with shown depths above.

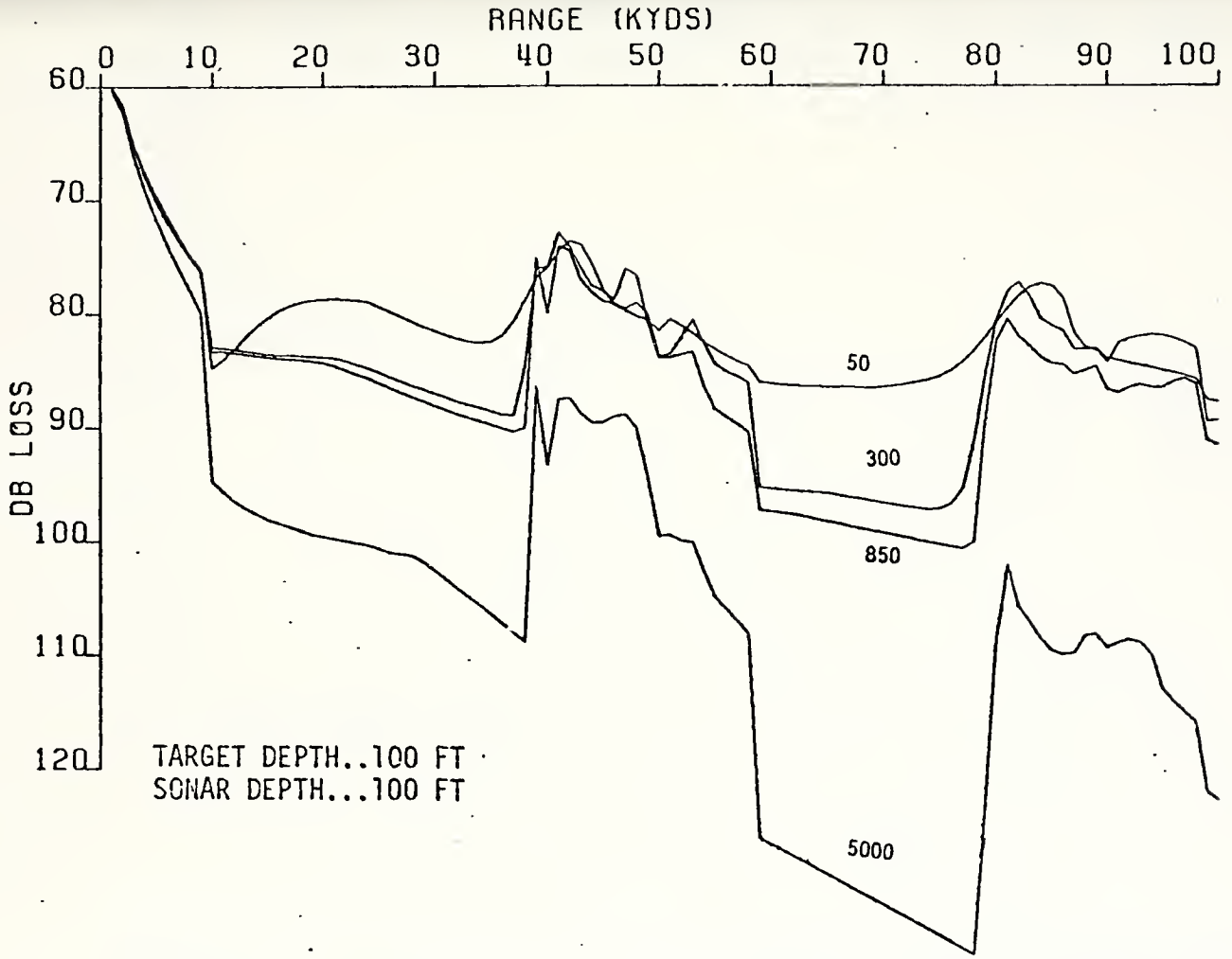

Figure 70. Transmission loss at point C in November with shown depths above.

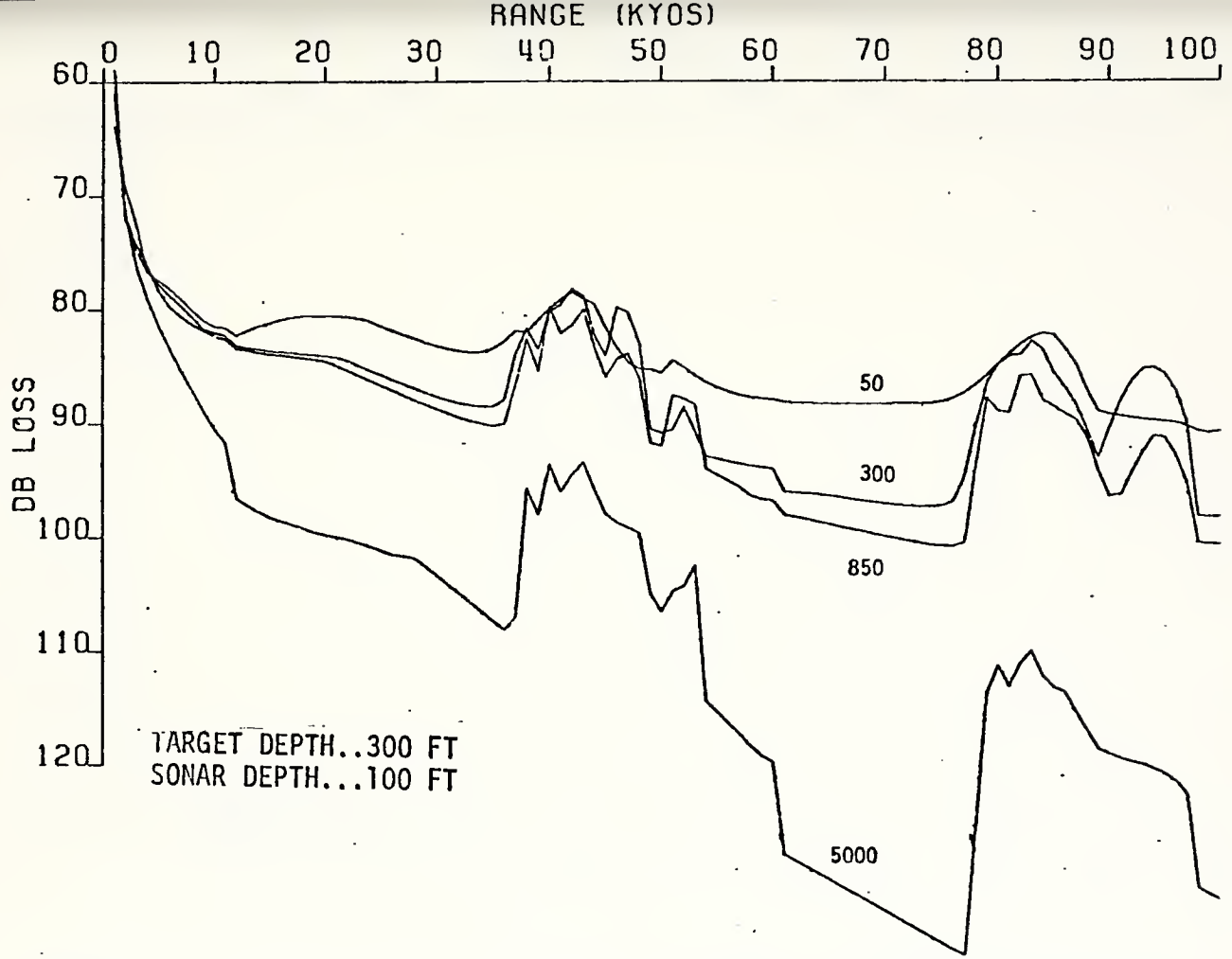

Figure 71. Transmission loss at point C in November with shown depths above.

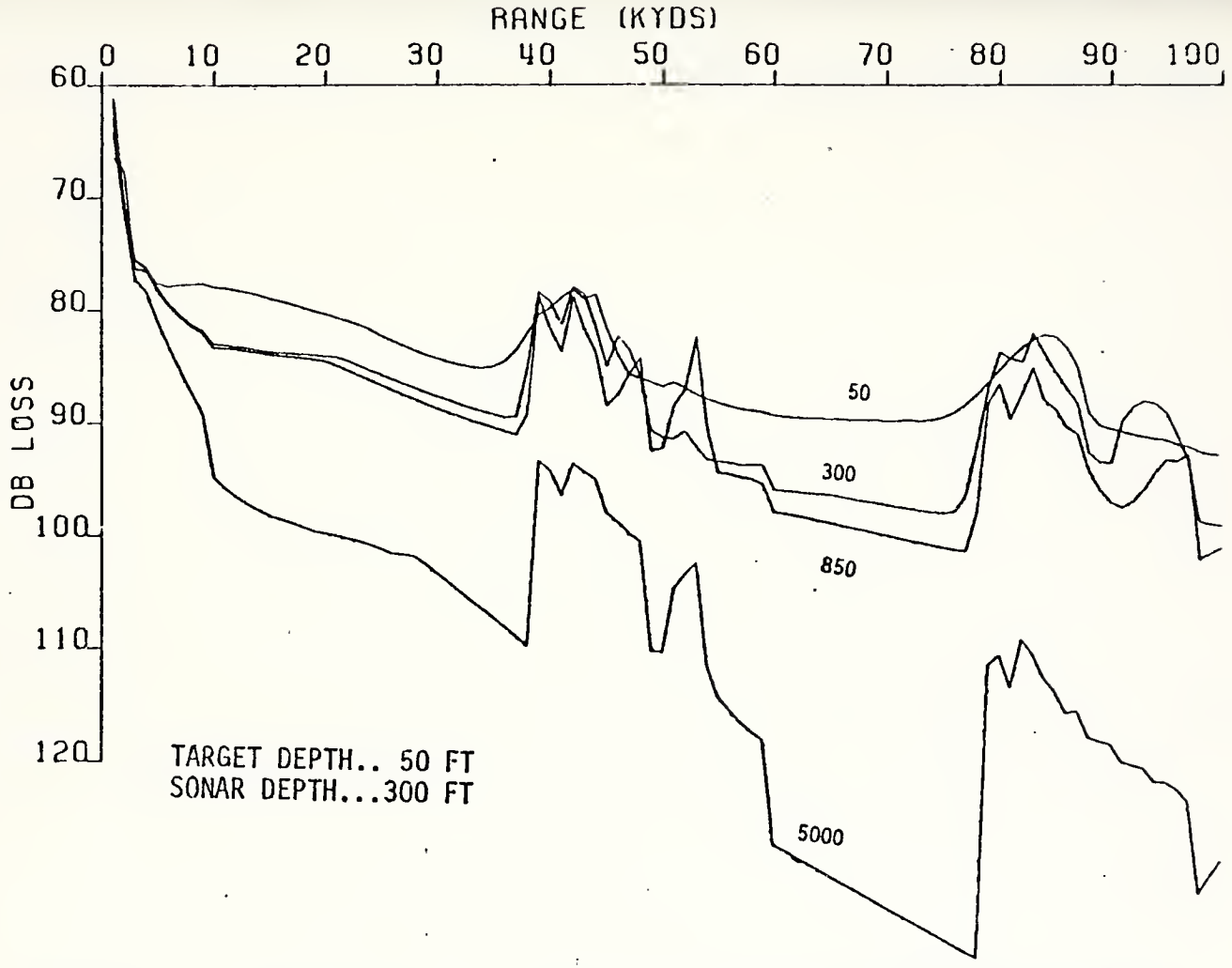

Figure 72. Transmission loss at point C in November with shown depths above.

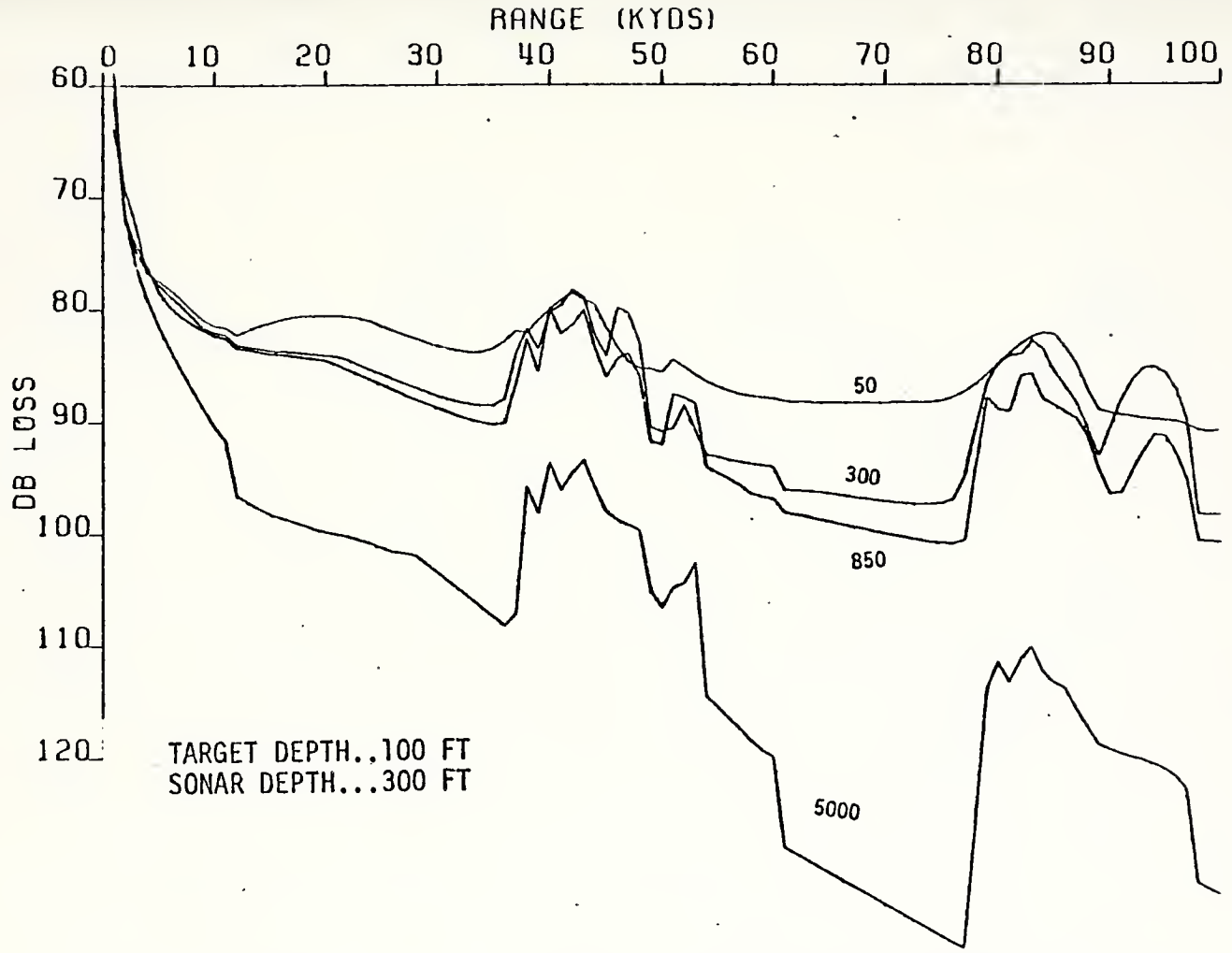

Figure 73. Transmission loss at point C in November with shown depths above.

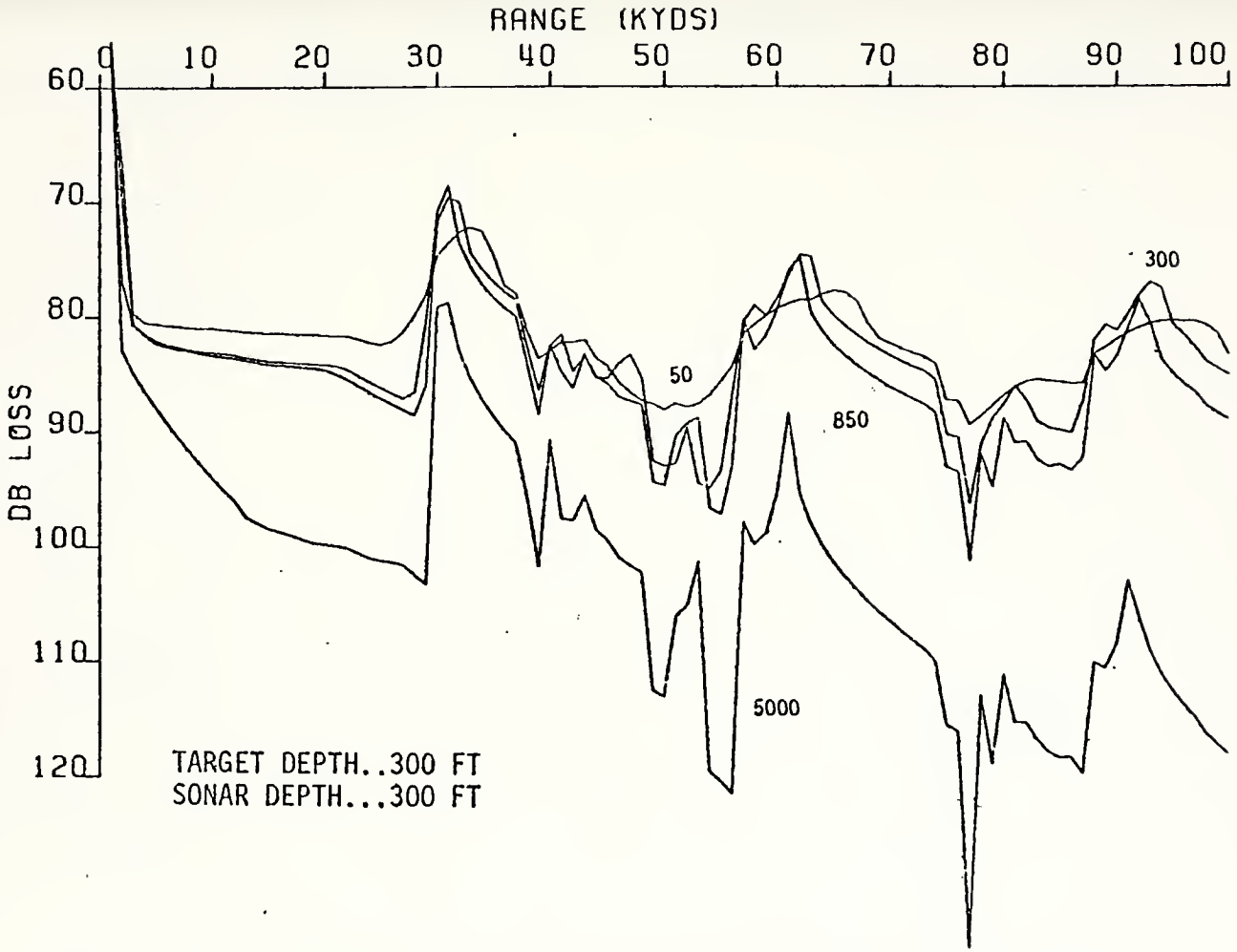

Figure 74. Transmission loss at point C in November with shown depths above.

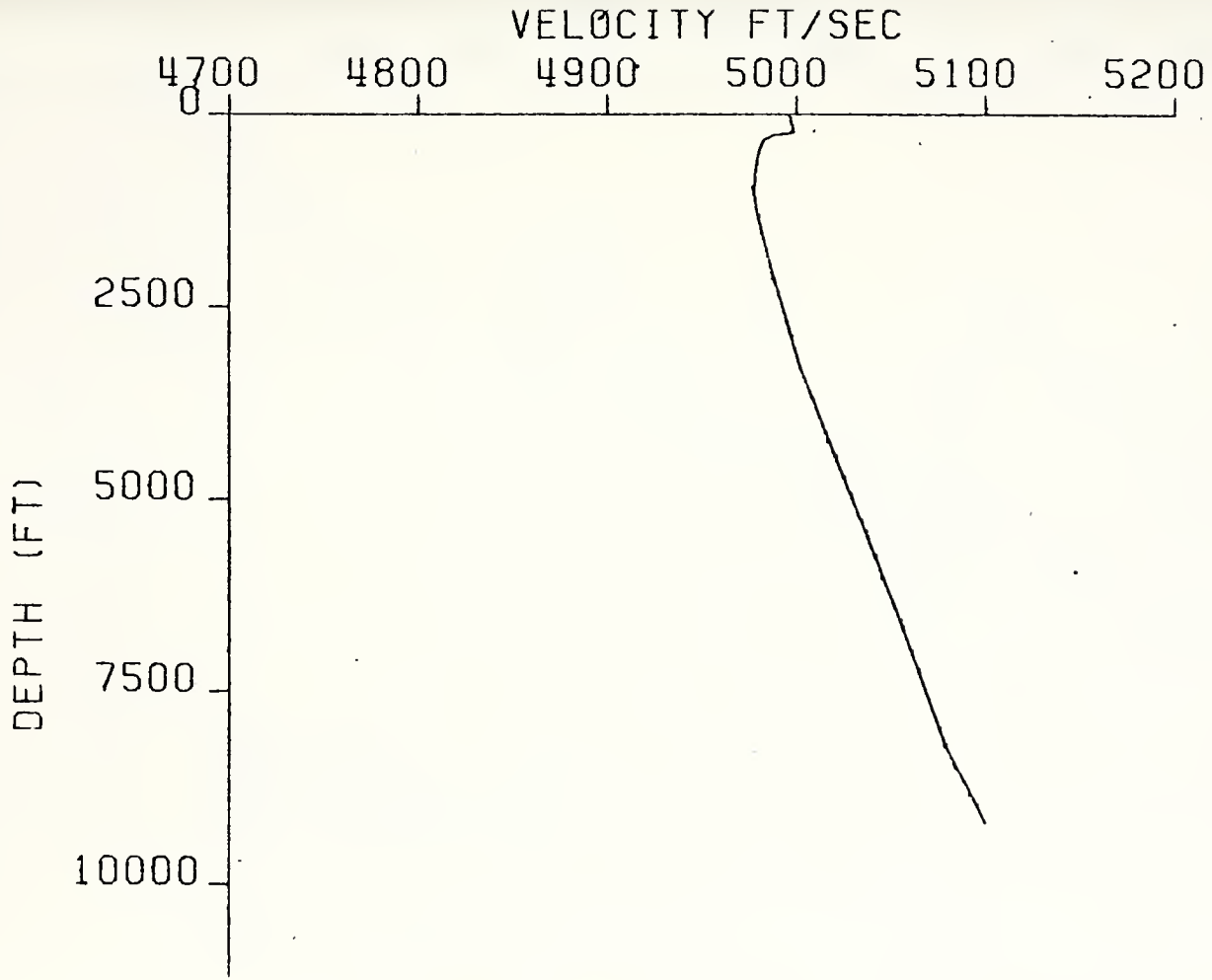

Figure 75. Sound velocity profile at point C in December.

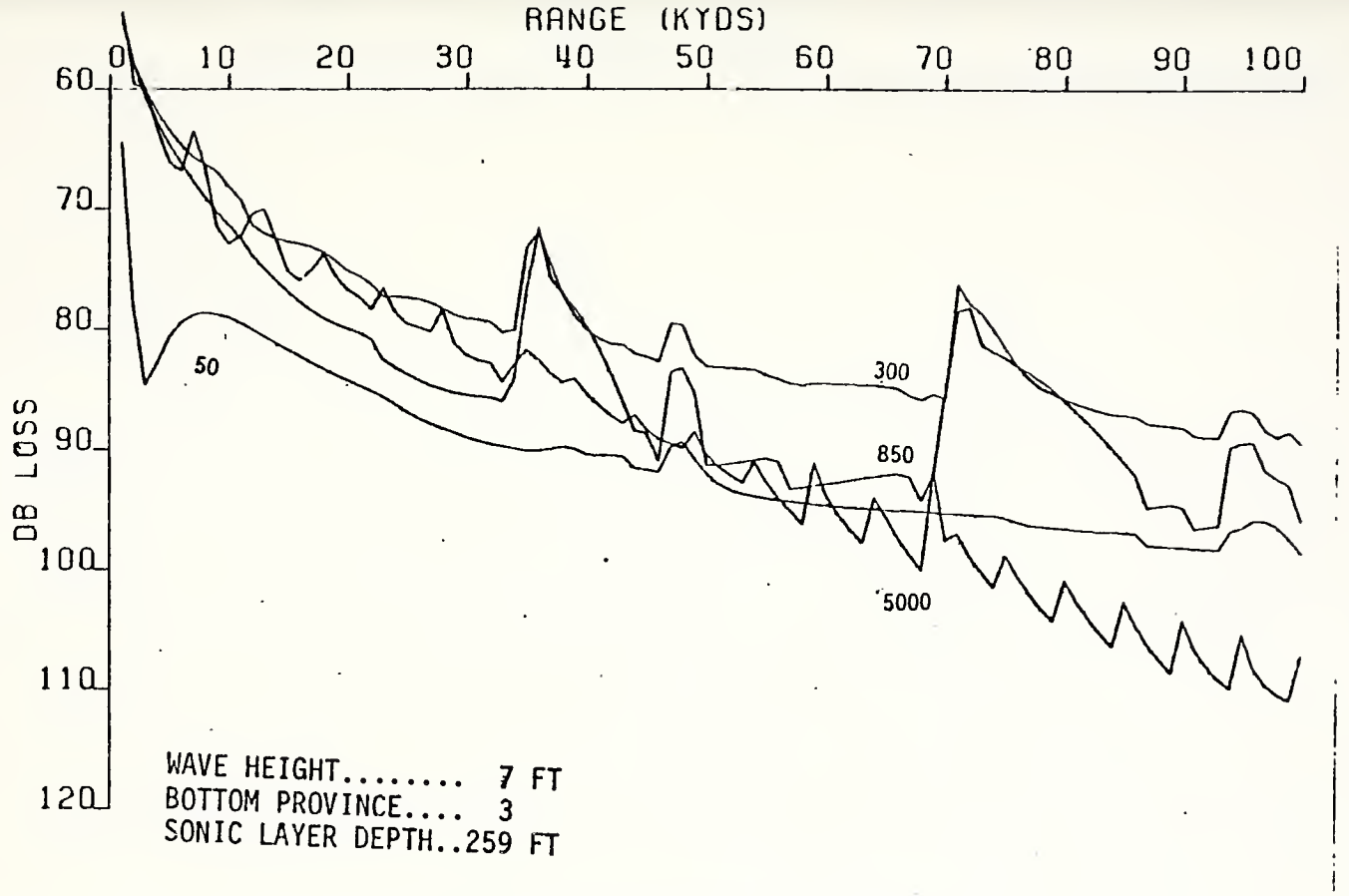

Figure 76. Transmission loss at point C in December.

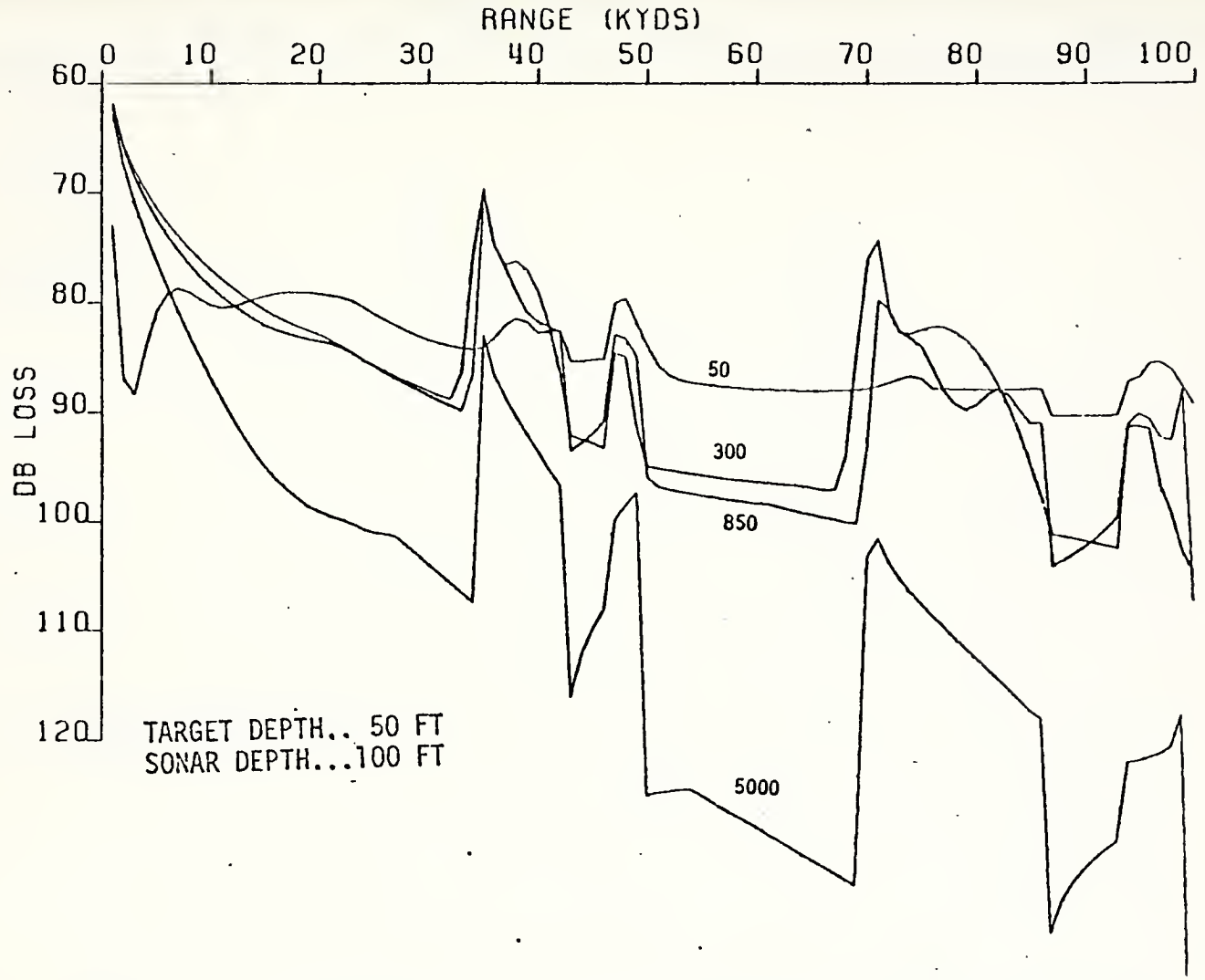

Figure 77. Transmission loss at point C in December with shown depths above.

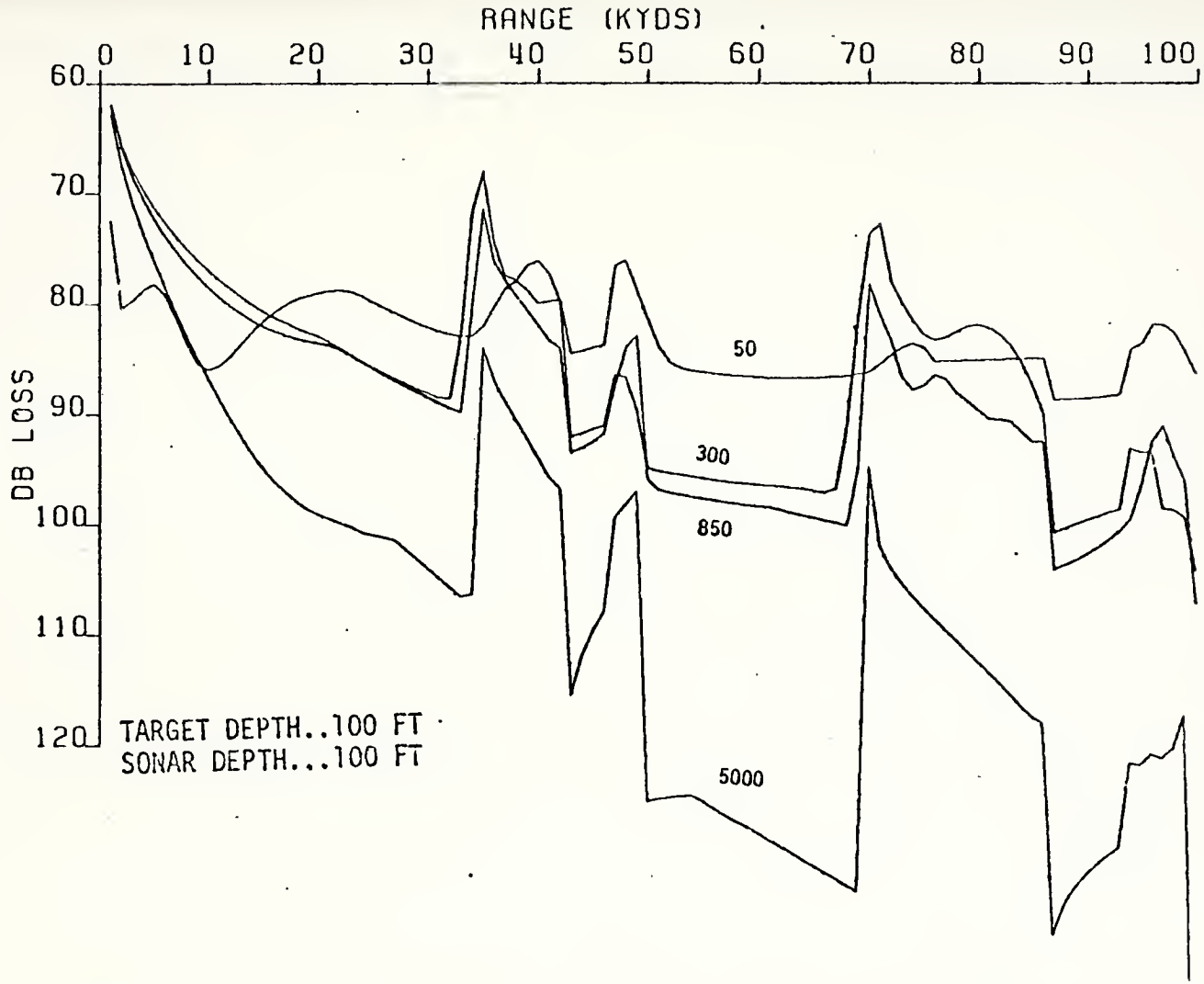

Figure 78. Transmission loss at point C in December with shown depths above.

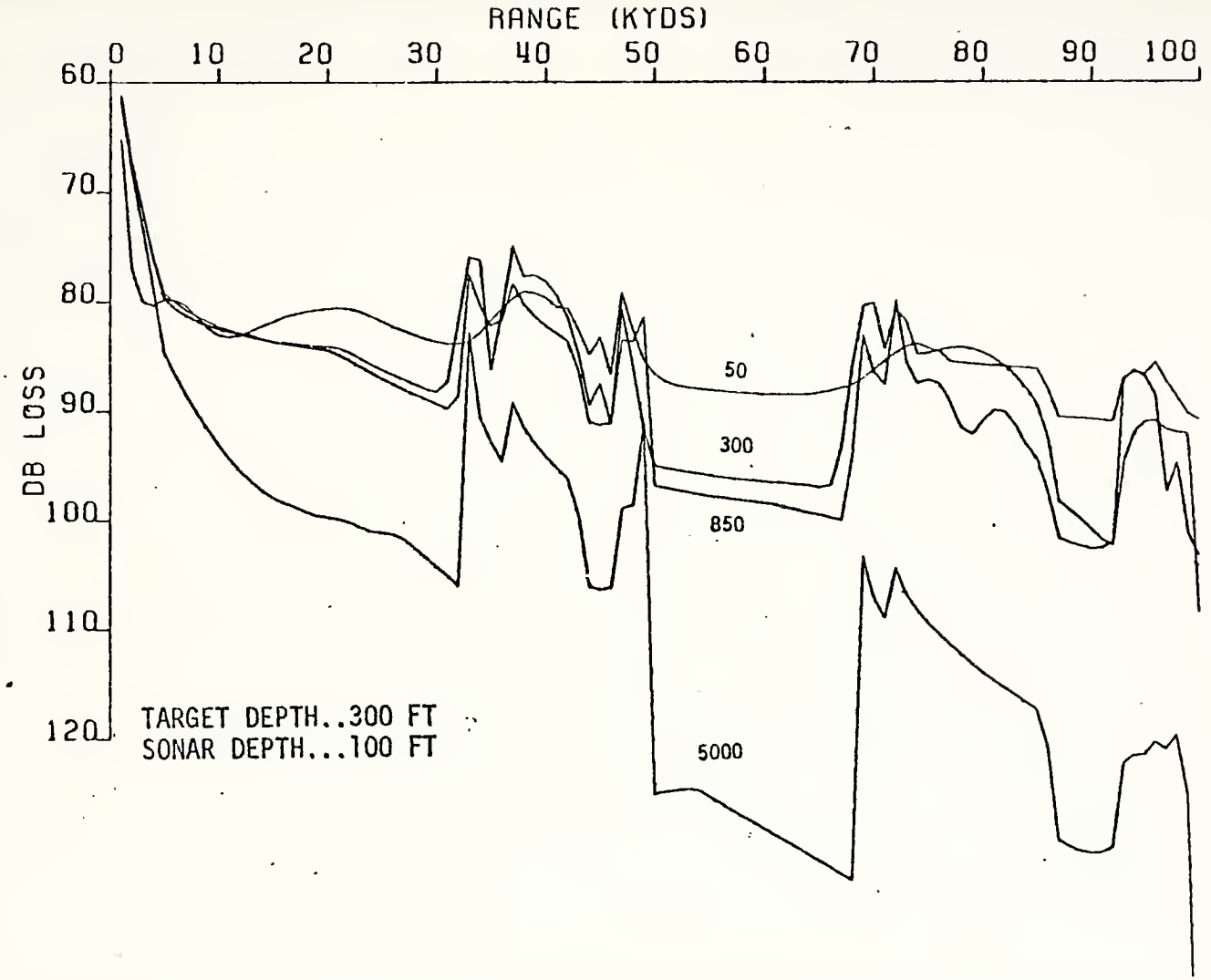

Figure 79. Transmission loss at point C in December with shown depths above.

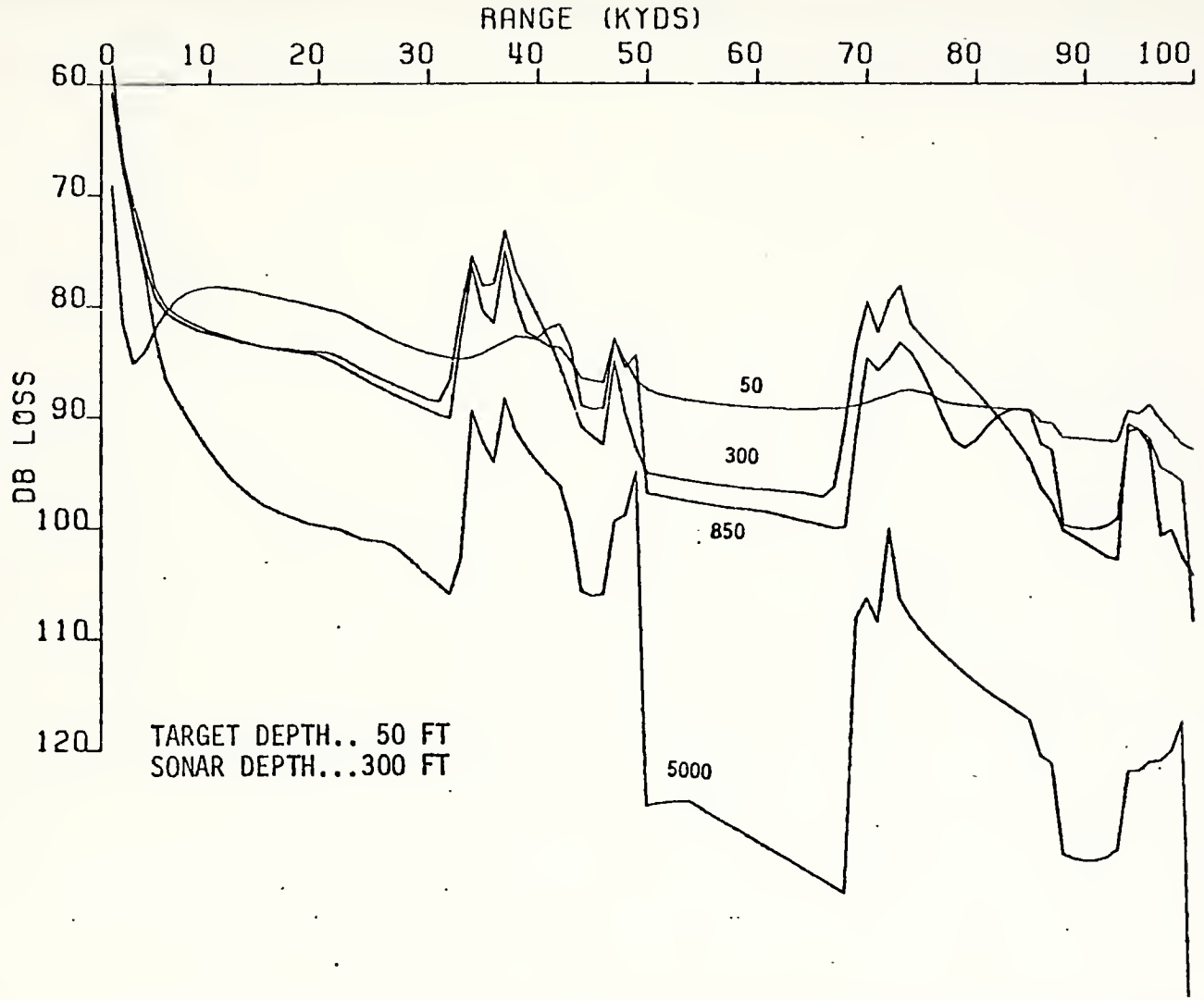

Figure 80. Transmission loss at point C in December with shown depths above.

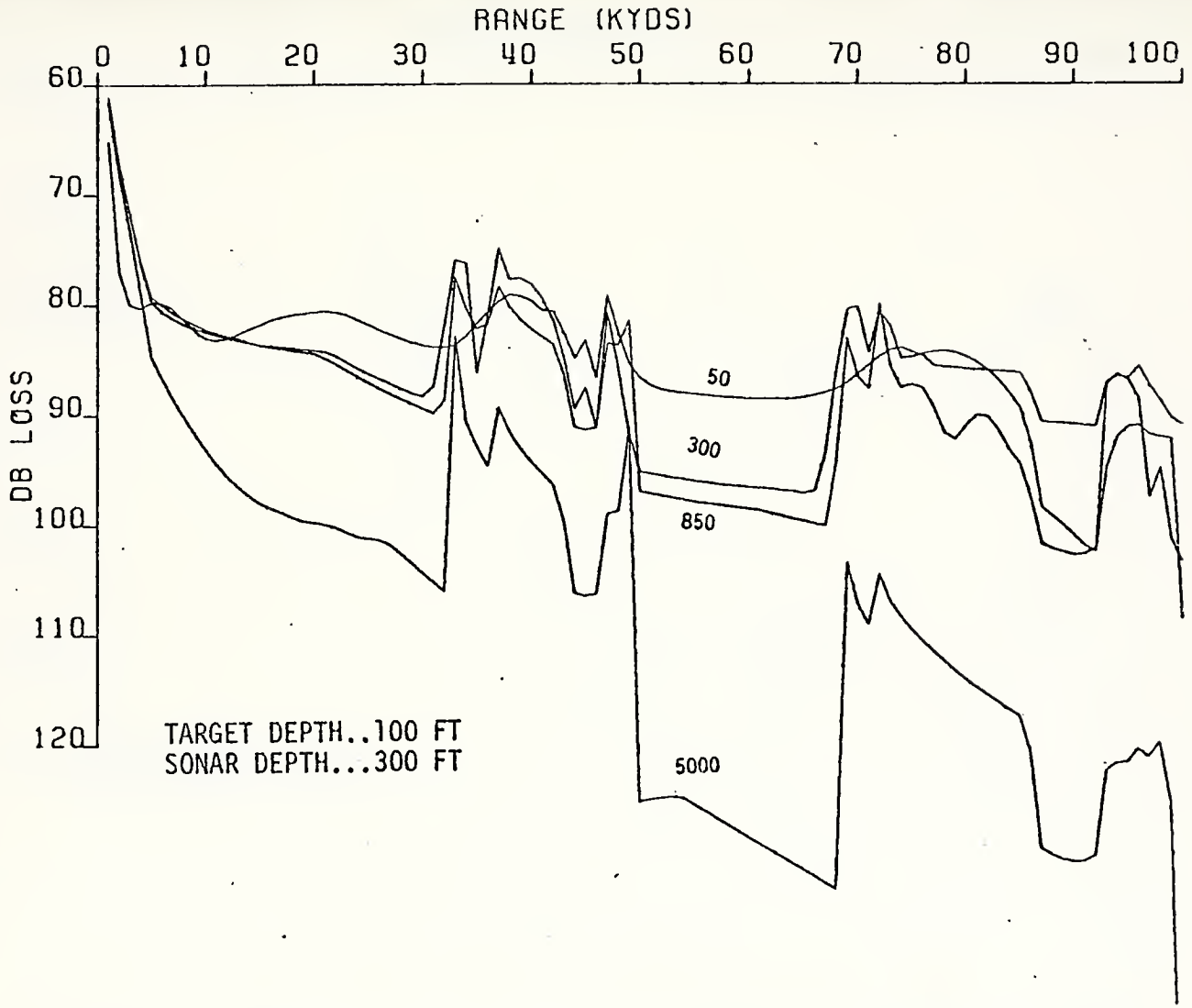

Figure 81. Transmission loss at point C in December with shown depths above.

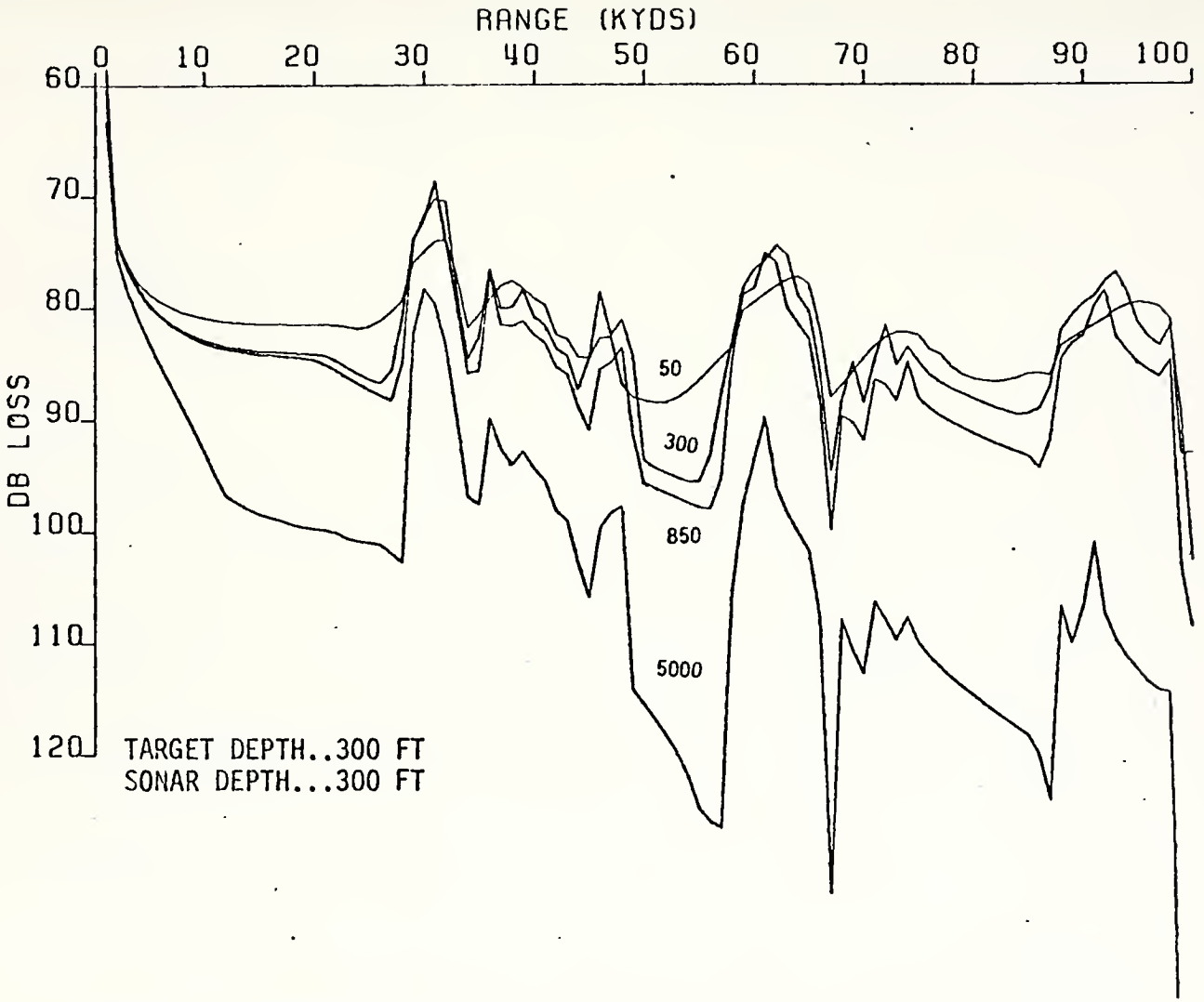

Figure 82. Transmission loss at point C in December with shown depths above.

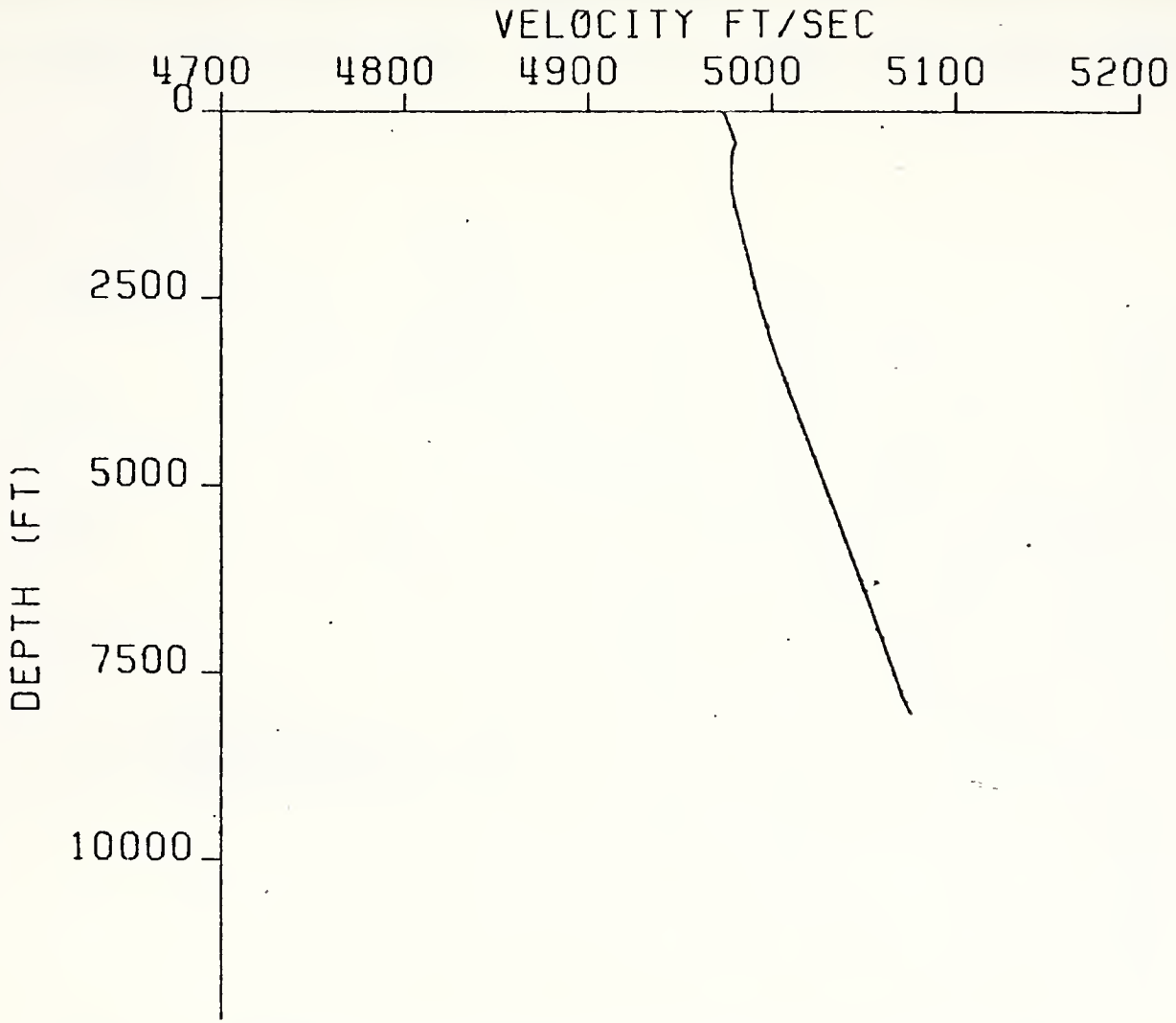

Figure 83. Sound velocity profile at point D in February.

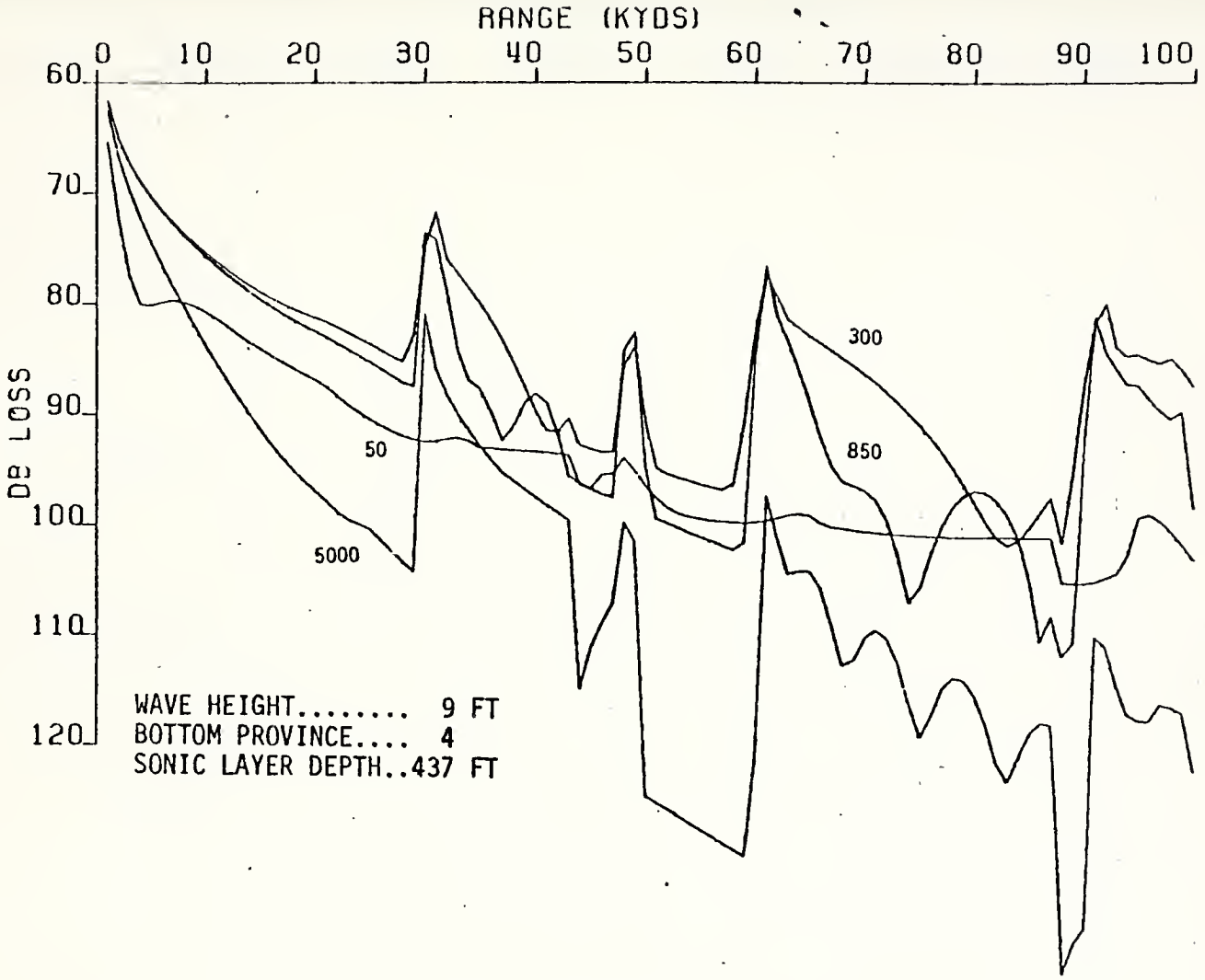

Figure 84. Transmission loss at point D in February.

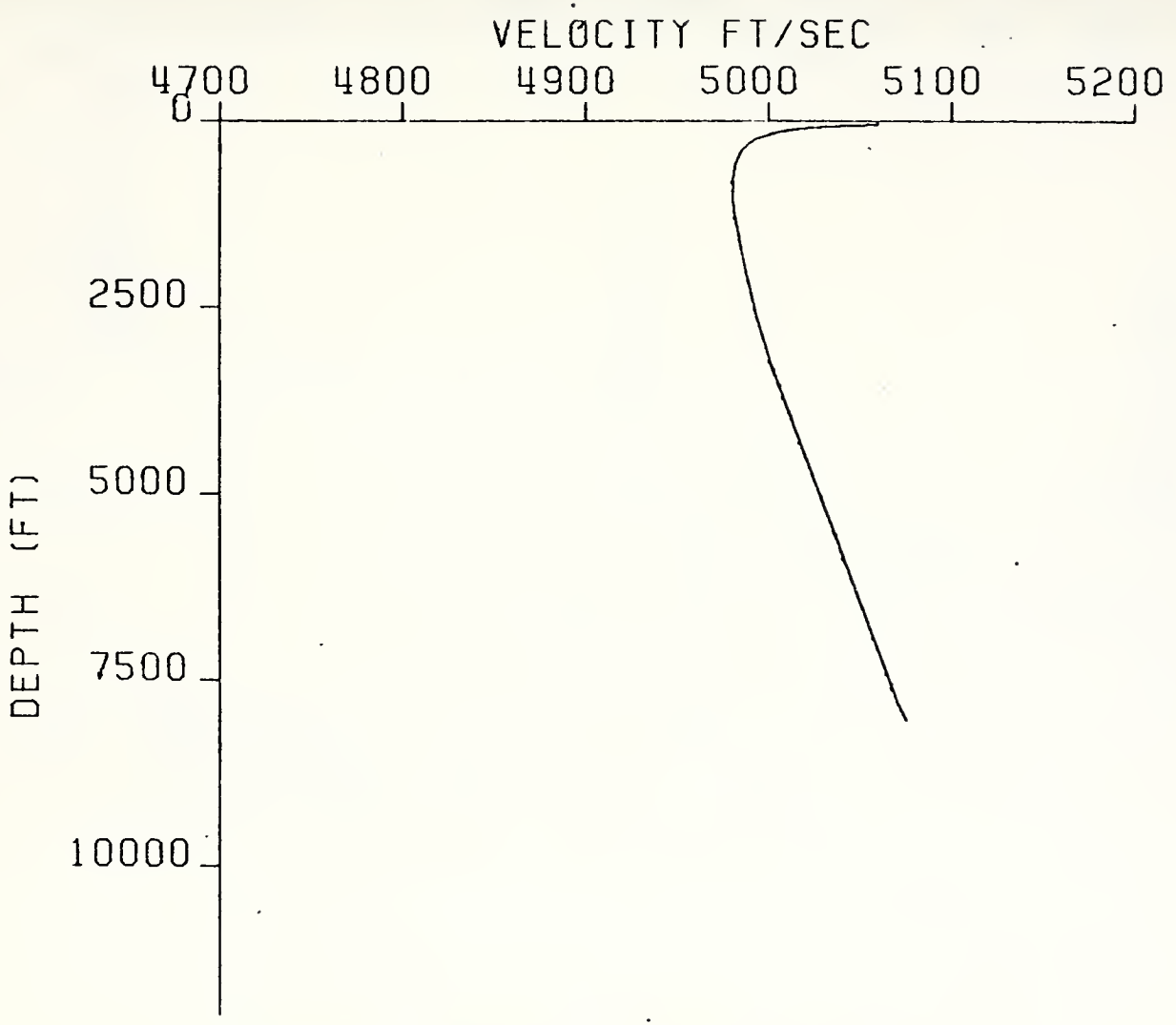

Figure 85. Sound velocity profile at point D in July.

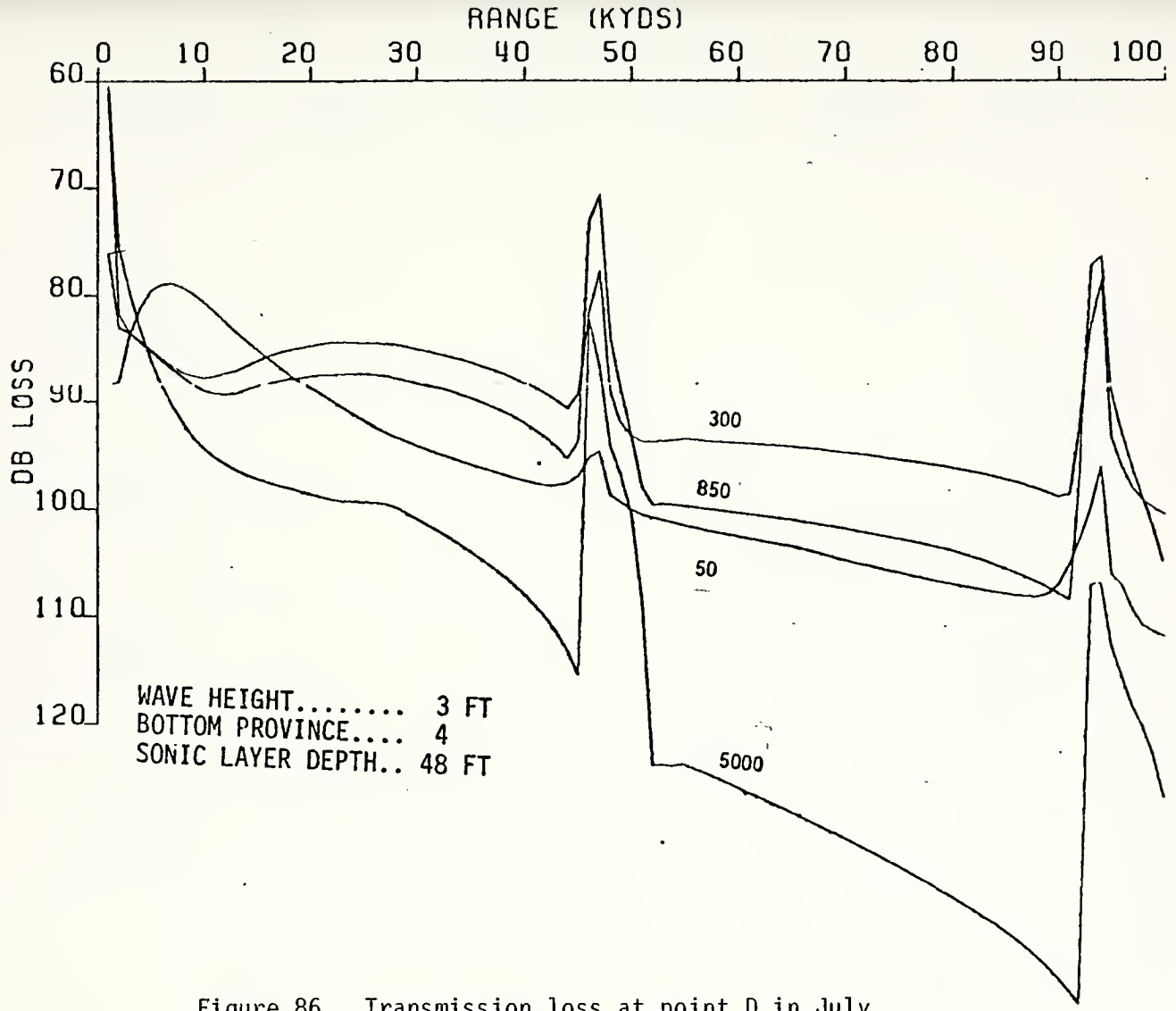

Figure 86. Transmission loss at point D in July.

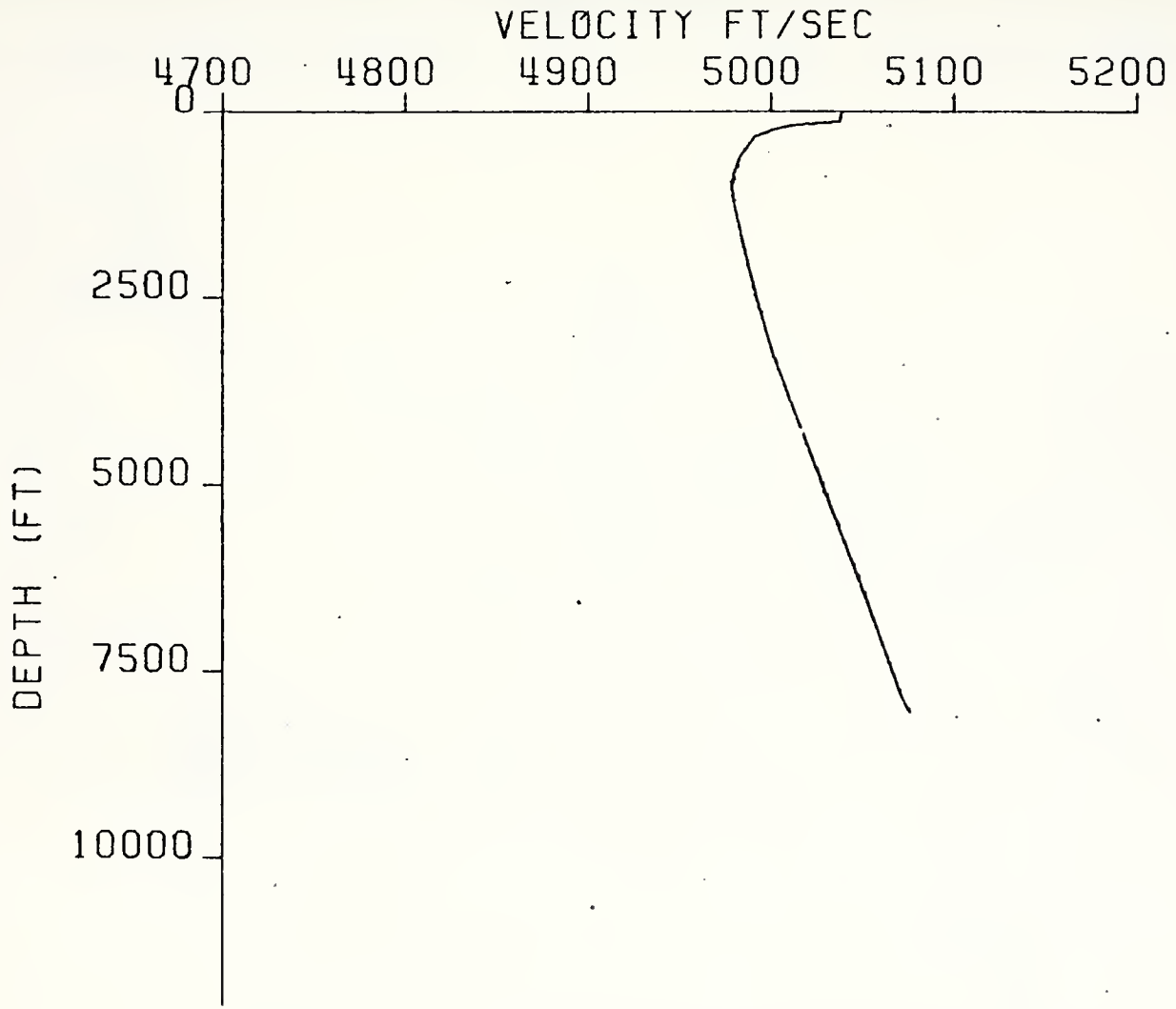

Figure 87. Sound velocity profile at point D in November.

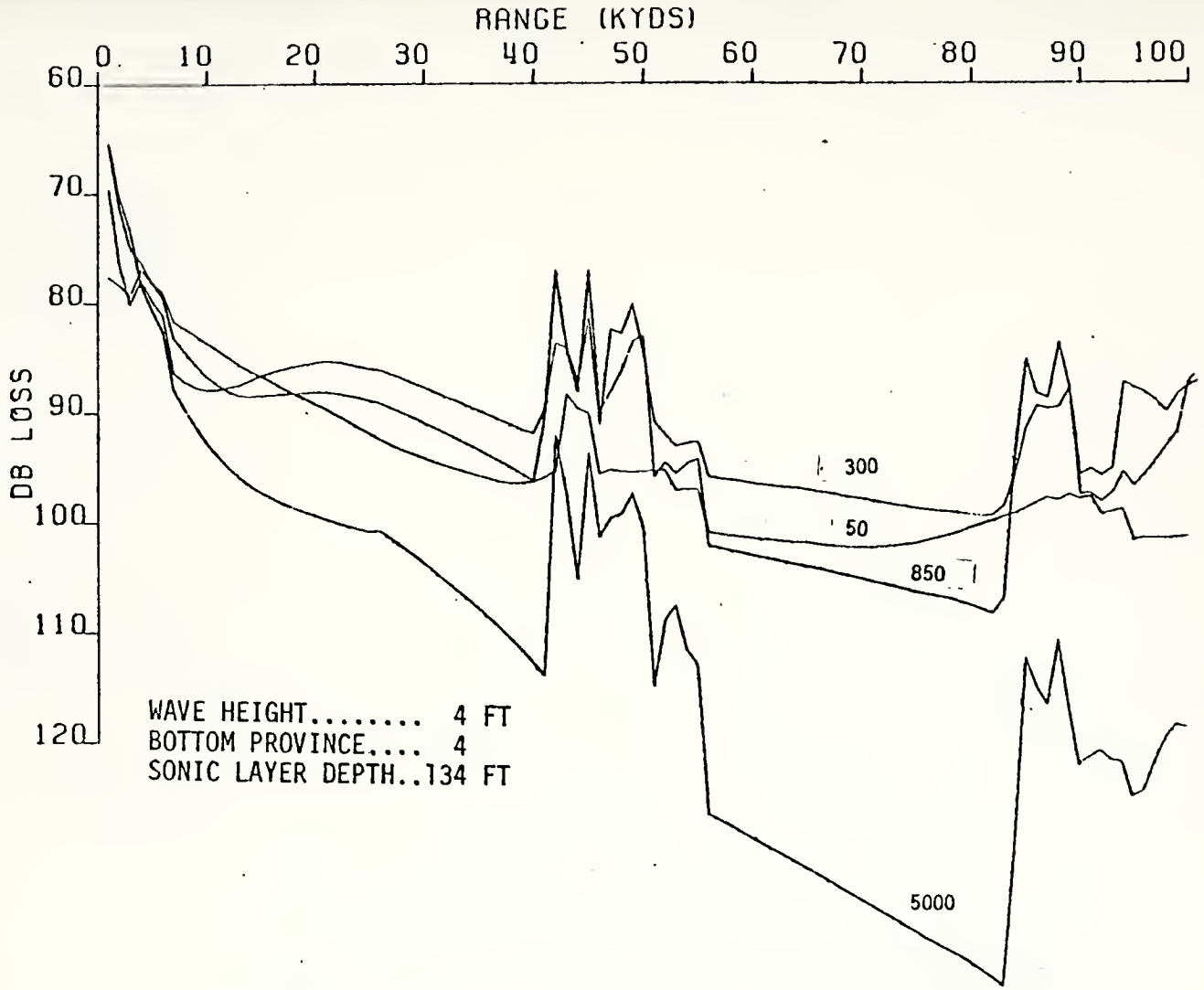

Figure 88. Transmission loss at point D in November.

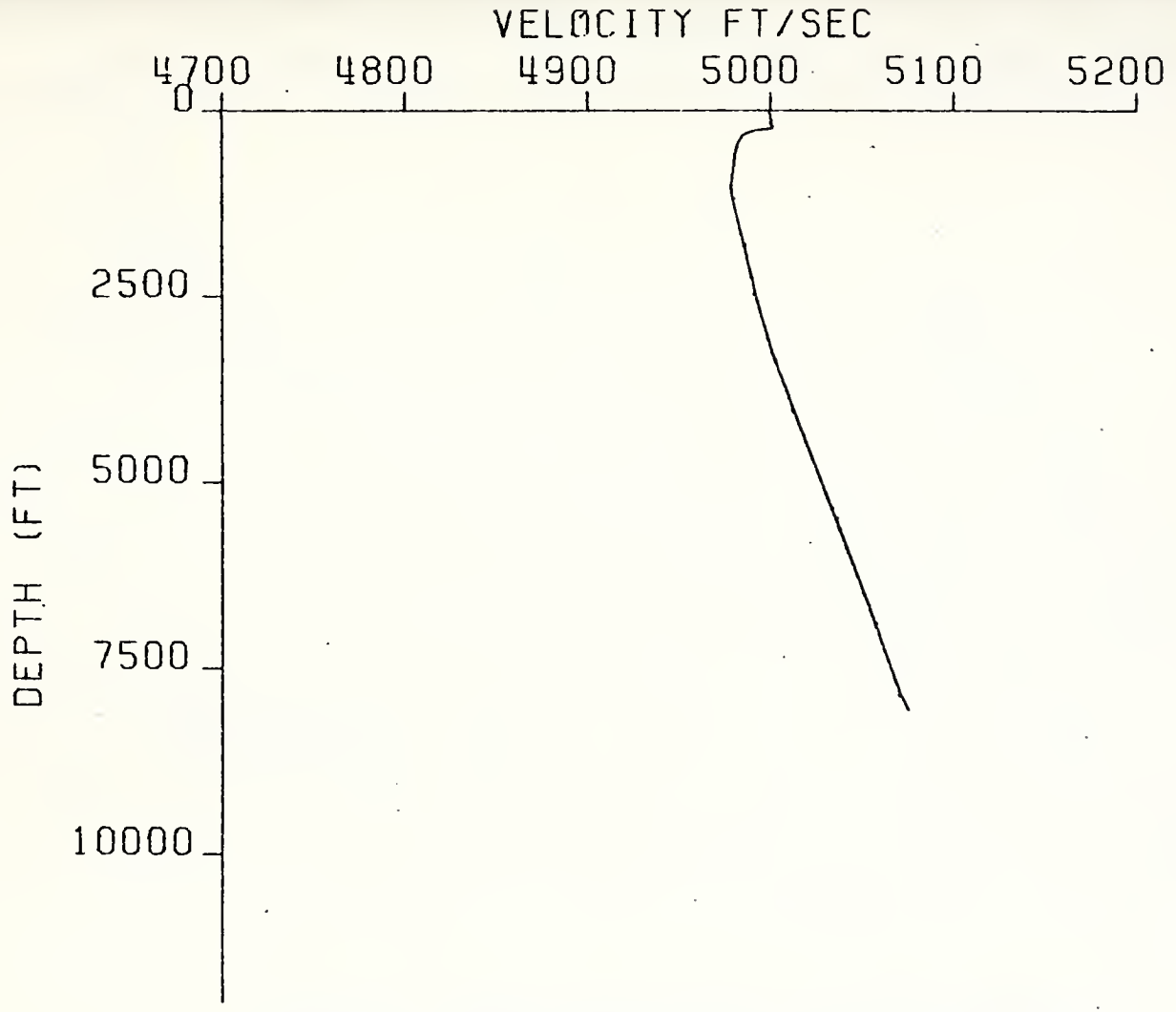

Figure 89. Sound velocity profile at point D in December.

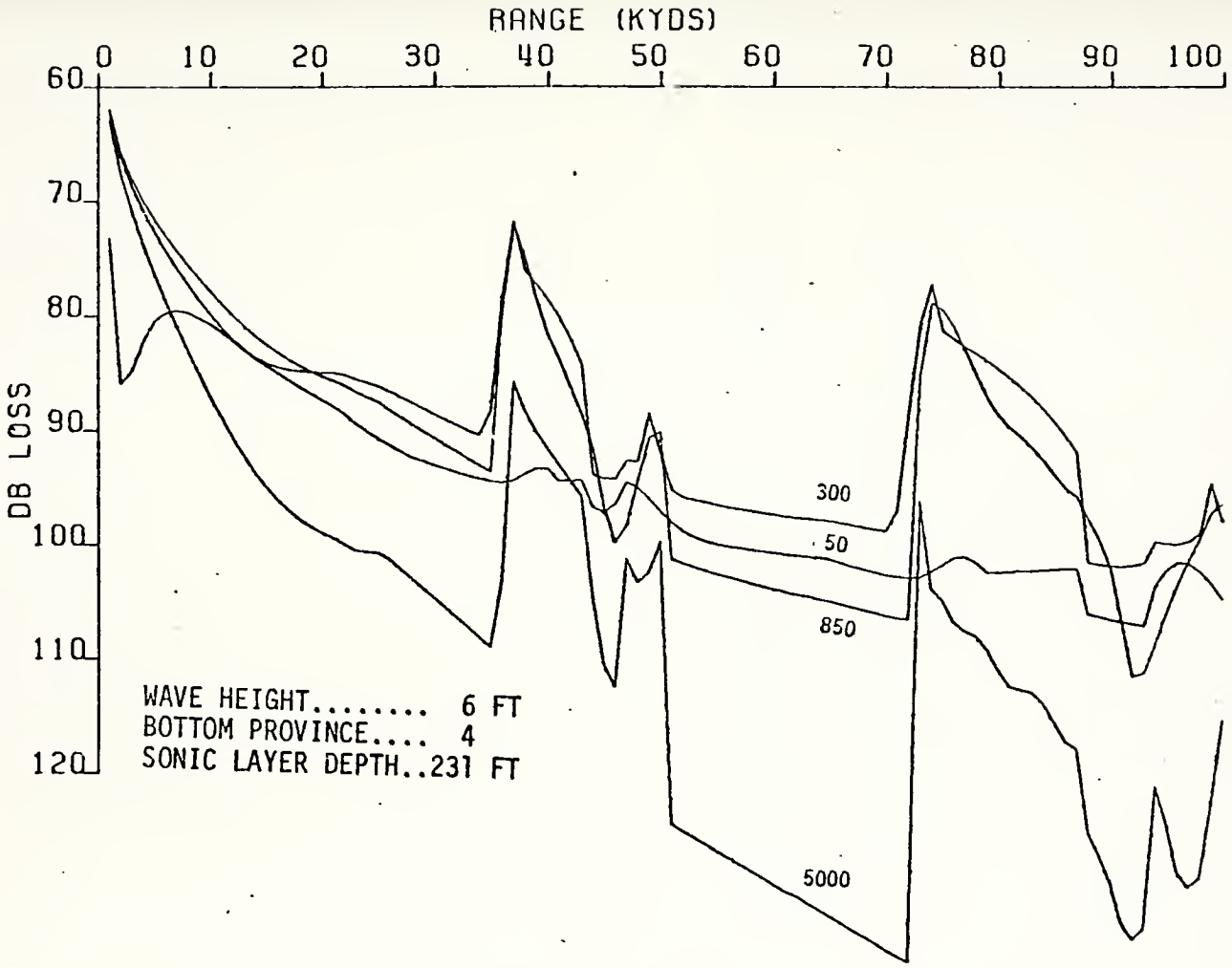

Figure 90. Transmission loss at point D in December.

APPENDIX B

MONTHLY BT DATA AT FOUR DIFFERENT LOCATIONS

(Data contains depth in meters, temperature in ^{o}C, salinity in parts per thousand, and sound velocity in meter/second.)

POINT A

0.00	16.42	38.83	1516.16
89.76	16.50	38.85	1517.89
97.38	16.21	38.85	1517.14
105.00	16.04	38.86	1516.77
120.24	15.86	38.87	1516.47
150.72	15.56	38.89	1516.18
182.88	15.38	38.91	1516.09
243.84	15.07	38.91	1516.13
304.80	14.84	38.90	1516.44
365.76	14.69	38.90	1516.95
600.00	14.31	38.79	1519.47
800.00	14.03	38.78	1521.90
1000.00	13.84	38.75	1524.58
1500.00	13.73	38.70	1532.47
2000.00	13.67	38.69	1540.67
2500.00	13.67	38.66	1549.08
3000.00	13.63	38.64	1557.46
3088.00	13.62	38.63	1558.91

POINT B

0.00	17.07	38.74	1517.97
60.96	17.07	38.80	1519.06
106.01	17.08	38.84	1519.66
113.63	16.71	38.85	1518.92
121.25	16.52	38.86	1518.48
136.49	16.31	38.87	1518.13
166.97	16.04	38.90	1517.84
243.84	15.33	38.91	1516.95
304.80	14.94	38.87	1516.69
365.76	14.73	38.84	1516.99
600.00	14.24	38.73	1519.18
800.00	13.90	38.67	1521.36
1000.00	13.72	38.67	1524.06
1500.00	13.65	38.63	1532.14
1900.00	13.66	38.61	1538.85

POINT C

0.00	16.93	39.07	1517.96
60.96	16.93	39.10	1519.01
102.36	16.94	39.10	1519.71
109.98	16.57	39.10	1518.74
117.60	16.37	39.10	1518.27
132.84	16.17	39.10	1517.92
163.32	15.91	39.08	1517.61
243.84	15.30	38.99	1516.96
304.80	14.91	38.94	1516.69
365.76	14.70	38.88	1516.94
600.00	14.24	38.75	1519.27
800.00	13.94	38.72	1521.53
1000.00	13.76	38.69	1524.24
1500.00	13.67	38.66	1532.25
2000.00	13.59	38.64	1540.36
2500.00	13.51	38.67	1547.93
2741.00	13.47	38.60	1551.16

POINT D

0.00	17.10	39.01	1517.35
60.96	17.10	39.04	1518.44
108.32	17.10	39.05	1520.23
115.94	16.66	39.06	1519.06
123.56	16.43	39.05	1518.51
138.80	16.23	39.07	1518.19
169.28	15.98	39.07	1517.91
243.84	15.43	39.04	1517.43
304.80	15.04	39.01	1517.18
365.76	14.82	38.97	1517.65
600.00	14.29	38.84	1519.91
800.00	13.92	38.76	1521.92
1000.00	13.66	38.73	1524.03
1500.00	13.54	38.65	1531.60
2000.00	13.43	38.62	1539.79
2370.00	13.18	38.59	1545.22

Figure 91. BT data in January.

POINT A

0.00	15.71	38.83	1514.01
60.96	15.72	38.85	1515.06
116.50	15.86	38.87	1516.46
126.12	15.67	38.87	1516.01
133.74	15.57	38.88	1515.87
148.98	15.46	38.89	1515.75
179.46	15.31	38.91	1515.81
243.84	15.06	38.91	1516.12
304.80	14.88	38.90	1516.55
365.76	14.74	38.90	1517.12
600.00	14.39	38.79	1519.72
800.00	14.11	38.78	1522.14
1000.00	13.90	38.75	1524.75
1500.00	13.76	38.70	1532.57
2000.00	13.68	38.69	1540.71
2500.00	13.67	38.66	1549.09
3000.00	13.63	38.64	1557.46
3088.00	13.62	38.63	1558.91

POINT B

0.00	16.24	38.74	1515.51
60.96	16.20	38.80	1516.46
144.41	16.14	38.88	1517.74
152.03	15.96	38.89	1517.33
159.65	15.85	38.90	1517.13
174.89	15.71	38.91	1516.98
205.37	15.49	38.93	1516.84
243.84	15.28	38.91	1516.79
304.80	14.92	38.87	1516.85
365.76	14.73	38.84	1517.00
600.00	14.28	38.73	1519.32
800.00	13.96	38.67	1521.52
1000.00	13.76	38.67	1524.20
1500.00	13.67	38.63	1532.22
1900.00	13.67	38.61	1538.90

POINT C

0.00	16.24	39.07	1515.89
60.96	16.18	39.10	1516.75
132.49	16.11	39.10	1517.72
140.11	15.97	39.10	1517.44
147.73	15.86	39.10	1517.29
162.97	15.76	39.08	1517.13
193.45	15.54	39.04	1516.91
243.84	15.26	38.99	1516.84
304.80	14.96	38.94	1516.85
365.76	14.77	38.88	1517.18
600.00	14.37	38.75	1519.62
800.00	14.06	38.72	1521.92
1000.00	13.85	38.69	1524.54
1500.00	13.72	38.66	1532.42
2000.00	13.61	38.64	1540.42
2500.00	13.31	38.67	1547.94
2741.00	13.07	38.60	1551.16

POINT D

0.00	16.24	39.01	1515.84
60.96	16.19	39.06	1516.74
133.24	16.12	39.06	1517.73
140.86	15.99	39.07	1517.46
148.48	15.90	39.07	1517.33
163.72	15.78	39.07	1517.20
194.20	15.57	39.07	1517.06
243.84	15.30	39.04	1517.03
304.80	14.99	39.01	1517.00
365.76	14.81	38.97	1517.42
600.00	14.39	38.86	1519.79
800.00	14.03	38.76	1521.98
1000.00	13.78	38.73	1524.33
1500.00	13.60	38.65	1531.99
2000.00	13.45	38.62	1539.87
2370.00	13.19	38.59	1545.25

Figure 92. BT data in February.

POINT A

0.00	15.82	38.83	1514.34
60.96	15.72	38.85	1515.06
98.91	15.66	38.85	1515.50
106.53	15.59	38.85	1515.40
114.15	15.53	38.86	1515.38
129.39	15.46	38.87	1515.41
159.87	15.32	38.90	1515.53
243.84	15.00	38.91	1515.92
304.80	14.79	38.91	1516.27
365.76	14.65	38.90	1516.84
600.00	14.32	38.79	1519.52
800.00	14.06	38.78	1522.01
1000.00	13.88	38.75	1524.68
1500.00	13.75	38.70	1532.54
2000.00	13.68	38.69	1540.70
2500.00	13.67	38.66	1549.09
3000.00	13.63	38.64	1557.46
3088.00	13.62	38.63	1558.91

POINT B

0.00	16.55	38.74	1516.42
60.96	16.41	38.80	1517.09
97.66	16.33	38.83	1517.49
105.28	16.19	38.84	1517.20
112.90	16.10	38.85	1517.06
128.14	15.97	38.86	1516.95
158.62	15.76	38.89	1516.86
243.84	15.33	38.91	1516.94
304.80	14.92	38.87	1516.62
365.76	14.71	38.84	1516.93
600.00	14.24	38.73	1519.19
800.00	13.92	38.67	1521.40
1000.00	13.73	38.67	1524.10
1500.00	13.66	38.63	1532.16
1900.00	13.66	38.61	1538.87

POINT C

0.00	16.70	39.07	1517.27
76.69	16.77	39.10	1518.80
84.31	16.55	39.10	1518.27
91.93	16.42	39.10	1517.99
107.17	16.25	39.10	1517.74
137.65	15.99	39.10	1517.44
182.88	15.67	39.05	1517.17
243.84	15.27	38.99	1516.87
304.80	14.85	38.94	1516.50
365.76	14.63	38.88	1516.74
600.00	14.19	38.75	1519.06
800.00	13.91	38.72	1521.42
1000.00	13.74	38.69	1524.18
1500.00	13.66	38.66	1532.22
2000.00	13.59	38.64	1540.35
2500.00	13.31	38.67	1547.93
2741.00	13.07	38.60	1551.16

POINT D

0.00	17.25	39.01	1518.82
75.02	17.28	39.06	1520.19
82.64	17.01	39.05	1519.52
90.26	16.84	39.05	1519.15
105.50	16.62	39.05	1518.75
135.97	16.26	39.06	1518.19
182.88	15.88	39.07	1517.82
243.84	15.40	39.04	1517.32
304.80	14.94	39.01	1516.85
365.76	14.71	38.97	1517.10
600.00	14.20	38.86	1519.23
800.00	13.86	38.76	1521.32
1000.00	13.65	38.73	1523.91
1500.00	13.52	38.65	1531.75
2000.00	13.42	38.62	1539.78
2370.00	13.18	38.59	1545.21

Figure 93. BT data in March.

POINT A

0.00	16.43	39.00	1516.39
16.17	16.44	38.96	1516.64
25.79	16.03	38.92	1515.52
33.41	15.83	38.90	1515.01
48.45	15.67	38.85	1514.71
79.13	15.51	38.79	1514.65
121.92	15.37	38.78	1514.91
182.88	15.19	38.84	1515.44
243.84	14.98	38.89	1515.83
304.80	14.77	38.89	1516.18
365.76	14.62	38.89	1516.73
600.00	14.27	38.79	1519.34
800.00	14.01	38.78	1521.83
1000.00	13.83	38.75	1524.55
1500.00	13.72	38.70	1532.46
2000.00	13.67	38.69	1540.67
2500.00	13.67	38.66	1549.08
3000.00	13.63	38.64	1557.46
3088.00	13.62	38.63	1558.91

POINT B

0.00	17.08	39.00	1518.32
23.32	17.08	38.90	1518.58
30.94	16.70	38.87	1517.53
38.56	16.49	38.84	1517.01
53.80	16.30	38.78	1516.61
84.28	16.05	38.70	1516.26
121.92	15.83	38.71	1516.23
182.88	15.52	38.64	1516.45
243.84	15.16	38.86	1516.37
304.80	14.88	38.84	1516.47
365.76	14.69	38.83	1516.86
600.00	14.24	38.73	1519.19
800.00	13.93	38.67	1521.42
1000.00	13.74	38.67	1524.13
1500.00	13.66	38.63	1532.19
1900.00	13.67	38.61	1538.88

POINT C

0.00	17.02	39.43	1518.66
27.81	17.03	39.29	1518.96
35.43	16.66	39.26	1517.97
43.05	16.47	39.23	1517.49
58.29	16.29	39.19	1517.16
88.77	16.08	39.13	1516.96
121.92	15.87	39.09	1516.81
182.88	15.52	39.04	1516.69
243.84	15.18	38.99	1516.59
304.80	14.86	38.94	1516.52
365.76	14.65	38.88	1516.80
600.00	14.22	38.75	1519.14
800.00	13.93	38.72	1521.49
1000.00	13.76	38.69	1524.23
1500.00	13.67	38.66	1532.25
2000.00	13.59	38.64	1540.36
2500.00	13.31	38.67	1547.93
2741.00	13.07	38.60	1551.15

POINT D

0.00	17.42	39.43	1519.85
29.24	17.42	39.34	1520.21
36.85	17.05	39.32	1519.23
44.48	16.85	39.30	1518.74
59.72	16.65	39.26	1518.35
90.19	16.39	39.17	1517.96
121.92	16.17	39.13	1517.77
182.88	15.73	39.07	1517.37
243.84	15.35	39.04	1517.17
304.80	14.96	39.00	1516.92
365.76	14.74	38.97	1517.21
600.00	14.25	38.86	1519.37
800.00	13.90	38.76	1521.45
1000.00	13.67	38.73	1524.00
1500.00	13.53	38.65	1531.79
2000.00	13.42	38.62	1539.79
2370.00	13.18	38.59	1545.22

Figure 94. BT data in April.

POINT A

0.00	19.04	39.00	1523.92
9.48	19.04	38.97	1524.06
17.10	17.63	38.95	1520.14
24.72	16.92	38.92	1518.17
39.96	16.36	38.88	1516.69
70.44	15.81	38.81	1515.44
121.92	15.37	38.78	1514.90
182.88	15.17	38.86	1515.38
243.84	14.97	38.89	1515.81
304.80	14.79	38.89	1516.25
365.76	14.65	38.89	1516.83
600.00	14.31	38.79	1519.48
800.00	14.05	38.78	1521.96
1000.00	13.86	38.75	1524.64
1500.00	13.74	38.70	1532.52
2000.00	13.68	38.69	1540.69
2500.00	13.67	38.66	1549.08
3000.00	13.63	38.64	1557.46
3088.00	13.62	38.63	1558.91

POINT B

0.00	18.70	39.00	1522.97
12.62	18.71	38.96	1523.16
20.24	17.55	38.94	1519.94
27.86	16.97	38.90	1518.35
43.10	16.51	38.80	1517.09
73.58	16.06	38.71	1516.13
121.92	15.61	38.71	1515.55
182.88	15.28	38.84	1515.72
243.84	14.99	38.86	1515.82
304.80	14.76	38.85	1516.08
365.76	14.60	38.83	1516.57
600.00	14.18	38.73	1519.00
800.00	13.89	38.67	1521.32
1000.00	13.72	38.67	1524.08
1500.00	13.66	38.63	1532.17
1900.00	13.67	38.61	1538.68

POINT C

0.00	20.53	39.43	1528.49
8.29	20.52	39.39	1528.56
15.91	19.08	39.35	1524.73
23.53	18.34	39.32	1522.72
38.77	17.67	39.26	1520.99
69.25	16.90	39.17	1519.13
121.92	16.27	39.08	1517.99
182.88	15.82	39.04	1517.62
243.84	15.38	38.99	1517.19
304.80	15.00	38.93	1516.95
365.76	14.76	38.88	1517.15
600.00	14.28	38.75	1519.35
800.00	13.96	38.72	1521.60
1000.00	13.77	38.69	1524.27
1500.00	13.67	38.66	1532.25
2000.00	13.59	38.64	1540.36
2500.00	13.31	38.67	1547.93
2741.00	13.07	38.60	1551.15

POINT D

0.00	21.47	39.43	1530.98
7.10	21.45	39.41	1531.03
14.72	19.95	39.39	1527.13
22.34	19.14	39.36	1525.01
37.58	18.36	39.30	1523.00
68.06	17.37	39.19	1520.52
121.92	16.63	39.09	1519.09
182.88	16.10	39.06	1518.49
243.84	15.52	39.04	1517.69
304.80	15.09	39.00	1517.33
365.76	14.66	38.97	1517.57
600.00	14.35	38.86	1519.70
800.00	13.98	38.78	1521.70
1000.00	13.73	38.73	1524.17
1500.00	13.56	38.65	1531.88
2000.00	13.43	38.62	1539.62
2370.00	13.19	38.59	1545.23

Figure 95. BT data in May.

POINT A

0.00	21.64	39.00	1530.92
11.87	21.64	38.96	1531.06
19.49	19.39	38.94	1525.14
27.11	18.24	38.92	1522.02
42.35	17.26	38.87	1519.39
72.83	16.20	38.81	1516.65
121.92	15.60	38.78	1515.61
182.88	15.32	38.84	1515.85
243.84	15.08	38.89	1516.15
304.80	14.89	38.89	1516.55
365.76	14.73	38.89	1517.07
600.00	14.34	38.79	1519.58
800.00	14.06	38.78	1521.98
1000.00	13.86	38.75	1524.63
1500.00	13.73	38.70	1532.50
2000.00	13.67	38.69	1540.68
2500.00	13.67	38.66	1549.08
3000.00	13.63	38.64	1557.46
3088.00	13.62	38.63	1558.91

POINT B

0.00	22.02	39.00	1531.89
14.21	22.01	38.96	1532.06
21.83	19.90	38.93	1526.56
29.45	18.81	38.89	1523.65
44.69	17.88	38.79	1521.13
75.17	16.85	38.71	1518.53
121.92	16.15	38.71	1517.20
182.88	15.73	38.84	1517.10
243.84	15.34	38.86	1516.94
304.80	15.05	38.85	1517.01
365.76	14.84	38.83	1517.33
600.00	14.34	38.73	1519.49
800.00	13.98	38.67	1521.59
1000.00	13.76	38.67	1524.21
1500.00	13.67	38.63	1532.21
1900.00	13.67	38.61	1538.89

POINT C

0.00	22.83	39.43	1534.45
11.20	22.83	39.37	1534.56
18.82	20.73	39.34	1529.23
26.44	19.62	39.31	1526.34
41.68	18.60	39.25	1523.67
72.16	17.35	39.16	1520.47
121.92	16.66	39.08	1519.17
182.88	16.22	39.04	1518.82
243.84	15.68	38.99	1518.12
304.80	15.25	38.93	1517.75
365.76	14.98	38.88	1517.83
600.00	14.42	38.75	1519.78
800.00	14.04	38.72	1521.84
1000.00	13.81	38.69	1524.39
1500.00	13.68	38.66	1532.29
2000.00	13.59	38.64	1540.36
2500.00	13.31	38.67	1547.92
2741.00	13.07	38.60	1551.15

POINT D

0.00	23.58	39.43	1536.29
9.30	23.57	39.40	1536.40
16.92	21.40	39.38	1531.01
24.54	20.23	39.36	1526.03
39.78	19.12	39.29	1525.16
70.26	17.72	39.19	1521.55
121.92	17.01	39.09	1520.21
182.88	16.57	39.06	1519.88
243.84	15.94	39.04	1518.96
304.80	15.49	39.00	1518.56
365.76	15.20	38.97	1518.64
600.00	14.56	38.86	1520.35
800.00	14.09	38.76	1522.06
1000.00	13.77	38.73	1524.32
1500.00	13.57	38.65	1531.91
2000.00	13.43	38.62	1539.81
2370.00	13.18	38.59	1545.22

Figure 96. BT data in June.

POINT A

0.00	23.66	39.00	1536.49
16.28	23.66	38.95	1536.69
23.90	20.40	38.93	1527.95
31.52	18.70	38.90	1523.39
46.76	17.41	38.86	1519.89
77.24	16.26	38.80	1516.90
121.92	15.65	38.78	1515.77
182.88	15.33	38.86	1515.87
243.84	15.06	38.89	1516.09
304.80	14.86	38.89	1516.48
365.76	14.71	38.89	1517.02
600.00	14.34	38.79	1519.58
800.00	14.06	38.78	1522.00
1000.00	13.87	38.75	1524.65
1500.00	13.74	38.70	1532.51
2000.00	13.67	38.69	1540.69
2500.00	13.67	38.66	1549.08
3000.00	13.63	38.64	1557.46
3088.00	13.62	38.63	1558.91

POINT B

0.00	24.65	39.00	1538.39
16.27	24.64	38.95	1538.58
23.89	21.20	38.92	1530.07
31.51	19.49	38.88	1525.54
46.75	18.13	38.78	1521.80
77.23	16.84	38.71	1518.51
121.92	16.16	38.71	1517.22
182.88	15.70	38.84	1517.00
243.84	15.30	38.86	1516.81
304.80	15.03	38.85	1516.94
365.76	14.82	38.83	1517.28
600.00	14.32	38.73	1519.45
800.00	13.97	38.67	1521.56
1000.00	13.76	38.67	1524.19
1500.00	13.67	38.63	1532.20
1900.00	13.67	38.61	1538.88

POINT C

0.00	25.65	39.43	1541.20
14.52	25.64	39.36	1541.34
22.14	22.12	39.32	1532.89
29.76	20.35	39.29	1528.34
45.00	18.89	39.24	1524.53
75.48	17.39	39.15	1520.64
121.92	16.44	39.08	1518.53
182.88	15.85	39.04	1517.69
243.84	15.38	38.99	1517.20
304.80	15.04	38.93	1517.09
365.76	14.80	38.88	1517.27
600.00	14.29	38.75	1519.35
800.00	13.95	38.72	1521.55
1000.00	13.75	38.69	1524.22
1500.00	13.66	38.66	1532.22
2000.00	13.59	38.64	1540.34
2500.00	13.31	38.67	1547.92
2741.00	13.07	38.60	1551.15

POINT D

0.00	26.04	39.43	1542.10
15.06	26.03	39.39	1542.28
22.68	22.48	39.36	1533.85
30.30	20.68	39.33	1529.28
45.54	19.19	39.27	1525.41
76.02	17.63	39.17	1521.38
121.92	16.64	39.09	1519.11
182.88	15.97	39.06	1518.07
243.84	15.53	39.04	1517.71
304.80	15.21	39.00	1517.70
365.76	14.96	38.97	1517.90
600.00	14.35	38.86	1519.71
800.00	13.94	38.78	1521.57
1000.00	13.68	38.73	1524.01
1500.00	13.53	38.65	1531.76
2000.00	13.42	38.62	1539.77
2370.00	13.18	38.59	1545.20

Figure 97. BT data in July.

POINT A

0.00	24.99	39.00	1539.20
20.07	24.98	38.94	1539.43
27.69	21.08	38.92	1529.82
35.31	19.16	38.89	1524.71
50.55	17.68	38.85	1520.70
81.03	16.31	38.79	1517.10
121.92	15.66	38.78	1515.79
182.88	15.30	38.86	1515.80
243.84	15.04	38.89	1516.03
304.80	14.81	38.89	1516.31
365.76	14.65	38.89	1516.83
600.00	14.28	38.79	1519.40
800.00	14.02	38.78	1521.86
1000.00	13.84	38.75	1524.56
1500.00	13.72	38.70	1532.46
2000.00	13.67	38.69	1540.67
2500.00	13.67	38.66	1549.08
3000.00	13.63	38.64	1557.46
3088.00	13.62	38.63	1558.91

POINT B

0.00	25.14	39.00	1539.55
19.04	25.14	38.94	1539.77
26.66	21.40	38.91	1530.64
34.28	19.55	38.86	1525.74
49.52	18.08	38.76	1521.75
80.00	16.66	38.70	1518.04
121.92	15.85	38.71	1516.30
182.88	15.40	38.84	1516.09
243.84	15.06	38.86	1516.04
304.80	14.77	38.85	1516.14
365.76	14.60	38.83	1516.58
600.00	14.20	38.73	1519.07
800.00	13.92	38.67	1521.39
1000.00	13.74	38.67	1524.14
1500.00	13.67	38.63	1532.21
1900.00	13.67	38.61	1538.90

POINT C

0.00	26.58	39.43	1543.31
18.37	26.56	39.34	1543.48
25.99	22.69	39.31	1534.39
33.61	20.74	39.28	1529.43
48.85	19.11	39.22	1525.20
79.33	17.41	39.14	1520.74
121.92	16.34	39.08	1518.21
182.88	15.74	39.04	1517.36
243.84	15.27	38.99	1516.86
304.80	14.92	38.93	1516.70
365.76	14.70	38.88	1516.95
600.00	14.27	38.75	1519.30
800.00	13.97	38.72	1521.63
1000.00	13.79	38.69	1524.33
1500.00	13.69	38.66	1532.30
2000.00	13.60	38.64	1540.38
2500.00	13.31	38.67	1547.93
2741.00	13.07	38.60	1551.16

POINT D

0.00	27.18	39.43	1544.65
17.44	27.16	39.38	1544.83
25.06	23.20	39.36	1535.69
32.68	21.18	39.32	1530.83
47.92	19.46	39.26	1526.19
78.40	17.60	39.16	1521.32
121.92	16.44	39.09	1518.53
182.88	15.80	39.06	1517.58
243.84	15.31	39.04	1517.04
304.80	14.94	39.00	1516.86
365.76	14.73	38.97	1517.16
600.00	14.27	38.86	1519.43
800.00	13.93	38.76	1521.54
1000.00	13.70	38.73	1524.09
1500.00	13.55	38.65	1531.85
2000.00	13.43	38.62	1539.82
2370.00	13.19	38.59	1545.23

Figure 98. BT data in August.

POINT A

0.00	24.51	39.00	1536.05
26.64	24.49	38.92	1538.36
34.26	20.77	38.90	1529.09
41.88	18.94	38.87	1524.20
57.12	17.54	38.84	1520.41
87.60	16.27	38.78	1517.07
121.92	15.72	38.78	1515.98
182.88	15.30	38.86	1515.80
243.84	15.02	38.89	1515.96
304.80	14.79	38.89	1516.24
365.76	14.63	38.89	1516.76
600.00	14.27	38.79	1519.36
800.00	14.01	38.78	1521.83
1000.00	13.83	38.75	1524.54
1500.00	13.72	38.70	1532.46
2000.00	13.67	38.69	1540.67
2500.00	13.67	38.66	1549.08
3000.00	13.63	38.64	1557.46
3088.00	13.62	38.63	1558.91

POINT B

0.00	24.62	39.00	1538.78
27.78	24.61	38.93	1539.10
35.40	21.26	38.85	1530.33
43.02	19.50	38.80	1525.68
58.26	18.13	38.74	1522.02
88.74	16.85	38.68	1518.71
121.92	16.28	38.71	1517.60
182.88	15.69	38.84	1516.95
243.84	15.22	38.86	1516.56
304.80	14.89	38.85	1516.50
365.76	14.69	38.83	1516.85
600.00	14.22	38.73	1519.13
800.00	13.99	38.67	1521.35
1000.00	13.72	38.67	1524.07
1500.00	13.65	38.63	1532.15
1900.00	13.66	38.61	1538.86

POINT C

0.00	25.39	39.43	1540.60
26.03	25.38	39.31	1540.88
33.65	21.69	39.28	1531.94
41.27	19.87	39.25	1527.19
56.51	18.44	39.20	1523.41
86.99	17.09	39.12	1519.92
121.92	16.46	39.08	1518.57
182.88	15.81	39.04	1517.58
243.84	15.30	38.99	1516.95
304.80	14.94	38.93	1516.76
365.76	14.72	38.88	1517.02
600.00	14.28	38.75	1519.33
800.00	13.98	38.72	1521.64
1000.00	13.79	38.69	1524.33
1500.00	13.68	38.66	1532.29
2000.00	13.60	38.64	1540.38
2500.00	13.21	38.67	1547.93
2741.00	13.07	38.60	1551.16

POINT D

0.00	26.00	39.43	1542.00
25.89	25.99	39.35	1542.32
33.51	22.21	39.32	1533.31
41.13	20.34	39.29	1528.49
56.37	18.85	39.23	1524.61
86.85	17.43	39.14	1520.94
121.92	16.75	39.08	1519.49
182.88	16.01	39.06	1518.21
243.84	15.43	39.03	1517.41
304.80	15.02	39.00	1517.09
365.76	14.80	38.97	1517.37
600.00	14.29	38.86	1519.52
800.00	13.94	38.78	1521.56
1000.00	13.70	38.73	1524.07
1500.00	13.55	38.65	1531.83
2000.00	13.43	38.62	1539.80
2370.00	13.18	38.59	1545.22

Figure 99. BT data in September.

POINT A

0.00	22.10	38.83	1531.90
39.96	21.96	38.84	1532.22
47.48	19.33	38.85	1525.32
55.10	18.02	38.85	1521.78
70.34	17.01	38.85	1519.10
100.82	16.08	38.85	1516.62
182.88	15.36	38.91	1516.04
243.84	15.07	38.91	1516.13
304.80	14.82	38.90	1516.36
365.76	14.67	38.90	1516.87
600.00	14.30	38.79	1519.45
800.00	14.03	38.78	1521.90
1000.00	13.85	38.75	1524.58
1500.00	13.73	38.70	1532.48
2000.00	13.67	38.69	1540.68
2500.00	13.67	38.66	1549.08
3000.00	13.63	38.64	1557.46
3086.00	13.62	38.63	1558.91

POINT B

0.00	23.01	38.74	1534.10
43.90	22.84	38.78	1534.44
51.52	20.05	38.79	1527.32
59.14	18.67	38.80	1523.63
74.38	17.58	38.81	1520.79
104.86	16.54	38.84	1518.26
182.88	15.67	38.92	1517.00
243.84	15.22	38.91	1516.59
304.80	14.89	38.87	1516.54
365.76	14.69	38.84	1516.88
600.00	14.22	38.73	1519.14
800.00	13.90	38.67	1521.35
1000.00	13.72	38.67	1524.07
1500.00	13.65	38.63	1532.15
1900.00	13.66	38.61	1538.86

POINT C

0.00	23.47	39.07	1535.61
38.50	23.26	39.08	1535.75
46.12	20.66	39.09	1529.21
53.74	19.35	39.10	1525.80
68.98	18.30	39.10	1523.09
99.46	17.23	39.11	1520.54
182.88	16.14	39.05	1518.59
243.84	15.55	38.99	1517.72
304.80	15.13	38.94	1517.35
365.76	14.87	38.88	1517.50
600.00	14.36	38.75	1519.60
800.00	14.01	38.72	1521.76
1000.00	13.80	38.69	1524.36
1500.00	13.68	38.66	1532.29
2000.00	13.59	38.64	1540.37
2500.00	13.31	38.67	1547.93
2741.00	13.07	38.60	1551.15

POINT D

0.00	24.31	39.01	1537.57
37.28	24.05	39.05	1537.61
44.90	21.37	39.06	1531.02
52.52	20.01	39.07	1527.54
67.76	18.87	39.06	1524.65
98.24	17.66	39.05	1521.70
182.88	16.48	39.06	1519.63
243.84	15.81	39.04	1518.59
304.80	15.34	39.00	1518.10
365.76	15.06	38.97	1518.21
600.00	14.44	38.86	1519.97
800.00	14.00	38.76	1521.76
1000.00	13.71	38.73	1524.13
1500.00	13.54	38.65	1531.82
2000.00	13.42	38.62	1539.79
2370.00	13.18	38.59	1545.21

Figure 100. BT data in October.

POINT A

0.00	20.23	38.82	1526.99
48.22	20.09	38.85	1527.44
55.84	18.30	38.85	1522.60
63.46	17.41	38.85	1520.16
78.70	16.71	38.85	1518.33
109.18	16.03	38.86	1516.80
182.88	15.35	38.91	1516.00
243.84	15.04	38.91	1516.06
304.80	14.80	38.90	1516.29
365.76	14.64	38.90	1516.80
600.00	14.28	38.79	1519.39
800.00	14.02	38.78	1521.86
1000.00	13.84	38.75	1524.56
1500.00	13.72	38.70	1532.47
2000.00	13.67	38.69	1540.67
2500.00	13.67	38.66	1549.08
3000.00	13.63	38.64	1557.46
3088.00	13.62	38.63	1558.91

POINT B

0.00	21.02	38.74	1528.98
51.52	20.86	38.79	1529.47
59.14	18.99	38.80	1524.53
66.75	18.05	38.81	1521.98
82.00	17.26	38.82	1519.96
112.48	16.42	38.85	1518.03
182.88	15.55	38.92	1516.61
243.84	15.11	38.91	1516.26
304.80	14.78	38.87	1516.19
365.76	14.60	38.84	1516.58
600.00	14.18	38.73	1518.99
800.00	13.89	38.67	1521.30
1000.00	13.72	38.67	1524.07
1500.00	13.65	38.63	1532.16
1900.00	13.66	38.61	1538.87

POINT C

0.00	22.17	39.07	1532.36
43.48	21.88	39.09	1532.37
51.30	19.92	39.10	1527.31
58.92	18.89	39.10	1524.59
74.16	17.94	39.10	1522.17
104.64	16.82	39.11	1519.39
182.88	15.75	39.05	1517.41
243.84	15.23	38.99	1516.74
304.80	14.86	38.94	1516.53
365.76	14.65	38.88	1516.80
600.00	14.24	38.75	1519.20
800.00	13.95	38.72	1521.57
1000.00	13.76	38.69	1524.30
1500.00	13.68	38.66	1532.29
2000.00	13.60	38.64	1540.38
2500.00	13.31	38.67	1547.93
2741.00	13.07	38.60	1551.16

POINT D

0.00	23.37	39.01	1535.29
41.66	23.02	39.05	1535.17
49.28	20.94	39.07	1529.98
56.90	19.83	39.06	1527.12
72.14	18.76	39.05	1524.40
102.62	17.40	39.05	1521.01
182.88	16.13	39.06	1518.58
243.84	15.50	39.04	1517.62
304.80	15.06	39.00	1517.24
365.76	14.83	38.97	1517.47
600.00	14.33	38.86	1519.63
800.00	13.97	38.76	1521.66
1000.00	13.72	38.73	1524.15
1500.00	13.56	38.65	1531.87
2000.00	13.43	38.62	1539.81
2370.00	13.18	38.59	1545.23

Figure 101. BT data in November.

POINT A

0.00	17.72	38.83	1519.99
69.17	17.70	38.85	1521.09
76.79	16.82	38.85	1518.64
84.41	16.38	38.85	1517.45
99.65	16.02	38.85	1516.61
130.13	15.64	38.88	1516.00
182.88	15.28	38.91	1515.78
243.84	15.02	38.91	1515.98
304.80	14.83	38.90	1516.38
365.76	14.68	38.90	1516.93
600.00	14.32	38.79	1519.50
800.00	14.04	38.78	1521.94
1000.00	13.85	38.75	1524.61
1500.00	13.73	38.70	1532.49
2000.00	13.67	38.69	1540.68
2500.00	13.67	38.66	1549.08
3000.00	13.63	38.64	1557.46
3086.00	13.62	38.63	1558.91

POINT B

0.00	18.58	38.74	1522.32
78.94	18.51	38.82	1523.53
86.56	17.46	38.82	1520.64
94.18	16.92	38.83	1519.19
109.42	16.46	38.84	1518.08
139.90	15.95	38.87	1517.10
182.88	15.54	38.92	1516.61
243.84	15.13	38.91	1516.33
304.80	14.85	38.87	1516.42
365.76	14.67	38.84	1516.80
600.00	14.22	38.73	1519.12
800.00	13.91	38.67	1521.37
1000.00	13.73	38.67	1524.09
1500.00	13.66	38.63	1532.17
1900.00	13.66	38.61	1538.87

POINT C

0.00	18.47	39.07	1522.42
72.76	18.38	39.10	1523.40
80.38	17.45	39.10	1520.83
88.00	16.97	39.10	1519.56
103.24	16.55	39.11	1518.59
133.72	16.10	39.10	1517.73
182.88	15.69	39.05	1517.22
243.84	15.29	38.99	1516.92
304.80	14.96	38.94	1516.82
365.76	14.74	38.88	1517.10
600.00	14.30	38.76	1519.40
800.00	13.99	38.72	1521.69
1000.00	13.80	38.69	1524.36
1500.00	13.59	38.65	1532.31
2000.00	13.60	38.64	1540.38
2500.00	13.31	38.67	1547.93
2741.00	13.07	38.60	1551.16

POINT D

0.00	18.78	39.01	1523.20
71.82	18.68	39.06	1524.17
79.44	17.69	39.06	1521.42
87.06	17.19	39.06	1520.13
102.30	16.75	39.05	1519.09
132.78	16.27	39.07	1518.17
182.88	15.84	39.07	1517.70
243.84	15.42	39.04	1517.38
304.80	15.06	39.01	1517.24
365.76	14.85	38.97	1517.54
600.00	14.35	38.86	1519.69
800.00	13.98	38.76	1521.70
1000.00	13.73	38.73	1524.17
1500.00	13.56	38.65	1531.88
2000.00	13.43	38.62	1539.62
2370.00	13.18	38.59	1545.23

Figure 102. BT data in December.

LIST OF REFERENCES

1. Armanda, M. Z., 1969. "Water Exchange Between the Adriatic and the Eastern Mediterranean." Deep Sea Research. 16:p.171-178.

2. Carter, T. G., Flanagan, J. P., Jones, C. R., Marchant, F. L., Murchison, R. R., Rebman, J. A., Sylvester, J. C., and Whitney, J. C., 1972. "A new bathymetric chart and physiography of the Mediterranean Sea." In: D. J. Stanley (editor), The Mediterranean Sea. Dowden, Hutchinson, and Ross, Stroudsburg, PA, p. 1-23.

3. Comninakis, P. E. and Papazachos, B. C., 1972. "Seismicity of the eastern Mediterranean and some tectonic features of the Mediterranean ridge." Geological Society of America Bulletin. 83: p.1093-1102.

4. Emelyanov, E. M., 1972. "Principal types of recent bottom sediments in the Mediterranean Sea: their mineralogy and geochemistry." In: D. J. Stanley (editor), The Mediterranean Sea. Dowden, Hutchinson, and Ross, Stroudsburg, PA, p. 355-386.

5. Emery, K. O., Heezen, B. C., and Allan, T. D., 1966. "Bathymetry of the eastern Mediterranean Sea." Deep Sea Research. 13: p. 173-192.

6. Engel, I., 1967. "Currents in the eastern Mediterranean." International Hydrographic Review. XLIV, no. 2, p. 23-40.

7. Engel, I., 1968. "Vertical hydrographic sections of the eastern Mediterranean." International Hydrographic Review. XLV, no. 1, p. 167-175.

8. Goncharov, V. P. and Mikhailov, O. V., 1964. "New data on the bottom relief of the Mediterranean." Deep Sea Research. 11: p. 625-628.

9. Horn, D. R., Horn, B. M., and Delach, M. N., 1968. "Correlation between acoustical and other physical properties of deep-sea cores." Journal of Geophysical Research. 73: no. 6, p. 1939-1957.

10. Keller, G. H. and Lambert, D. N., 1972. "Geotechnical properties of submarine sediments, Mediterranean Sea." In: D. J. Stanley (editor), The Mediterranean Sea. Dowden, Hutchinson, and Ross, Stroudsburg, PA, p. 25-36.

11. Lacombe, H. and Tchernia, P., 1972. "Caracteres hydrologiques et circulation des eaux en Mediterranee." In: D. J. Stanley (editor), The Mediterranean Sea. Dowden, Hutchinson, and Ross, Stroudsburg, PA, p. 25-36.

12. Morcos, S. A., 1972. "Sources of Mediterranean intermediate water in the Levantine Sea." In: A. L. Gordon (editor), Studies in Physical Oceanography. Gordon and Breach, New York, p. 185-206.

13. Moskalenko, L. V. and Ovchinnikov, I. M., 1965. "The water masses of the Mediterranean Sea." In: Basic Features of the Geological Structure of the Hydrologic Regime and Biology of the Mediterranean Sea. U. S. Naval Oceanographic Office, Washington, D. C., p. 202-206.

14. Nielsen, N. J., 1912. "Hydrography of the Mediterranean and adjacent waters." Rap. Dan. Oceanogr. Exped. Medit., I, p. 77-192.

15. Oceanographic Atlas of the North Atlantic Ocean, 1963, U. S. Naval Oceanographic Office, Washington, D. C.

16. Ovchinnikov, I. M. and Fedoseyev, A. F., 1968. "The horizontal circulation of the water of the Mediterranean Sea during the summer and winter seasons." In: Basic Features of the Geological Structure of the Hydrologic Regime and Biology of the Mediterranean Sea. U. S. Naval Oceanographic Office, Washington, D. C.

17. Pollak, M. J., 1951. "The sources of the deep water of the eastern Mediterranean Sea." Journal of Marine Research, X, 1.

18. Schieferdecker, A. A. G., 1959. Geological Nomenclature. Gorinchem. J. Noorduijn en zoon N.V.

19. Sverdrup, H. U., Johnson, M. W., and Fleming, R. H., 1942. The Oceans. Prentice-Hall, N.J., p. 643.

20. Swanson, B. K., 1966. Oceanography for Long Range Sonar Systems, Part I. U. S. Naval Oceanographic Office.

21. Urick, R. J., 1967. Principles of Underwater Sound for Engineers. McGraw-Hill, p. 155.

22. Venkatarathnam, K. and Ryan, W. B. F., 1971. "Dispersal patterns of clay minerals in the sediments of the eastern Mediterranean Sea." Marine Geology, 11, p. 261-282.

23. Wong, H. K. and Zarudzki, E. F. K., 1969. "Thickness of unconsolidated sediments in the eastern Mediterranean Sea." Geological Society of America Bulletin, 80: p. 2611-2614.

24. Wüst, G., 1951. "On the vertical circulation of the Mediterranean Sea." Journal of Geophysical Research, 77, no. 6, p. 3261-3271.

INITIAL DISTRIBUTION LIST

		No. Copies
1.	Defense Documentation Center Cameron Station Alexandria, Virginia 22314	2
2.	Library, Code 0142 Naval Postgraduate School Monterey, California 93940	2
3.	LCDR. A. B. Chace Department of Oceanography, Code 63 Naval Postgraduate School Monterey, California 93940	1
4.	Prof. W. C. Thompson Department of Oceanography, Code 68 Naval Postgraduate School Monterey, California 93940	1
5.	Nazım Çubukçu Ziya Erdem Sokak No. 20/2 yeşilköy-ISTANBUL-TURKEY	3
6.	Commanding Officer Fleet Numerical Weather Central Monterey, California 93940	1
7.	Commanding Officer Naval Environmental Prediction Research Facility Monterey, California 93940	1
8.	Department of the Navy Commander Oceanographic System Pacific Box 1390 Pearl Harbor, Hawaii 96860	1
9.	Department of Oceanography, Code 68 Naval Postgraduate School Monterey, California 93940	3
10.	Department of Oceanography Library University of Washington Seattle, Washington 98105	1
11.	Department of Oceanography Library Oregon State University Corvallis, Oregon 97331	1

12. Director — 1
Naval Oceanography and Meteorology
National Space Technology Laboratories
NSTL Station, Mississippi 39529

13. Deniz Kuvvetleri Komutanligi — 3
Personel egitim Sb.Mudurlugu
Ankara, TURKEY

14. Dz. Kuvvetleri Seyir ve Hidrografi Dairesi Bsk. — 3
Cubuklu, Istanbul
TURKEY

15. Orta-Dogu Teknik Universitesi — 1
Ankara,
TURKEY

16. Istanbul Teknik Universitesi — 1
Taskisla, Istanbul
TURKEY

17. Library, Code 3330 — 1
Naval Oceanographic Office
Washington, D. C. 20373

18. NORDA — 1
NSTL Station, Mississippi 39529

19. Oceanographer of the Navy, Code N-45 — 1
Hoffman Building No. 2
200 Stovall Street
Alexandria, Virginia 22332

20. Office of Naval Research — 1
Code 410
NORDA
NSTL Station, Mississippi 39529

21. SIO Library — 1
University of California, San Diego
P. O. Box 2367
La Jolla, California 92037

22. Dr. Robert E. Stevenson — 1
Scientific Liaison Office, ONR
Scripps Institution of Oceanography
La Jolla, California 92037